

**PALACKÝ UNIVERSITY IN OLOMOUČ**

**Faculty of Science**

**Department of Analytical Chemistry**



**Metabolomics of clinically important  
*Aspergillus fumigatus* and *Rhizopus  
microsporus* in the diagnoses of invasive  
fungal infections**

**DOCTORAL THESIS**

Author: Rutuja Hiraji Patil  
Field of study: Analytical Chemistry  
Supervisor: prof. Ing. Vladimír Havlíček, Dr.

**Olomouc 2023**

## Declaration

I hereby declare that I have worked on this thesis under the guidance of my supervisor, and I have written the dissertation thesis myself. All the sources of the utilized information are appropriately indicated in the references.

I agree that this work will be accessible in the library of the Department of Analytical Chemistry, Faculty of Science, Palacký University in Olomouc.

In Olomouc

Mgr. Rutuja Hiraji Patil

## ACKNOWLEDGEMENT

My PhD journey has been a truly extraordinary experience and would not have been possible without the support and guidance I received from many people worldwide.

Firstly, I am highly indebted to thank my supervisor, prof. Vladimír Havlíček, not only for his continuous guidance and insights in science but also for music and sports enthusiasm. He has inspired me to become an independent researcher, and his constructive criticism helped me realize the power of critical reasoning. I appreciate his support in writing grant proposals and travelling and presenting work to several conferences, which allowed me to explore and meet many other great minds from different research fields all over the world.

My big thanks also belong to other laboratory members for creating a friendly environment, great discussions and for helping me whenever required. Along with others, mainly I would like to mention Andrea Palyzová and Helena Marešová for all the help and guidance during microbiology, Tomáš Pluháček for his all-time advice on statistics and analytical chemistry, Anton Škríba for teaching me operating FT-ICR mass spectrometer, Hynek Mácha and Jiří Houšť for all the fun and craziness we had in the lab. I would also like to thank all my colleagues from the Department of Analytical Chemistry for both social and scientific interactions.

Next, I would like to express my gratitude to all our collaborators from other labs. Ioly Kotta-Loizou for providing me opportunity to do my research stay at Imperial College London, UK. David A. Stevens (California Institute for Medical Research and Stanford University School of Medicine, USA), Radim Dobiáš (Public Health Institute in Ostrava and University of Ostrava, CZ) and Jiří Hrdý (Charles University, CZ) for providing their expertise and biological samples during my study.

I would also like to acknowledge the Internal Grant Agency of Palacký University grant IGA\_PrF\_2022\_023 and Czech Science Foundation, grant No. 21-17044S (2021-2023) for financial support.

Last but not least, my family and my other half who continuously encouraged and comforted me day after day, through thick and thin: my love and gratitude for them cannot be expressed in words.

## SUMMARY

*Aspergillus fumigatus* and *Rhizopus microsporus* are globally distributed pathogenic fungi responsible for causing a wide spectrum of infections called aspergillosis and mucormycosis, respectively. The diagnosis of these infections still faces challenges due to various factors such as non-specific clinical symptoms, overlapping risk factors, non-discrimination between colonization and invasive infection and limited sensitivity to already existing diagnostic tools. Moreover, the increase in antifungal resistance and vaccine unavailability to these infections emphasizes the critical need for specific and timely diagnostics.

One area of research is using mycotoxins and microbial metallophores, specifically siderophores, which play crucial roles in fungal growth, survival, and pathogenesis; as a result, their complex structures could enable high diagnostic specificity. Liquid chromatography-mass spectrometry-based metabolomics can provide accurate and rapid detection of these fungal metabolites and can also specify a comprehensive overview of pathogen-induced changes to the host cells following infection.

Therefore, the main goal of this thesis is the liquid chromatography-mass spectrometry (MS) based characterization of *A. fumigatus* and *R. microsporus* siderophores and other metabolites. The thesis focuses on the following four topics: introduction of infection metallomics, characterization of *R. microsporus* siderophores, characterization of *A. fumigatus* siderophores and mycotoxins to distinguish between colonization and invasion, as well as during inter-kingdom interaction with bacterial pathogen-*Pseudomonas aeruginosa*, host cells-neutrophils and polymycovirus and finally, infection metallomics based diagnosis of human and equine aspergillosis.

The theoretical part covers general information on *A. fumigatus* and *R. microsporus*, related infections, secondary metabolites, and specific knowledge about each mentioned topic. Experimental, results and discussion parts are divided into corresponding sections to each topic. The first section introduces infection metallomics, a MS platform based on the central concept that microbial metallophores are specific, sensitive, noninvasive, and promising biomarkers of invasive infectious diseases. The second section of this thesis includes *R. microsporus in vitro* cultivation, followed by liquid chromatography-mass spectrometry analysis of its siderophores. The third section involves *in vitro* cultivation of *A. fumigatus* with subsequent growth stage-specific siderophore and mycotoxin quantification to distinguish between colonization and invasive infection. Additionally, this



section deals with the time course quantification of *A. fumigatus* secondary metabolites during its interaction with neutrophils, bacterial pathogen *P. aeruginosa* and polyomavirus. The analysis is performed using developed metabolite extraction protocol and mass spectrometry methods. The fourth and last part focuses on applying infection metallomics-based diagnosis in human invasive pulmonary aspergillosis and equine aspergillosis.

Taken together, this thesis shows the performance of the non-invasive infection metallomics armoury and makes difference towards the standard serology, cultivation, microscopy, or nucleic acid analyses routinely used in invasive fungal infection diagnostics. The thesis documents why the innovative non-invasive approach based on mass spectrometry based microbial metallophores detection with benefit of isotope data filtration is inherently more sensitive and specific in selected applications than classical clinical standards.

## SOUHRN

*Aspergillus fumigatus* a *Rhizopus microsporus* jsou celosvětově rozšířené patogenní houby způsobující široké spektrum infekcí obecně nazývaných aspergilóza a mukormykóza. Diagnostika těchto infekcí stále čelí problémům kvůli nespecifickým klinickým příznakům, překrývajícím se rizikovým faktorům, neschopnosti rozlišit mezi kolonizací a invazí patogenu a omezené citlivosti současných diagnostických metod. Nárůst rezistence vůči antimykotikům a nedostupnost vakcín proti těmto infekcím podtrhuje kritickou potřebu specifické a včasné diagnostiky.

Jedna z oblastí výzkumu cílí na využití mikrobiálních metaloforů (konkrétně sideroforů) a mykotoxinů, které hrají klíčovou roli v růstu, přežívání a patogenezi hub. Metabolomika založená na kapalinové chromatografii a hmotnostní spektrometrii těchto biomarkerů může poskytnout rychlou, přesnou a specifickou detekci těchto patogenů. Zároveň může také reflektovat komplexní přehled změn vyvolaných patogenem v hostitelských buňkách po infekci.

Hlavním cílem této práce je charakterizace sideroforů a dalších metabolitů *A. fumigatus* a *R. microsporus* pomocí kapalinové chromatografie a hmotnostní spektrometrie. Práce je rozdělena do čtyř témat: představení infekční metalomiky, charakterizace sideroforů *R. microsporus*, charakterizace sideroforů a mykotoxinů *A. fumigatus* pro rozlišení kolonizace, invaze a mezidruhové interakce s bakteriálním patogenem *Pseudomonas aeruginosa*, hostitelskými neutrofily a polymykovirem, a na závěr diagnostika aspergilózy u lidí a koní za využití infekční metalomiky.

Teoretická část zahrnuje obecné informace o houbách *A. fumigatus* a *R. microsporus*, o infekcích, které tyto patogeny způsobují a o konkrétních sekundárních metabolitech. Experimentální část, výsledky a diskuse jsou rozděleny do příslušných oddílů ke každému tématu. První oddíl představuje infekční metalomiku, hmotnostně spektrometrickou platformu založenou na ústředním konceptu, že mikrobiální metalofory jsou specifické, citlivé, neinvazivní a slibné biomarkery invazivních infekčních onemocnění. Druhá část této práce zahrnuje kultivaci *R. microsporus in vitro*, po níž následuje analýza jeho sideroforů pomocí kapalinové chromatografie a hmotnostní spektrometrie.

Třetí část zahrnuje kultivaci *A. fumigatus in vitro* s následnou kvantifikací sideroforů a mykotoxinů specifických pro daná růstová stadia s cílem rozlišit mezi kolonizací a invazivní infekcí. Dále se tato část zabývá kvantitativním popisem časového

průběhu sekundárních metabolitů *A. fumigatus* při jeho interakci s neutrofilý, bakteriálním patogenem *P. aeruginosa* a polymykovirem. Analýza se provádí pomocí námi vyvinutého protokolu extrakce metabolitů a metod hmotnostní spektrometrie. Čtvrtá a poslední část je zaměřena na aplikaci infekční metalomiky při diagnostice invazivní plicní aspergilózy u lidí a u koní.

Tato práce ukazuje výkonnost neinvazivního přístupu infekční metalomiky v porovnání s rutinně používanými diagnostickými metodami, jako je standardní sérologie, kultivace, mikroskopie nebo analýza nukleových kyselin. Práce dokumentuje inovativní a neinvazivní přístup založený na detekci mikrobiálních metaloforů pomocí hmotnostní spektrometrie s využitím izotopové datové filtrace, jež je ve vybraných aplikacích citlivější a specifičtější metoda v porovnání s klasickými diagnostickými přístupy.

## TABLE OF CONTENTS

<b>1</b>	<b>INTRODUCTION</b> .....	10
<b>2</b>	<b>THEORETICAL PART</b> .....	11
<b>2.1</b>	<b><i>Aspergillus fumigatus</i></b> .....	11
2.1.1	The growth phases of <i>A. fumigatus</i> .....	11
2.1.2	<i>A. fumigatus</i> related infections.....	12
2.1.2.1	Chronic pulmonary aspergillosis.....	13
2.1.2.2	Allergic bronchopulmonary aspergillosis.....	13
2.1.2.3	Invasive pulmonary aspergillosis.....	13
2.1.2.3.1	Diagnosis of pulmonary aspergillosis.....	14
2.1.2.3.2	Treatment of pulmonary aspergillosis.....	15
<b>2.2</b>	<b>Secondary metabolites of <i>A. fumigatus</i></b> .....	16
2.2.1	Fungal siderophores – structures, functions, and applications.....	16
2.2.2	Mycotoxins-structure, biosynthesis and their roles in infections.....	19
<b>2.3</b>	<b><i>A. fumigatus</i> in interaction studies <i>in vitro</i></b> .....	21
2.3.1	<i>A. fumigatus</i> -innate immune cells mutual interplay.....	22
2.3.2	<i>A. fumigatus</i> - <i>Pseudomonas aeruginosa</i> are frenemies.....	24
2.3.2.1	<i>P. aeruginosa</i> molecular defence mechanisms.....	24
2.3.2.2	<i>A. fumigatus</i> molecular weapons for combat within consortia.....	25
2.3.3	<i>A. fumigatus</i> -mycovirus intracellular interaction.....	26
<b>2.4</b>	<b><i>Rhizopus</i> species and mucoromycosis</b> .....	27
<b>2.5</b>	<b>Secondary metabolites of <i>R. microsporus</i></b> .....	28
<b>3</b>	<b>AIMS OF THE THESIS</b> .....	30
<b>4</b>	<b>EXPERIMENTAL PART</b> .....	31
4.1	Liquid chromatography-mass spectrometry (LC-MS) based characterization of <i>R. microsporus</i> siderophores.....	31
4.2	LC-MS based <i>A. fumigatus</i> growth-specific siderophore and mycotoxin quantitation to distinguish between colonization and invasive infection.....	32
4.2.1	<i>A. fumigatus</i> siderophores and mycotoxins production during interaction with neutrophils and <i>P. aeruginosa</i> .....	35
4.2.2	<i>A. fumigatus</i> siderophores and mycotoxins production during interaction with polymycovirus.....	37

4.3	Infection metallomics-based diagnostics.....	40
4.3.1	Human invasive pulmonary aspergillosis.....	40
4.3.2	Equine aspergillosis.....	41
<b>5</b>	<b>RESULTS AND DISCUSSION.....</b>	<b>42</b>
5.1	Introduction to infection metallomics.....	42
5.2	LC-MS based characterization of <i>R. microsporus</i> siderophores.....	49
5.3	LC-MS based <i>A. fumigatus</i> growth-specific siderophore and mycotoxin quantitation to distinguish between colonization and invasive infection.....	52
5.3.1	<i>A. fumigatus</i> siderophores and mycotoxins production during interaction with neutrophils and <i>P. aeruginosa</i> .....	54
5.3.2	<i>A. fumigatus</i> siderophores and mycotoxins production during interaction with polmycovirus.....	58
5.4	Infection metallomics-based diagnosis.....	63
5.4.1	Human invasive pulmonary aspergillosis.....	63
5.4.2	Equine aspergillosis.....	66
<b>6</b>	<b>CONCLUSIONS.....</b>	<b>68</b>
	<b>REFERENCES.....</b>	<b>70</b>
	<b>LIST OF ABBREVIATIONS.....</b>	<b>88</b>
	<b>CURRICULUM VITAE.....</b>	<b>90</b>

# 1 INTRODUCTION

Throughout history, infectious diseases caused by pathogenic bacteria, fungi, and viruses have afflicted humans. The recent COVID-19 (Coronavirus disease 2019) pandemic is a daunting reminder that this susceptibility continues even in the medically/scientifically enhanced world. Unfortunately, some of these microbial threats are still unrecognized or neglected, and fungi infecting billions of people yearly are examples of such overlooked threats. Fungal infections represent emerging global diseases, accounting for approximately 1.7 million deaths annually [3]. During the COVID-19 pandemic, invasive fungal infection incidence increased significantly among hospitalized patients [4]. Regardless of the high mortality, invasive fungal infections remain understudied and underdiagnosed compared to other infectious diseases. Most fungal infections lack rapid, sensitive and timely diagnostics. Additionally, the long-term prophylactic use of antifungal drugs in high-risk patients has stimulated multidrug resistance in fungi. With growing concern, World Health Organization recently released a fungal priority pathogen list wherein *Aspergillus fumigatus* belonging to the critical propriety group and Mucorales from the high priority group will be mainly discussed in this thesis [5].

The need for high-throughput techniques capable of capturing diverse aspects of the disease, such as defining and monitoring changes in metabolites and proteins, has unlocked the door for mass spectrometry (MS)-based techniques in clinical diagnostics. MS with electrospray ionization (ESI) and matrix-assisted laser desorption/ionization (MALDI) was introduced in the late 1980s to detect large protein molecules. Moreover, coupling liquid chromatography (LC) with ESI-MS added another dimension for analysing the crude biological mixture in less time, expanding the analytical dynamic range. MS technologies are constantly evolving by designing new ion sources, boosting resolution and sensitivity, and miniaturization to bench-top instruments. Though MS-based tools are still underused in some clinical settings, they can potentially extend the current capabilities of detecting disease markers or therapeutic drug levels with exceptional precision, accuracy, and reproducibility. In this thesis, I will show the capability of MS-based detection of infectious disease biomarkers with their subsequent application in diagnostics.

## 2 THEORETICAL PART

### 2.1 *Aspergillus fumigatus*

*A. fumigatus* is a ubiquitous saprotrophic mould with the ability to survive up to 70 °C through a vegetative mycelial lifecycle occurring in the soil, air or decaying organic material. *A. fumigatus* produces asexual conidia on specialized hyphal structures called conidiophores to survive in adverse conditions or for reproduction. These conidia are usually small (2 to 5µm) in size, metabolically less active and are the primary source of distribution of *Aspergilli* in the environment. A healthy human inhales 100-1000 conidia daily, which travel through the respiratory tract to the alveoli and begin the infection route [6]. In immunocompetent individuals, macrophages quickly clear inhaled conidia. However, if not eliminated by the immune system and with the help of a favourable environment such as water and nutrients, it starts germination leading to invasive hyphal growth, which can penetrate pulmonary tissue.

#### 2.1.1 The growth phases of *A. fumigatus*

The germination of *A. fumigatus* conidia involves a specific morphological transition critical for colonising *A. fumigatus* in the suitable host (**Fig. 2.1**).

##### A. Dormant phase

Dormant conidia are stress-tolerant with characteristic cell wall structure, allowing them to remain viable for up to one year in the environment. The cell wall of the resting conidium comprises three layers. The innermost layer is composed of  $\alpha$ -glucans, and above it is the dihydroxy naphthalene (DHN) melanin necessary for the structure and the stiffness of the cell wall. The outermost is the rodlet layer composed of hydrophobin RodA proteins, associated with survival and sensitivity to external stresses like desiccation and physical damage [7].

##### B. Isotropic phase

It starts with breaking the dormancy of resting conidium upon exposure to a carbon source and uptake of water resulting in an increased intracellular osmotic pressure. The outer conidial cell wall sheds, and aspartic proteases degrade the rodlet layer. Conidia grow

isotropically for up to six hours (h), where the diameter of the cell doubles. Isotropically expanding of the conidia are associated with metabolic activities such as protein synthesis and carbohydrate metabolism [8].

#### C. Polarised phase

After 6 h of conidial germination, swollen conidia form a germ tube to one side of the cell to grow in a polarised manner, which further elongates to become hyphae. After the emergence of the germ tube, the melanin layer is disrupted, and the polysaccharides on the surface of the cell wall are also modified to others, such as chitin and  $\beta$ -1,3-glucan (BDG) [9].

#### D. Mycelial formation

Hyphae continue to elongate and branch by 12 h, eventually forming a mycelial mat. These mature hyphae can form branches at the hyphal tip or from basal regions over one another, forming a monolayer at the bottom surface. The mycelial growth has characteristics of a classic microbial biofilm defined by extracellular matrix production, cell wall changes, surface adhesion and increased antifungal drug resistance [10].

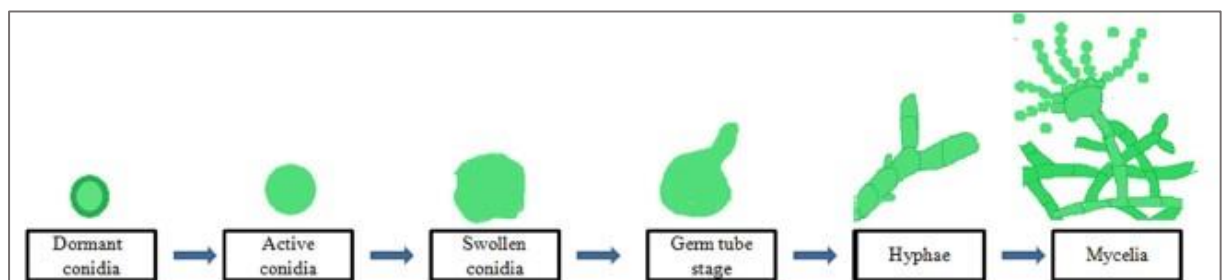


**Figure 2.1** *Aspergillus* transition with different morphotypes during germination. It is adapted from reference [1].

### 2.1.2 *Aspergillus fumigatus*-related infections

Among the widespread genus *Aspergilli*, including over 185 species, aspergillosis is primarily caused by *A. fumigatus* and less frequently by *A. flavus*, *A. terreus*, and *A. niger*. The broad spectrum of disease caused by *Aspergillus* depends on the status of the host immune system. Each form of pulmonary aspergillosis is mentioned below, with particular emphasis on invasive pulmonary aspergillosis (IPA), which is involved in this work.



### **2.1.2.1 Chronic pulmonary aspergillosis**

Chronic pulmonary aspergillosis (CPA) principally affects patients with a previous or underlying pulmonary condition such as tuberculosis, chronic obstructive pulmonary disease (COPD), sarcoidosis or bronchiectasis [11]. Chronic cavitary pulmonary aspergillosis (CCPA) is the most common form of CPA, which in the absence of treatment, may progress to chronic fibrosing pulmonary aspergillosis. *Aspergillus* nodules and simple aspergilloma are less common forms of CPA. CCPA is characterized by cavity formation and progression without overt tissue invasion, whereas aspergilloma are fungal ball consisting of *Aspergillus* hyphae, fibrin and cellular debris that arise in pulmonary cavities as a late manifestation of CPA. *Aspergillus* nodules are less commonly present as solitary or multiple lesions (<3cm) and are most commonly diagnosed after an excision biopsy. Patients usually show symptoms including chronic cough, shortness of breath, sputum production and chest pains [12]. The diagnosis is based on representative symptoms and radiologic features present in patients with *Aspergillus* IgG antibodies detection.

### **2.1.2.2 Allergic bronchopulmonary aspergillosis**

Allergic bronchopulmonary aspergillosis (ABPA) represents a hypersensitivity reaction to colonized *Aspergillus* conidia in the airways. It is predominantly found in patients with asthma and cystic fibrosis (CF), with few reported cases in patients with COPD, a history of tuberculosis, or lung transplantation [13, 14]. ABPA, with significant morbidity, approximately 4.8 million affected individuals worldwide, has a global prevalence of 2.5% among asthmatic and 7.8% in CF patients [15]. Symptoms include chronic cough, wheezing, fever, chest pain, hemoptysis, night sweats and weight loss, often overlapping with the predisposing lung condition. Diagnostic criteria include elevated immunoglobulin E (IgE) (>1000 IU/mL) against *A. fumigatus*, high IgG and eosinophil count [16]. Nevertheless, the main clinical challenge in ABPA is poor diagnosis as it shares similar clinical features with both asthma and CF.

### **2.1.2.3 Invasive pulmonary aspergillosis**

IPA is considered a life-threatening type of *Aspergillus*-related pulmonary infection. Over 1 million people globally are affected by IPA, with a mortality rate of 30% to 95% [17]. It mainly targets immunocompromised hosts and is characterized by lung tissue invasion by *Aspergillus* hyphae. The classical risk factors include neutropenia, hematologic malignancy following chemotherapy, hematopoietic stem cell transplantation,

glucocorticoid and immunosuppressive therapy [18]. Other emerging risk factors cover critically ill patients in intensive care unit settings, solid organ transplantation, COPD and superinfection with influenza or COVID-19 [19, 20]. The lungs are usually the common site of primary infection, with the symptoms such as cough, sputum production, dyspnoea, pleuritic chest pain and haemoptysis following angioinvasion. IPA is one of the most common sources of haemoptysis in neutropenic patients, which might be related to cavitation that occurs with neutropenia recovery [21].

#### **2.1.2.3.1 Diagnosis of pulmonary aspergillosis**

The histopathological examination of lung tissue obtained by thoracoscopic or open-lung biopsy, computed tomography scanning, and microscopic examination can detect the presence of septate, acute and branching hyphae invading lung tissue. The histopathology, even though considered the gold standard method for IPA diagnosis, has been shown to differ according to the underlying host. Chest radiography is of less use in the early stages of IPA because of the high incidence of nonspecific signs than classic radiographic signs (such as the halo or air crescent sign) [22]. The recent advances in IPA diagnosis involve *Aspergillus* antigens, galactomannan (GM) and BDG detection in body fluids, such as serum or bronchoalveolar lavage fluid (BALF). These methods' reported sensitivity and specificity largely depend on the host characteristics. Serum GM has substantial false positivity rates caused by early antigen clearance from the blood due to circulating neutrophils [23]. As a result, BALF GM detection with sensitivity (81–86%) and specificity (88–91%) reported in many studies is preferred for critically ill non-neutropenic patients suspected of IPA [24, 25]. Still, the limitation of GM detection in BALF includes false positivity by *Aspergillus* colonization without clinical and radiographic evidence of infection and other non-*Aspergillus* invasive fungal infections [26]. Detection of serum BDG, a fungal cell wall component also found to have similar sensitivity and specificity to serum GM [27]. However, the combination of both tests showed improved specificity and positive predictive value to the individual test.

Polymerase chain reaction (PCR) is another technique in IPA diagnosis involving the detection of *Aspergillus* DNA in BALF and serum. The sensitivity and specificity of PCR analysis in BALF samples were obtained in the range of 67–100% and 55–95%, respectively [28], while for serum samples, sensitivity and specificity were 100% and 65–92%, respectively [29, 30]. Together with the restriction of specialized laboratories with skilled workers, PCR is often associated with false-positive results where distinguishing

colonization from infection is impossible. Hence, combining at least two different methods, especially GM and PCR, is recommended to diagnose IPA. Studies have demonstrated that *A. fumigatus* PCR in BAL combined with GM can increase sensitivity and specificity up to 83% and 95%, respectively [31]. The lateral flow device (LFD) test involving the detection of glycoprotein secreted by *Aspergillus* spp. in BALF and serum is also used. The individual LFD test showed an overall pooled sensitivity of 73-90% and specificity of 86-93% in BALF for patients with IPA [32, 33], whereas when checked together with PCR had more promising sensitivity [34]. LFD testing requires further multicenter studies to receive routine clinical practice recommendations.

Despite advances in diagnostic methods, IPA remains challenging to diagnose as the performance and clinical utility of these tests vary not only by the stage of the fungal disease but also by patient groups. Although the combination of diagnostic methods seems to improve sensitivity and specificity, demand for new diagnostic tools is still growing to improve the accuracy and timeliness of IPA diagnosis.

#### **2.1.2.3.2 Treatment of pulmonary aspergillosis**

Three classes of antifungal agents, such as polyenes, azoles, and echinocandins, are mainly used to treat IPA. Amphotericin B, an ergosterol-binding polyene, causes the disintegration of the fungal membrane [35]. Broad-spectrum triazoles inhibiting ergosterol synthesis in the membrane of fungi include voriconazole, isavuconazole, and posaconazole. Posaconazole is commonly used as salvage therapy for IPA refractory to standard antifungal therapy [36]. Voriconazole, currently considered the treatment of choice in many patients with IPA, is more effective than itraconazole or amphotericin B in animal models of IPA [37]. Isavuconazole, another triazole with similar efficacy to voriconazole, is an alternative option in cases where voriconazole cannot be tolerated [38]. Echinocandins, such as caspofungin, micafungin, and anidulafungin, are antifungal agents that block the synthesis of BDG of fungal cell walls. While echinocandins have limited activity against *Aspergillus*, they may be used as adjunctive therapy in combination with other antifungal agents [39]. The choice of antifungal therapy depends on various factors, such as infection severity, underlying health status, drug interactions, and potential side effects. Despite the introduction of several antifungal agents, treatment of IPA remains challenging, and mortality rates are still high. Moreover, no available vaccine and the worldwide emergence of antifungal drug resistance to *A. fumigatus* seriously threatens the human population [40].

## 2.2 Secondary metabolites of *A. fumigatus*

Depending on growth conditions and for survival in hostile environments, *A. fumigatus* can produce a large number of secondary metabolites. Production of these metabolites benefits fungi during combat with host immune cells and increases competitiveness over other microbes, whereas some allow the fungus to acquire essential cofactors. One of the ways that *A. fumigatus* can thrive in the human body is through the production of secondary metabolites called siderophores. Even so, the production of these metabolites at specific stages of *A. fumigatus* growth and during its interaction with other microbes/cells is not well known. As a result, secondary metabolites, mainly siderophores and mycotoxins production, together with their potential role in diagnosis, are the main topic in this work.

### 2.2.1 Fungal siderophores – structures, functions, and applications

Iron, the most abundant element on the Earth, is a vital cofactor for various cellular processes, including DNA replication and electron transfer reactions. Nevertheless, excessive iron can be harmful due to its toxicity and ability to form cell-damaging reactive oxygen species (ROS); therefore, its bioavailability in humans is tightly regulated. In particular, most of the iron in circulation is tightly bound to proteins such as ferritin, transferrin, and lactoferrin. *A. fumigatus* uses siderophore-mediated iron uptake and reductive iron assimilation mechanisms to ensure the supply of iron. However, it was found that *A. fumigatus* virulence is primarily dependent siderophores-based mechanism than reductive iron-assimilation during infection in a mouse model for pulmonary aspergillosis [41].

Siderophores are small molecular weight,  $\text{Fe}^{3+}$  ion-specific chelators produced, secreted and reabsorbed during iron starvation. Most fungal siderophores are hydroxamate-type, structurally grouped into four categories, fusarinines, coprogens, ferrichromes, and rhodotorulic acid. The only exceptions are carboxylate rhizoferrin (RHF) (mentioned in this thesis) secreted by Mucorales [42] and the catecholate pistillarin secreted by the *Penicillium bilaii* [43]. *A. fumigatus* produces two types of siderophores (**Fig. 2.2 A**): fusarinine-type for iron uptake, including fusarinine C (FsC) and its derivative triacetylfusarinine C (TafC) as well as ferrichrome-type ferricrocin (Fc) and hydroxyferricrocin (Hfc) (**Fig. 2.2 B**) for iron storage and distribution in hyphae and conidia [44] respectively.

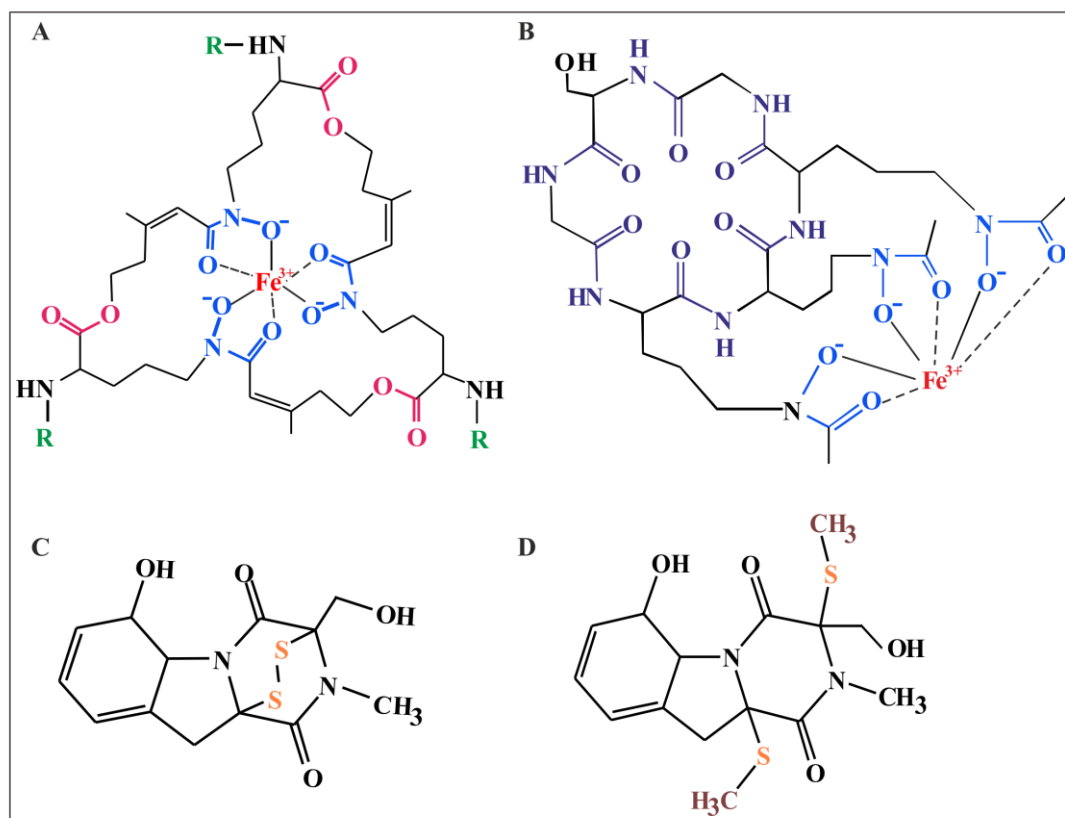


**Figure 2.2** Structure of *A. fumigatus* siderophores and mycotoxins. **A)** Extracellular fusarinine C (R=H) and its N<sup>2</sup>-acetyl derivative triacetylfusarinine C (TafC) (R=acetyl). **B)** Intracellular ferricrocin (Fc) with cyclic hexapeptide Gly-Ser-Gly-(N5-acetyl-N5-hydroxy-L-ornithine) in violet and HfC, hydroxylated Fc with unknown hydroxylation location. **C)** Gliotoxin **D)** Bismethyl gliotoxin. Iron chelating hydroxamate groups in blue, ester bonds in pink, sulphur in orange and methyl group in brown.

Biosynthesis of siderophores in *A. fumigatus* involves several enzyme-catalyzed reactions as well as regulation of gene expression (**Fig. 2.3**). Ornithine-N5-monooxygenase SidA catalyzes the first step, after which biosynthesis pathways split for intra and extracellular siderophores with the binding of different acyl groups. The non-ribosomal peptide synthetase (NRPS) SidC is essential for the biosynthesis of Fc and Hfc, whereas the acetyltransferase SidG and the NRPS SidD are involved in the biosynthesis of TafC and FsC, respectively [44].

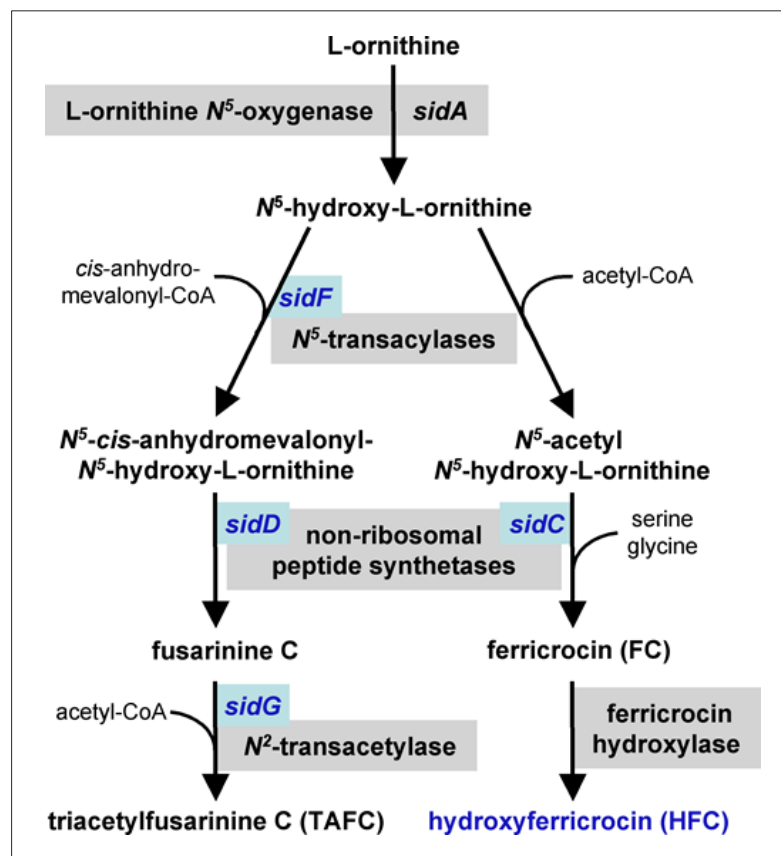


**Figure 2.3** Postulated siderophore biosynthetic pathway of *A. fumigatus*. FsC and Fc are assembled by the non-ribosomal peptide synthetases SidD and SidC, respectively. TafC is derived from FsC catalyzed by SidG. Adapted from [41, 44].

Extracellular siderophores bound with ferric ions cross the fungal membrane via siderophore-iron transporters such as MirB and Sit1 which are involved in transporting secreted TafC and Fc, respectively [45, 46]. Subsequent to uptake inside the cytosol, iron-complexed TafC and FsC are hydrolyzed by the esterase EstB and SidJ, respectively [47]. The iron is then supplied to the metabolism or transferred to Fc for hyphal iron storage. As the production of siderophores is controlled by iron availability in the environment, two transcription factors, SreA and HapX, are involved in iron regulation in *A. fumigatus*. Under high iron conditions, SreA represses the expression of genes involved in siderophore biosynthesis to avoid iron toxicity. Conversely, HapX is activated under iron depletion, causing the upregulation of genes involved in iron uptake and storage.

### 2.2.2 Mycotoxins-structure, biosynthesis and their roles in infections

*A. fumigatus* secretes several mycotoxins, including, among others, fumiquinazolines, fumitremorgin, gliotoxin (Gtx) and fumagillin in response to environmental stimuli [48]. These mycotoxins exhibit antifungal (pseurotin) [49], (fumitremorgin B) [50] or anti-inflammatory (fumigaclavine C) [51] activity, while some provide competitive survival advantages. Moreover, mycotoxins such as fumagillin, melanins, tryptacidin and Gtx are involved during interaction with the host immune system. The production of these metabolites is often influenced by environmental factors, such as nutrients and temperature, and could be modulated by genetic and epigenetic factors as well.

Gtx, with a molecular mass of 326 Da, is one of the most abundant epipolythiodioxopiperazine mycotoxins produced by *A. fumigatus* (**Fig. 2.2 C**). It is characterized by the internal disulphide bridge, which can undergo repeated cleavage and reformation, thereby regulating its biological activity, including immunosuppression and redox activity [52]. The functional genomics studies revealed a *gli* cluster containing 13 genes responsible for Gtx biosynthesis and its related metabolites' production (**Fig. 2.4**) [53]. The pathway begins with forming the intermediate cyclo-phenylalanyl-serine catalyzed by the NRPS, GliP. *gliG* gene, which encodes for a glutathione S-transferase form bis-glutathionylated intermediate responsible for the sulfurization of Gtx. The resulting product is then modified by a series of enzymes in a coordinated manner, including GliK (glutamyltransferase), GliJ (a dipeptidase), GliI (aminotransferase), two cytochromes p450 monooxygenases (GliC and GliF) and finally by GliN (N-methyltransferase) to form a Gtx backbone. Furthermore, gliotoxin is generated by a disulfide bridge cyclization catalyzed by oxidoreductase GliT while GliA exports it outside the cell. GtmA functions as bis-thiomethyltransferase to form bisdethiobis(methylthio)-gliotoxin (BmGtx). Moreover, gliotoxin biosynthesis is controlled by a variety of environmental and cellular factors. The transcription factor GliZ has been shown to positively regulate the expression of *gli* gene clusters in response to oxidative stress, wherein the disruption of GliZ could abolish the production and gliotoxin [54]. The global regulators LaeA [55] and VeA [56] also positively modulate Gtx production.

Due to its ability to manipulate the immune system, Gtx has garnered significant attention in recent years. Gtx is known to cause apoptotic cell death in macrophages and monocytes. The toxin can suppress the activity of macrophages by inhibiting the production of ROS and nitric oxide [57]. Gtx is reported to block phagocytosis and activation of

nuclear transcription factor NF- $\kappa$ B, thereby stalling inflammatory response and cytokine production [58]. Moreover, Gtx could positively exacerbate aspergillosis by altering several neutrophil functions. The toxin is proven to hamper the oxidative burst of human neutrophils by inhibiting NADPH oxidase activity [59]. Gtx has been reported to modulate dendritic cell function by blocking antigen presentation and affecting subsequent T-cell responses [60]. Overall, the production of Gtx by *A. fumigatus* is an essential factor in its pathobiology and ability to cause disease in humans and other animals and could serve as a potential biomarker for diagnosing IPA.

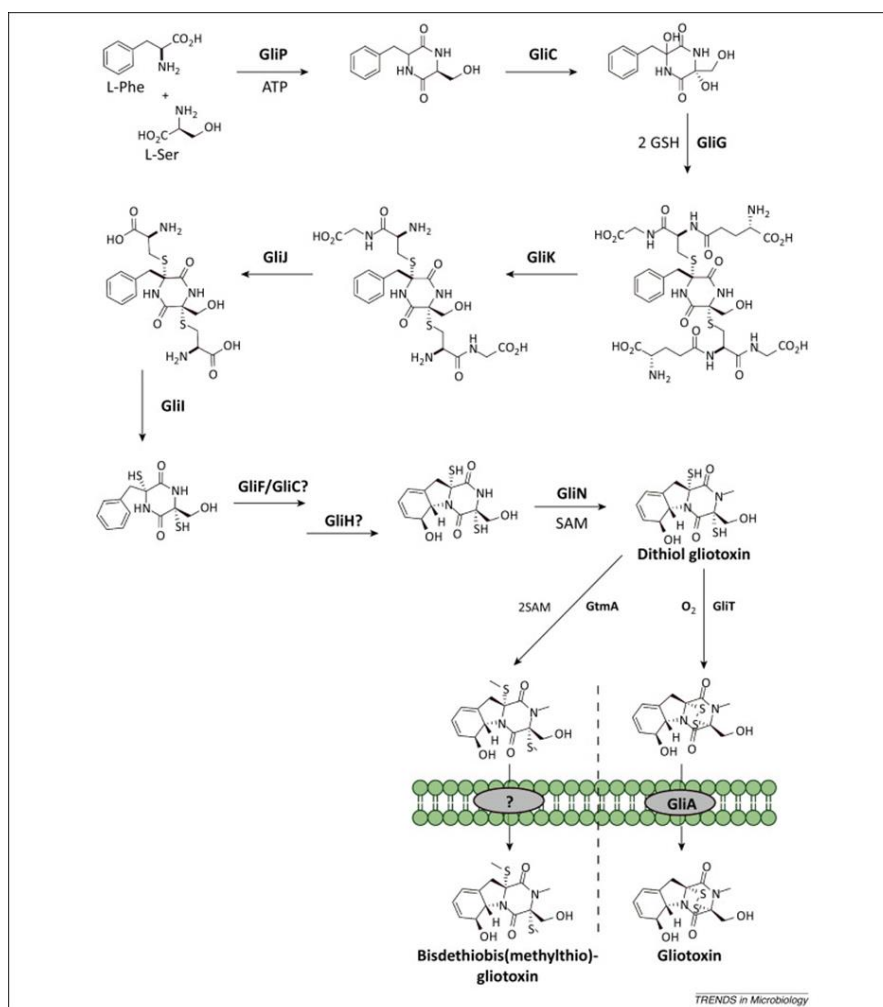


**Figure 2.4** The proposed biosynthetic pathway of Gtx and BmGtx. A series of enzyme-catalyzed steps are described to form dithiol gliotoxin, a co-substrate for either Gtx or BmGtx formation. GSH, glutathione S-transferase; SAM, S-adenosylmethionine; GtmA, S-methyltransferase, Gtx, gliotoxin; BmGtx, bismethylgliotoxin; adapted from reference [61].



BmGtx, a dimethyl derivative of Gtx (**Fig. 2.2 D**), is a negative regulator of Gtx biosynthesis, where increased Gtx levels induce *gtmA* expression, facilitating BmGtx formation. This results in the depletion of dithiol gliotoxin and consequently reduces GliT-mediated gliotoxin biosynthesis [62]. Therefore, BmGtx acts as a detoxifying agent against Gtx cytotoxicity, confirmed by its delayed production than Gtx *in vitro* and in alveolar epithelial and macrophage cell models [63]. BmGtx is also reported to be a more stable molecule than Gtx, indicating its potential use as a biomarker [64].

Overall, the production of secondary metabolites by *A. fumigatus* is a complex process regulated by various environmental and cellular factors. The selected secondary metabolites, particularly siderophores and mycotoxins, act as front-line virulence factors. As a result, the timing and profile of secretion of these metabolites during the course of *A. fumigatus* infection as well as during interaction with other cells is reported in this thesis.

### 2.3 *A. fumigatus* in interaction studies *in vitro*

*A. fumigatus* exists in diverse microbial communities, and studying its molecular interactions with other microorganisms and the host can provide insights into its pathogenic and survival strategies (**Fig. 2.5**).

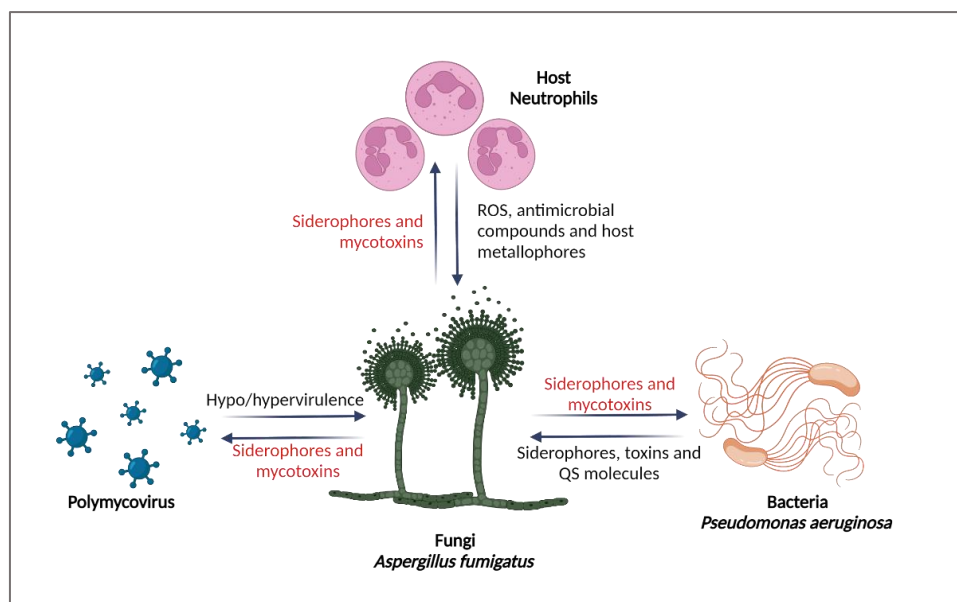


**Figure 2.5** *A. fumigatus* interplay with siderophores and mycotoxin production. Consecutively, host innate immune cells neutrophils secrete reactive oxygen species (ROS) and antimicrobial compounds, and bacterial pathogen *P. aeruginosa* secretes its own siderophores, toxins and quorum sensing (QS) molecules, and poly mycovirus affects fungal virulence.

### 2.3.1 *A. fumigatus*-innate immune cell mutual interplay

Following inhalation, *A. fumigatus* conidia are confronted with stage-specific innate immune responses (**Fig. 2.6**). In immunocompetent individuals, anatomical barriers, mainly lung epithelial cells, represent the first line of contact with inhaled conidia. Most inhaled conidia are cleared by mucociliary clearance; however, few can reach and interact with the alveolar epithelial cells [65]. Further, they encounter the first line of immune defence cells, alveolar macrophages, which also play an essential role in host iron homeostasis [66]. Alveolar macrophages express several soluble receptors such as pentraxin 3 (Ptx3), surfactant protein D, and surface pattern recognition receptors (PRRs) such as dectins and toll-like receptors (TLRs). PRR mediates conidial recognition via pathogen-associated molecular patterns. The detection of *A. fumigatus* cell wall components BDG, chitins and galactomannan by particular PRRs, leads to phagocytosis, conidial killing and the secretion of inflammatory chemokines and cytokines [67]. Mainly, dectin-1 allows macrophages to differentiate between the different morphological forms of *A. fumigatus* by recognizing BDG moieties on swollen and germinating conidia but not responding to resting conidia [68]. *In vitro*, studies have also shown macrophage-mediated, more efficient phagocytosis of swollen conidia than resting ones [69]. Dectin-2, a new C-type lectin receptor, was reported to be expressed at increased levels by human lung alveolar macrophages in response to *A. fumigatus* and also displayed an NF- $\kappa$ B-dependent proinflammatory response in a time-dependent manner against swollen, but not resting conidia [70].

Conidia that escaped macrophage attack can germinate and penetrate through the alveolar space. Secreted pro-inflammatory mediators thereby recruit neutrophils, considered to be the vital innate immune cells for host defence against *A. fumigatus*. Studies have reported that neutrophil-depleted mice infected with *A. fumigatus* conidia stimulated high mortality rates and hyphae-induced lesions in the lung. However, macrophage-depleted infected mice could still prevent conidial germination resulting in 100 % survival [71]. Like macrophages, neutrophils recognize *A. fumigatus* using various PRRs, including dectin-1 and TLRs [72]. Neutrophil utilizes both oxidative and non-oxidative mechanisms to kill *A. fumigatus* conidia and hyphae. Oxidative mechanisms involve NADPH oxidase-mediated ROS production [73]. The neutrophil granules contain antimicrobial compounds such as serine proteases, defensins, Ptx3 and lysozyme comprising non-oxidative mechanisms for direct pathogen killing [74]. Ptx3 secreted in response to conidia and

inflammatory signal TNF- $\alpha$  has been reported to improve phagocytic and fungicidal immune response activities *in vivo* [75]. Neutrophil extracellular traps (NETs), composed of bound DNA with histones and antimicrobial proteins, have been implicated as another form of neutrophil-mediated protective mechanism against *A. fumigatus*. However, the NET-based killing of *A. fumigatus* is not well clarified since a recent study excluded the role of NETs in killing *Aspergillus* hyphae [76]. Conversely, the same study identified that the extracellular killing of *A. fumigatus* hyphae depends on ROS production, whereas intracellular inhibition of conidial germination mainly involves lactoferrin-mediated iron sequestration. In turn, *A. fumigatus* fights back by secreting several metabolites. Melanins, namely pyomelanin and DHN melanin, being part of the outer surface of the conidial cell wall, can protect *A. fumigatus* against ROS [47]. Furthermore, apart from the immunosuppressive ability of Gtx mentioned above, other secreted toxins, such as fumagillin proved to hamper neutrophil function by inhibiting NADPH oxidase activity [48].

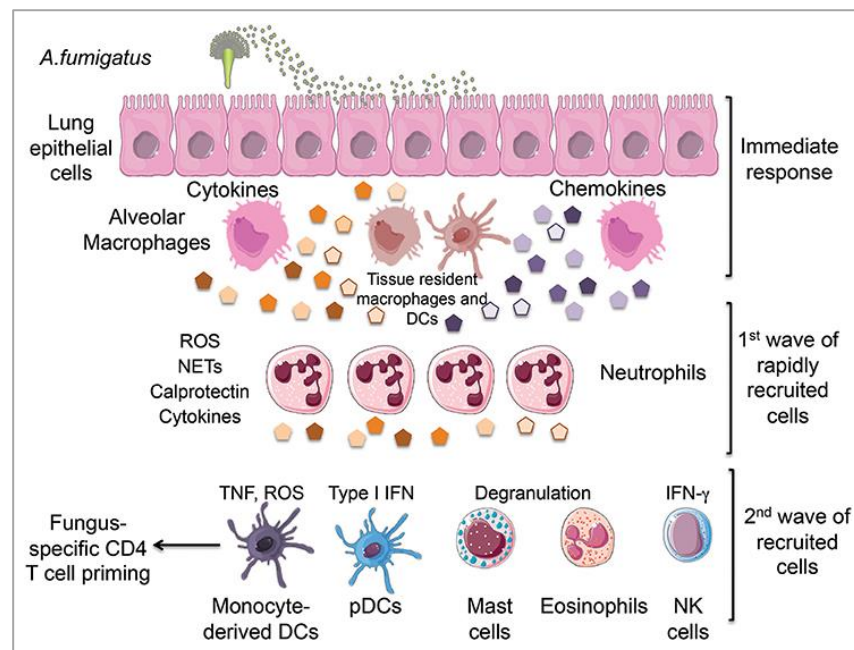


**Figure 2.6** Innate immune response upon inhalation of *A. fumigatus* conidia. Initial recognition occurs via lung epithelial cells and alveolar macrophages. This results in the production of chemokines promoting the rapid recruitment of neutrophils, followed by the subsequent arrival of second-wave cells such as monocytes, pDCs, mast cells, eosinophils and NK cells. All of these innate cells cooperate in eliminating fungal conidia by producing a combination of cytokines and antifungal compounds. ROS, reactive oxygen species; NETs, neutrophil extracellular traps; TNF, tumour necrosis factor; IFN, interferon; pDCs, plasmacytoid dendritic cells. Adapted from [2].

The whole host-pathogen interaction between *A. fumigatus* and immune cells engages in a nutrient war to carry out their necessary functions. As iron is one of the critical elements to *A. fumigatus* virulence, upon infection, the host strategically sequesters iron away from the invading pathogen via a phenomenon termed nutritional immunity. Neutrophils employ nutritional immunity mechanisms via lactoferrin and lipocalin-1-mediated iron and fungal siderophore sequestration [77]. As the host can reduce nutrient availability, *A. fumigatus* exploit siderophores to scavenge metal ions even from tightly bound carrier proteins. TafC is stated to be able to extract iron *in vitro* from serum iron-binding protein transferrin [78]. Therefore, the interaction between *Aspergillus* and immune cells is dynamic, where the fungus and the host both try to gain the upper hand in the infection (**Fig. 2.5**).

### **2.3.2 *A. fumigatus*-*Pseudomonas aeruginosa* are frenemies**

Microbial interactions in polymicrobial infections can affect their individual fitness and impact the immune system's response. *A. fumigatus* and *Pseudomonas aeruginosa* are common opportunistic fungal and bacterial pathogens, respectively, co-existing in immunocompromised and immunocompetent individuals. The combined presence of both pathogens in the airways of cystic fibrosis (CF) patients is reported to aggravate disease progression [79]. From several studies, the prevalence of *A. fumigatus* colonization in CF patients was reported to be 16-58% [79, 80], whereas; the reported prevalence of both pathogens together is 15.8% [81]. The potential of interspecies interactions could be vast and lead to both beneficial and antagonistic relationships.

#### **2.3.2.1 *P. aeruginosa* defence mechanism**

Virulence of *P. aeruginosa* contributes to significant morbidity and mortality in CF lung disease, shown to be influenced by other microorganisms co-inhabiting the CF airways [82, 83]. *P. aeruginosa* cells communicate through a quorum sensing (QS) system by synthesizing small signalling molecules that regulates biological activities such as virulence, motility, biofilm formation and interaction with the host [84]. *P. aeruginosa* inhibits *A. fumigatus* through the secretion of an array of virulence factors, including QS molecules such as homoserine lactones, quinolones, phenazines, and siderophores. QS molecules-based inhibition of *A. fumigatus* was demonstrated in *P. aeruginosa* QS knockout strains [85]. Specifically, homoserine lactones and quinolones restricted *A. fumigatus* hyphae formation and reduced fungal biofilm mass [86, 87]. Phenazines, as

endogenous redox-active molecules comprising pyocyanin, phenazine-1-carboxamide, 1-hydroxy phenazine (1-HP), and phenazine-1-carboxylic acid (PCA), can promote *P. aeruginosa* growth and survival under iron-limiting conditions in CF patients [88]. At high iron concentrations, phenazines inhibit *A. fumigatus* growth by producing reactive oxygen and nitrogen species, thereby damaging the mitochondrial ultrastructure of *A. fumigatus* hyphae. However, in an iron-limited environment, pyocyanin, phenazine-carboxamide and phenazine-carboxylic acid could promote the growth of *A. fumigatus* by reduction of ferric iron to ferrous iron. Dirhamnolipids another class of signal molecules hinder *A. fumigatus* growth by altering BDG synthase from the fungal cell wall [89].

In addition to inter-microbial signals, nutrient competition is a further mechanism exploited by *P. aeruginosa* during *A. fumigatus* interaction. During the battle for iron necessary for the metabolism of both pathogens in a shared microenvironment, *P. aeruginosa* secretes two siderophores, pyoverdines and pyochelin, for iron acquisition and storage. Less inhibitory activity against *A. fumigatus* growth in *P. aeruginosa* pyoverdine-lacking mutants indicated its importance in fungal inhibition [90]. Pyoverdine alone can inhibit *A. fumigatus* growth and biofilm formation by reducing iron availability and increasing *A. fumigatus* siderophore secretion. Denial of iron to *A. fumigatus* is also employed by *P. aeruginosa*-produced bacteriophage Pf4 to inhibit the *A. fumigatus* biofilm formation [91].

### **2.3.2.2 *A. fumigatus* molecular weapons for combat within consortia**

Despite a range of fungicidal properties of *P. aeruginosa*, *A. fumigatus* manages to survive within the shared ecosystem of the CF airways, indicating its ability to counteract the antagonistic actions of *P. aeruginosa*. The antifungal capacity of *P. aeruginosa* diminishes during *A. fumigatus* conidial transition into hyphae. Moreover, compared to preformed biofilm, the mature filamentous *A. fumigatus* biofilms were found to be more resistant to an inhibitory effect of *P. aeruginosa* [92]. *A. fumigatus* can produce various mycotoxins such as demethoxyfumitremorgin C, fumitremorgin, Gtx, and pyripyropene during biofilm formation in co-culture with *P. aeruginosa* [93]. It upregulates the secretion of Gtx explicitly, possessing antibacterial activity against *P. aeruginosa* in mixed biofilm formation [93, 94]. As a further line of defence to counteract iron denial by *P. aeruginosa*, *A. fumigatus* produces its siderophores. The role of *A. fumigatus* siderophores, mainly hydroxamate types, was confirmed using mutant strains lacking the *sidA* gene, which exhibited poor capacity in preserving *A. fumigatus* biofilms than wild-type strains during

exposure to phenazine and pyoverdine [95]. Furthermore, *A. fumigatus* also possess the ability to bio-transform phenazines into alternative forms, including conversion of PCA to 1-HP, thereby inducing siderophore production [96]. Nonetheless, at a molecular level, the extent and role of *A. fumigatus* siderophore production as an antagonistic mechanism when exposed to *P. aeruginosa* is still unexplored and will be reported in this thesis.

### **2.3.3 *A. fumigatus*-mycovirus intracellular interaction**

Mycoviruses, also known as fungal viruses, are widespread in fungal species. Most do not integrate into the host genome and are transmitted horizontally via hyphal fusion or vertically via conidiospores. They are classified into families based on their single or double-stranded RNA genomes [97]. Mycoviruses can have diverse effects on their fungal hosts, ranging from impact on growth, morphology, or altering pathogenicity, toxin production or drug resistance. In *Saccharomyces cerevisiae*, mycovirus encode glycoprotein toxin with the ability to kill other yeast without any cell contact [98]. Particular mycovirus infection was shown to modulate fungal toxins production, such as suppressing carcinogenic aflatoxins in *A. flavus* [99] or inducing a secondary metabolite and mycotoxin tenuazonic acid and ochratoxin A in plant pathogenic fungus *Magnaporthe oryzae* [100] and *A. ochraceus* [101] respectively.

Mycoviruses infecting *Aspergilli* have been extensively studied, where around 7-19% of *A. fumigatus* clinical isolates were found virus-infected [102]. *A. fumigatus* polymycovirus 1 (AfuPmV-1) [103], a member of the family Polymycoviridae, was initially uncovered in the *A. fumigatus* Af293 isolate [104]. Differential effects of AfuPmV-1 infection in *A. fumigatus* have been extensively studied under several conditions, such as high salt and antifungal drugs. The results indicated that AfuPmV-1 infection sensitized *A. fumigatus* towards nikkomycin Z, an antifungal affecting chitin synthesis [105] and high salt stress [106]. The authors reported less virulence in mice [107] and mild hypervirulence in the wax moth infection model in virus-infected fungus [108]. Moreover, a recent study showed that mycovirus infection weakened *A. fumigatus* via altered fungal stress responses during inter-microbial interaction with *P. aeruginosa* [103].

To date, no direct correlation between the presence of mycovirus and the quantitative or qualitative modulation of *A. fumigatus* siderophores and mycotoxins has been studied, which is reported in this thesis. Even though the clinical relevance of *A. fumigatus* virus infection is controversial, understanding mycovirus–fungal host interactions could further illustrate their potential in the control of fungal infections.

## 2.4 *Rhizopus* species and mucormycosis

After *Aspergillus*, Mucorales are the next common fungal pathogens in animals and humans. Mucorales are saprotrophic fungi comprising *Rhizopus* spp., *Mucor* spp., *Lichthiemia* spp., and some others that represent a permanent part of the human environment, as commonly found in soil, animal excrements and decaying material. Nevertheless, some species are widely used for the biotransformation of several medically and pharmaceutically necessary compounds, such as steroids and terpenoids and in the fermentation of food and a variety of cheese. The genus *Rhizopus* is differentiated by the formation of pigmented sporangiophores, 3-11 µm in diameter, arising alone or in whorls bearing sporangia from horizontally growing aerial hyphae called stolons (**Fig. 2.7**) [109]. Young sporangia are white, while mature sporangia are black, containing over 1000 spores. *Rhizopus* species have gained importance in both human health and industry as some species can act as plant pathogens causing spoilage of crops, while others are used in the fermentation of tempeh and ragi [110].

Mucormycosis is a life-threatening, angioinvasive disease caused by spore inhalation of fungi belonging to the order Mucorales. *R. oryzae* is the predominant agent identified, followed by *R. microsporus* and *R. homothallicus* associated with mucormycosis [111-113]. The major risk factors include uncontrolled diabetes mellitus in ketoacidosis, corticosteroid treatment, organ transplantation, neutropenia, trauma and burns, malignant hematologic disorders, and immunosuppressive therapies [114, 115]. The global incidence of mucormycosis is rising, but the rise is excessive in countries such as India and China amongst patients with uncontrolled diabetes mellitus. It is indicated that the expected prevalence of mucormycosis in India is almost 70 times higher than the global average [116]. Invasive mucormycosis has mortality ranging from 23-80% in adult patients and up to 72.7% in paediatric patients [5]. Early diagnosis of mucormycosis is still challenging. The current diagnostic strategies rely on clinical findings, risk factor analysis, histopathology, and culture of specimens. The primary concern about these methods is that clinical signs may vary with the form and stage of the infection. Moreover, low sensitivity and false negativity are reported in culture methods in 50% of mucormycosis cases [117]. Culture-independent molecular methods such as conventional PCRs, restriction fragment-length polymorphism and DNA sequencing of defined gene regions are developed; however, the efficiency of these assays is yet to be studied [118, 119]. Moreover, there is no circulating antigen detection test similar to GM or BDG detection we know for invasive

aspergillosis available for diagnosing mucormycosis. Surgical debridement and antifungal agents such as liposomal amphotericin B and posaconazole are used in the treatment; however, even with treatment, mortality rates can be as high as 80% [120]. As early diagnosis is the key factor for successful disease management, diagnostic methods with more specific and sensitive molecular markers and secondary metabolite identification still need development in mucormycosis.

## 2.5 Secondary metabolites of *R. microsporus*

Recently polyketide synthase, NRPS, and L-tryptophan dimethylallyl transferase encoding genes were identified in Mucoromycota [121]. The availability of host iron plays a critical role in predisposing patients to mucormycosis. Clinical observation demonstrated that the level of available free iron in serum is a crucial factor affecting diabetic ketoacidosis patients to mucormycosis [122], while in other observation, dialysis patients treated with the iron chelator deferoxamine were found to be susceptible to a deadly form of mucormycosis [123]. *Rhizopus* is known to secrete polycarboxylate siderophore RHF (**Fig. 2.7**) to supply iron through a receptor-mediated, energy-dependent process [124].

RHF production is reported in *R. delemar*, *Mucor circinelloides*, *Lichtheimia corymbifera*, *Syncephalastrum racemosum*, *Mucor heimalis*, *Rhizomucor pusillus* and *Cunninghamella echinulata*. Several RHF analogues have also been described by directed fermentation [125]. The RHF biosynthetic gene, a member of the NRPS-independent siderophore family, has recently been identified in *R. delemar* [126]. Moreover, RHF is inefficient in capturing iron from serum; however, *Rhizopus* can use xenosiderophores such as deferoxamine to obtain iron from the host [127]. To overcome the lack of knowledge on virulence factors and for further development of a new tool for non-invasive diagnosis, *R. microsporus* metabolome was studied using high-performance [128] LC-MS in this thesis.



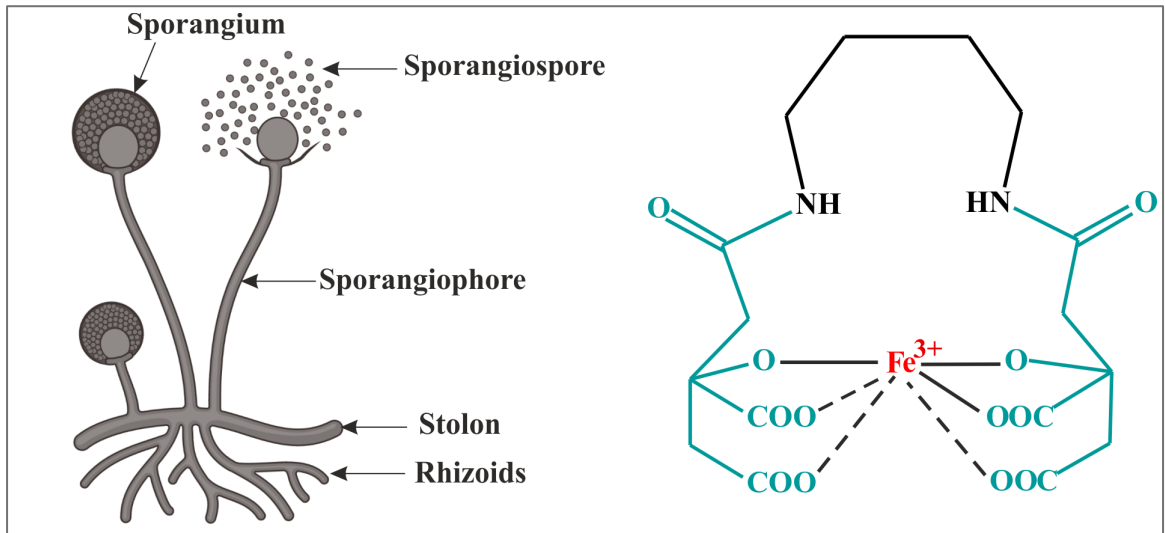


**Figure 2.7** Vegetative structure of *Rhizopus* characterised by the presence of stolons and branched rhizoids (left). Sporangiphores bear sporangium, which carries asexual spores. Rhizoferrin structure is composed of two molecules of citric acid (green) linked to 1,4-diaminobutane (black) through two amide bonds [129].

## 2 OBJECTIVES OF THE THESIS

The aim of this dissertation thesis is to comprehensively characterize *R. microsporus* and *A. fumigatus* siderophores and mycotoxins *in vitro* using LC-MS and demonstrate their utility in the diagnosis of invasive fungal infection in humans and animals.

The specific goals include:

- To design infection metallomics – a MS-based platform in a wide range of pathogen-related functional studies
- To analyze the siderophore production in *R. microsporus in vitro* using MS.
- To quantitatively assess *A. fumigatus* growth stage-specific siderophore and mycotoxin production to distinguish between colonization and invasive infection
- To explore *A. fumigatus* siderophores and mycotoxins production during interaction with immune cells (neutrophils), bacterial pathogen (*P. aeruginosa*) and AfuPmV-1.
- To demonstrate the application potential of infection metallomics to the invasive or noninvasive diagnoses of human IPA and equine aspergillosis.

## 4 EXPERIMENTAL PART

### 4.1 LC-MS-based characterization of *R. microsporus* siderophores

Materials presented in this section have been published in ref. [130].

#### ***R. microsporus* identification and growth conditions**

*R. microsporus* isolate obtained from the sputum of an immunocompromised patient was grown in iron-depleted mineral medium (residual content 235.5 µg of Fe/L) containing 55 mM glucose, 50 mM NH<sub>4</sub>Cl, 11.2 mM KH<sub>2</sub>PO<sub>4</sub>, 7 mM KCl, 2.1 mM MgSO<sub>4</sub>·7H<sub>2</sub>O, 68 µM CaCl<sub>2</sub>·2H<sub>2</sub>O, and 20 µM ZnSO<sub>4</sub>·7H<sub>2</sub>O (pH 6.5). The medium was inoculated with spore suspension (10<sup>7</sup> spores/mL) and incubated for 48h at 30°C with shaking (190 rpm). The supernatant from the culture was separated by centrifugation (5,000× g, 4 °C, 15 min) and subsequently lyophilized.

#### **Metabolite extraction**

The lyophilized sample was re-dissolved in water, extracted two times with ethyl acetate and dried under reduced pressure. The remaining aqueous phase was mixed with four equivalents of methanol (MeOH) and incubated at –80 °C for 1 h. Precipitated proteins were removed by centrifugation (14,000×g, 4°C, 10 min), and the supernatant layer was transferred to a vial with the residual evaporated ethyl acetate fraction and concentrated under reduced pressure using a SpeedVac (catalog number SPD121P; Thermo Scientific, Pardubice, Czechia).

#### **HPLC-MS analysis**

The pooled extract was re-suspended in 5% LC-MS-grade acetonitrile (ACN) and injected onto an Acquity HSS T3 C18 analytical column (1.8 µm, 1.0 × 150 mm, Waters, Milford, MA, USA). Analytes were gradient-eluted with a 50 µL/min flow rate (A: 1% ACN with 0.1% formic acid (FA) in water, B: 95% ACN with 0.1% aqueous FA): 0 min, 2%; 2 min, 2%; 9 min, 60%; 11.0 min, 99%; 14 min, 99%; 14.5 min, 2%; and 20 min, 2% of B. The metabolites were quantified using HPLC-MS on a Dionex UltiMate 3000 Ultra HPLC system (Thermo Fisher Scientific, Waltham, MA, USA) connected to a SolariX 12T Fourier transform ion cyclotron resonance (FTICR) MS (Bruker Daltonics, Billerica, MA, USA) in electrospray positive-ion mode. A quadrupole filter to 200–700 and 500–1500 Daltons adjusted with two continuous accumulations of selected ion windows.

## Data processing

All samples were measured in triplicates. Our in-house CycloBranch [40] version 2.0.8 and Bruker Data Analysis 5.0 software performed qualitative and quantitative data processing, respectively. RHF and bis-imido-RHF were quantified in fermentation broths by the standard addition method. The limit of detection (LOD) and limit of quantitation (LOQ) were defined as the sum of the background average with 3 and 10 multiples of standard deviation [131] [131], respectively.

## 4.2 LC-MS based *A. fumigatus* growth-specific siderophore and mycotoxin quantitation to distinguish between colonization and invasive infection

Materials presented in this section have been published in ref. [132].

### *A. fumigatus* identification and growth conditions

*A. fumigatus* strain EI278 was isolated from a clinical sample received from the University Hospital in Motol (Prague, Czechia) and identified by phylogenetic analysis of the internal transcribed spacer regions 1 and 2. *A. fumigatus* conidia were harvested in phosphate-buffered saline (PBS) containing 0.01% Tween 80 from a culture grown at 37°C on malt extract agar (17, 3, and 20 g/L of malt extract, mycological peptone, and agar, respectively, adjusted to pH 5.4 before sterilization). The suspension was filtered using a 5- $\mu$ m SyringeStrainer (Pluriselect, San Diego, CA, USA). *A. fumigatus* conidia ( $10^8$ /mL) were inoculated into iron-limited minimal medium (pH 7) consisting of Na<sub>2</sub>HPO<sub>4</sub>·12H<sub>2</sub>O (14.62 g/L), KH<sub>2</sub>PO<sub>4</sub> (3 g/L), NaCl (0.5 g/L), NH<sub>4</sub>Cl (1 g/L); source of carbon: glucose (5 g/L); trace elements: MgSO<sub>4</sub>·7H<sub>2</sub>O (0.2 g/L), CaCl<sub>2</sub>·2H<sub>2</sub>O (0.05 g/L), ZnSO<sub>4</sub>·7H<sub>2</sub>O (0.01 g/L), MnSO<sub>4</sub>·H<sub>2</sub>O (0.017 g/L), CoCl<sub>2</sub>·6H<sub>2</sub>O (0.0048 g/L), CuSO<sub>4</sub>·5H<sub>2</sub>O (0.003 g/L), Na<sub>2</sub>MoO<sub>4</sub> (0.0045 g/L). The experiment with four biological replicates was performed with 10-mL cultures shaken in 50-mL Erlenmeyer flasks on an orbital shaker (190 rpm) at 37°C for 72 h. To detect fungal metabolites, samples of conidia, the residual fungal mass, and the supernatant were collected from each biological replicate at incubation times of 0 h, 3 h, 5 h, 6 h, 7 h, 8 h, 9 h, 10 h, 12 h, 14 h, 18 h, 24 h, 48 h, and 72 h. Before further sample processing, the supernatants were filtered through a Whatman membrane (5  $\mu$ m; VWR International, Strábrná Skalice, Czechia) using a sterile syringe. The residual fungal mass

was washed three times with sterile water, centrifuged (14,000 x g for 2 min) at room temperature, and lyophilized.

### **Microscopy**

Samples of 60 to 100 conidia collected up to 10 h of incubation were fixed in 37% formaldehyde. Their germination was observed using a DN45 light microscope (Lambda Praha Ltd., Prague, Czechia), and images were captured with an Eos 700D digital single-lens reflex (SLR) camera (Canon, Inc., Tokyo, Japan). The recorded images were calibrated using the Fiji software suite [133] with a stage objective micromanipulator.

### **Extraction and quantitation of metabolites**

Siderophores (Fc, Hfc, FsC, TafC, and triacetylfusarinine B (TafB)) and mycotoxins (Gtx, fumigaclavine A, fumiquinazoline C, fumiquinazoline D, 3-hydroxy-fumiquinazoline A, and tryptoquivaline F/J) were extracted from *A. fumigatus* as mentioned in **section 4.1** with some modifications. Briefly, samples (50  $\mu$ L of conidia, the residual fungal mass suspension, or the supernatant) were spiked with a ferrioxamine E (FoxE) (50 ng/mL) internal standard and ferrated with FeCl<sub>3</sub> (100  $\mu$ M) and were subjected to two-step liquid-liquid extraction using ethyl acetate (150  $\mu$ L) and MeOH (200  $\mu$ L). Calibration standards of Fc, TafC, Gtx, fumigaclavine A, and fumiquinazoline D were prepared at final concentrations of 0.5, 1, 5, 10, 50, 100, 500, 750, and 1,000 ng/mL. The extracts were vacuum dried for 2 h at 35°C using a SpeedVac (catalog number SPD121P; Thermo Scientific, Pardubice, Czechia) and stored at -80°C until HPLC-MS analysis.

### **HPLC-MS analysis**

Before the HPLC-MS analysis in triplicates, all samples were re-constituted in 150  $\mu$ L of 15% ACN. Previously reported LC settings (**section 4.1**) were applied for the separation of analytes. Siderophores and mycotoxins were detected using a Solarix 12T (FT-ICR) MS (Bruker Daltonics, Billerica, MA, USA) with electrospray positive-ion mode. MS parameters were tuned and adjusted to optimize the signal intensity of the analytes of interest by applying a quadrupole filter to facilitate the continuous accumulation of the selected ions at 100 to 700 and 500 to 1,500  $m/z$  intervals for analyses of mycotoxins and siderophores, respectively.

## Data processing and method validation

All acquired LC-MS data were processed using DataAnalysis v.5.0 software (Bruker Daltonics, Germany). Fumiquinazoline C, 3-hydroxy-fumiquinazoline A, and tryptoquivaline F/J were annotated from mass spectra by matching the exact  $m/z$  values and product ion mass spectra. The detected analytes were quantified using external calibration standards. Assuming similar ionization efficiencies, Hfc was semiquantified using the Fc calibration curve, and fumiquinazoline C, 3-hydroxy-fumiquinazoline A, and tryptoquivaline F/J were semiquantified using the fumiquinazoline D calibration curve, while FsC and TafB were semiquantified using the TafC calibration curve. The results were averaged from triplicates. The sample preparation methods were validated using control growth medium samples, according to U.S. Food and Drug Administration guidelines for validating bioanalytical methods [134], in terms of the calibration curve (linearity), LOD, LOQ, intra- and interday accuracy and precision, selectivity, specificity, sensitivity, carryover, and autosampler stability. Instrumental LOD and LOQ values were defined as the lowest concentrations for which the SD [131] of the intercept equaled 3.3 and 10, respectively. The LOD, LOQ, linearity, and sensitivity were determined using a set of prepared nonzero calibration standards. A system suitability test using an HPLC peptide standard mixture (Sigma-Aldrich, Prague, Czechia) checked the instrument's performance.

## Statistical analysis

The variations in the measured siderophores and mycotoxins from four biological replicates of *A. fumigatus* cultures at each stage of germination and subsequent growth were characterized in terms of means, SDs, standard errors of the means, and coefficients of variation using MS Excel 2016 and graphically visualized using OriginPro version 22 software (OriginLab Corporation, Northampton, MA, USA). Data were presented as box plots displaying means  $\pm$  SD.

#### **4.2.1 *A. fumigatus* siderophores and mycotoxins production during interaction with neutrophils and *P. aeruginosa***

##### **Neutrophils isolation and *A. fumigatus* infection**

Neutrophils were isolated from anticoagulated blood using a neutrophil direct isolation kit employing (negative selection, StemCells; <https://www.stemcell.com/products/easysep-direct-human-neutrophil-isolation-kit.html>) based on manufacturer's instructions. Cells were counted using trypan blue and Turck solution (50 $\mu$ L of cell suspension + 950 $\mu$ L of diluted trypan blue or Turck solution) by light microscopy (Olympus) at the beginning of the experiment. At every time point, the viability of cells was visualized using trypan blue and determined by light microscopy (Olympus). For the infection experiment, neutrophils ( $1 \times 10^6$  cells/mL) were transferred to a complete growth medium (RPMI 1640, 10% fetal bovine serum) in 24-well plates and incubated with *A. fumigatus* strain EI278 hyphae at 37 °C for 48 h in 5% CO<sub>2</sub> atmosphere in triplicates. Entire plated neutrophils were transferred to a sterile tube and centrifuged for 300g for 10 min. Supernatants collected were immediately stored at -80°C until further processing. PBS was used to wash cell pellets, with successive centrifugation at 300g for 10 min.

##### ***A. fumigatus* and *P. aeruginosa* dual cultivation**

*A. fumigatus* (EI278) conidia ( $10^7$  conidia/mL) and *P. aeruginosa* (PAO1) cells ( $10^7$  cells/mL) were inoculated into iron-limited minimal medium (composition of the medium is similar to **section 4.2**). The experiment with three biological replicates was conducted as 100 mL culture into 500 mL Erlenmeyer flask shaken at 37°C on an orbital shaker (190 rpm). For metabolite analysis, supernatants were collected at 0 h, 6 h, 9 h, 12 h, 18 h, 24 h, 36 h, 48 h, and 72 h of incubation and immediately stored at -80 °C.

##### **Extraction of metabolites**

For siderophores (Fc, TafC and TafB), samples of supernatant were spiked with a FoxE (50 ng/mL) internal standard and ferrated with FeCl<sub>3</sub> (10 mM) and were subjected to previously reported liquid-liquid extraction protocol (**section 4.2**). For Gtx and its metabolites, several solvent and solid phase extractions (SPE) were tested to reduce dilution due to tremendous siderophore production and to improve mycotoxin detection sensitivity. Initially, liquid-liquid extraction using chloroform-MeOH and

dichloromethane-MeOH was checked. Next, SPE (HLB and Sep-Pak, Waters, Milford, MA, USA) using appropriate elution solvent composition (50%, 60% and 100% MeOH+0.1% FA and 50%, 60% and 100% ACN+0.1% FA) were examined. Based on the results, a protocol using SPE HLB 3cc (150 mg) cartridge was finalized. The samples of supernatant (50  $\mu$ L) were spiked with 2-heptyl-4(1H)-quinolone (10 ng/mL) as internal standard and were loaded on SPE cartridges preconditioned with 1mL MeOH +0.1% FA and equilibrated with 1mL 5% MeOH +0.1% FA. Polar impurities were removed with 1mL of 5%MeOH+0.1% FA, with the subsequent addition of 2mL of 60% MeOH +0.1% FA. The compounds of interest were eluted with 1mL of MeOH+0.1% FA. The extracts were then vacuum dried for 2 h at 35°C and stored at -80°C until HPLC-MS analysis.

### **HPLC-MS analysis**

All the extracted samples from interaction with neutrophils and *P. aeruginosa* were reconstituted in 150  $\mu$ L of 15% ACN. Siderophores (Fc, TafC, TafB) were analyzed by an Acquity M-class HPLC system connected to a Synapt G2-Si Q-TOF MS (Waters Corporation, Manchester, UK). Each sample was loaded onto an Acquity HSS T3 C18 analytical column (1.8  $\mu$ m, 1.0  $\times$  150 mm, Waters Corporation, Manchester, UK). Gradient elution was performed at a 50  $\mu$ L/min flow rate: 0 min, 5%; 2 min, 5%; 10 min, 50%; 14 min, 95%; 16.5 min, 95%; 17 min, 5%; and 20 min, 5% of B. Solvent A contained 0.1% FA in the water, and solvent B contained 0.1% FA in ACN. The spectrometer was operated in electrospray positive-ion mode within 200–1200  $m/z$ .

Reconstituted samples for mycotoxins (Gtx and BmGtx) analysis were injected into an Acquity HSS C18/1.8-mm, 2.1 by 5-mm VanGuard precolumn connected to an Acquity HSS T3/1.8-mm, 1.0 x 150-mm analytical column (both from Waters, Prague, Czechia). Previously reported LC gradient conditions (**section 4.1**) were applied and detection was performed using a Solarix 12T (FT-ICR) MS (Bruker Daltonics, Billerica, MA, USA) with electrospray positive-ion mode. MS parameters were tuned and adjusted to optimize the signal intensity of the analytes of interest by applying a quadrupole filter for the continuous accumulation of the selected ions at 200 to 600  $m/z$  intervals.

### **Data processing**

Data for siderophores and mycotoxins were processed by MassLynx 4.1 software (Waters Corporation, Manchester, UK) and Cyclobranch [135] version 2.1.32, respectively. The detected analytes were quantified using external calibration standards in



technical duplicates. Instrumental LOD and LOQ values were defined as the lowest concentrations for which the SDs of the intercept equalled 3.3 and 10, respectively.

### **Statistical analysis**

The obtained results were statistically analysed using GraphPad Prism 8.0.1 software (GraphPad, San Diego, CA, USA). A non-parametric Mann-Whitney test is used to compare between two groups for each time point where a *P* values of < 0.05 were considered statistically significant. The box plots are expressed as a mean  $\pm$  SD.

### **4.2.2 A. *fumigatus* siderophores and mycotoxins production during interaction with the polymycovirus AfuPmV-1**

Materials presented in this section have been published in ref. [136] for siderophore analysis.

#### **Isolates**

In a masked study, five *A. fumigatus* strains as mentioned below, were maintained on malt extract agar (1.7% malt extract, 0.3% mycological peptone, 3% Bacto agar, pH 5.4, for 10 days, at 37 °C.

Strain 18–42 (VF);	UK Af293 cured from AfuPmV-1
Strain 18–95 (VI);	UK Af293 with AfuPmV-1
Strain 10–53 (VI);	USA Af293 with AfuPmV-1
Strain 19–40 (VR);	18–42 re-infected with AfuPmV-1
Strain 19–47 (VR);	18–42 re-infected with AfuPmV-1

*A. fumigatus* UK AF293 strain (18–95) was cured using the protein synthesis inhibitor cycloheximide [104], producing a VF strain now designated 18–42. AfuPmV-1 was purified by differential polyethylene glycol precipitation and ultracentrifugation. Purified AfuPmV-1 was re-introduced in the VF *Aspergillus* by protoplast transfection, producing re-infected strains designated as 19–40 and 19–47. Strain 19-47 was misprinted, thereby corrected to 19-42 [137].

### **Fungal strains cultivation**

For the detection of siderophores, strains 18-42, 18-95, 10-53, 19-40 and 19-42 ( $10^8$  conidia/mL) were grown in an iron-limited mineral medium with a similar composition mentioned in **section 4.2**. The samples of mycelia and supernatants were collected at 48, 52, or 24, 31, 48, 54, and 72 h, respectively.

For detection of mycotoxins, strains 18-42, 18-95 B, 19-40 and 19-42 ( $10^8$  conidia/mL) were inoculated into a minimal medium (composition is similar to **section 4.2**) along with  $\text{FeCl}_3 \cdot 6 \text{H}_2\text{O}$  ( $10 \mu\text{M}$ ). The supernatant was collected at 18 h, 24 h, 36 h, 48 h, 72 h and 96 h of growth and immediately stored at  $-80^\circ\text{C}$ .

For gene expression analysis, conidia ( $10^7$  conidia/mL) were inoculated in media containing  $\text{Na}_2\text{HPO}_4 \cdot 12\text{H}_2\text{O}$  (14.62 g/L),  $\text{KH}_2\text{PO}_4$  (3 g/L),  $\text{NaCl}$  (0.5 g/L),  $\text{NH}_4\text{Cl}$  (1 g/L); source of carbon: glucose (5 g/L); trace elements:  $\text{MgSO}_4 \cdot 7\text{H}_2\text{O}$  (0.2 g/L),  $\text{CaCl}_2 \cdot 2\text{H}_2\text{O}$  (0.05 g/L),  $\text{FeCl}_3 \cdot 6 \text{H}_2\text{O}$  ( $10 \mu\text{M}$ ). The cultures were shaken for 48 h in flasks, at  $39^\circ\text{C}$ , on an orbital shaker (190 rpm). The experiment was carried out with three biological replicates, and mycelia were collected at 48 h. The mycelia were washed with sterile water and centrifuged twice at  $14,000 \times g$ , 2 min, at room temperature before RNA extraction.

### **Extraction of metabolites**

Previously mentioned liquid-liquid extraction (**section 4.2**) and SPE protocol (**section 4.2.1**) was applied for siderophores (Fc, TafC and TafB) and mycotoxins (Gtx and BmGtx) respectively.

### **HPLC-MS analysis**

Before the HPLC-MS analysis in triplicates, all samples were reconstituted in 150  $\mu\text{L}$  of 15% ACN. Previously reported LC-MS settings **section 4.1** and **section 4.2.1** were applied for quantification of siderophores and mycotoxins, respectively.

### **RNA extraction, complementary c-DNA synthesis and quantitative polymerase chain reaction (qPCR)**

Total RNA was extracted from each strain 18-42, 18-95 B, 19-40 and 19-42 grown in three biological replicates for 48 h using the RNeasy mini kit (Qiagen). Following treatment with DNase I (Promega) and quantification by Nanodrop spectrophotometry, equal amounts of RNA were utilised as a template for cDNA synthesis using the SuperScript VI Reverse Transcriptase (Invitrogen). The qPCR assays were performed in the OneStepPlus Real-Time qPCR System (Applied Biosystems) utilizing the Power

SYBR Green PCR Master Mix (Applied Biosystems) and the relative standard curve quantitation method. *A. fumigatus*  $\beta$ -tubulin sequence was used as an endogenous control. Target-specific primer pairs were designed using PrimerBlast and are listed in (**Tab. 4.1**).

Gene	Forward primer	Reverse primer
AfuPmV-1	ATAGGTCACGCCATAGCACG	CCCAGCACTGAGAAGAGGTG
$\beta$ -tubulin	AATTGGTGCCGC TTTCTGG	CTATTCCGTCCCGACAACCT
<i>gliG</i>	GCGACCCTCCGATCTTGTAG	TGACGGTGTGTGTGTGGA
<i>gliN</i>	ACTCCGAAAACGGCTACCTC	AGGACTCGCAGATTGGGTTG
<i>gliA</i>	TACCTGCCGACCTACTTCCA	TCCAGGTTCGAGGGTGTAGAG
<i>gliT</i>	CTTCGACTCTGGCGTCTACC	TCGAACAGCTGGTTGGTCTC
<i>gtmA</i>	TCCAGCGTACTCAACCACAC	GAAGACCGGTGTCTAACGCA

**Table 4.1** The list of forward and reverse primers used.

### Statistical analysis

Each sample was analysed in three technical replicates by MS, providing nine points for statistical analyses (3 x 3). The differences in the metabolite levels among *A. fumigatus* strains were presented as standard box plots with outliers plotted as individual points. The box plots were built using MS Excel 2016. Kruskal–Wallis One-Way ANOVA with Bonferroni (All-Pairwise) Multiple Comparison and Friedman’s Q Rank Test was used to compare the differences between the intra and extracellular metabolite levels in VF and VI *A. fumigatus* strains. Friedman’s Q Rank Test was explicitly used to test how the strain and growth-phase time affected siderophore levels. Statistical analysis was performed by NCSS 9 statistical software (NCSS, Kaysville, UT, USA).

For LC-MS-based mycotoxin analysis, each sample was analysed in two technical replicates. Data are presented as box plots displaying means  $\pm$  SD built using MS Excel 2016.

For gene expression analysis of mycotoxins, the results from three technical replicates were plotted as box plots displaying means  $\pm$  standard error of mean using MS Excel 2016.

### **4.3 Infection metallomics-based diagnosis**

#### **4.3.1 Diagnosis of human invasive pulmonary aspergillosis**

Materials presented in this section have been published in ref. [132].

##### **Extraction of metabolites**

According to a previously reported protocol, siderophores and mycotoxins were extracted from human urine and serum samples [138]. Briefly, urine and serum samples from patients and healthy individuals were centrifuged at 6,000 rpm for 30 s. All centrifuged samples (50  $\mu$ L) were spiked with the FoxE (100 ng/mL) internal standard. Urine and serum samples from healthy individuals were used to prepare calibration standards of Fc, TafC, and Gtx at final concentrations of 0.1, 0.5, 1, 5, 10, 50, 100, 500, 1,000, and 5,000 ng/mL. The samples were loaded onto Sep-Pak C18 1-mL Vac SPE cartridges (Waters, Prague, Czechia) preconditioned with MeOH+0.1% FA and equilibrated with H<sub>2</sub>O-0.1% FA. Impurities were removed with 200  $\mu$ L of 2%MeOH+0.1% FA, and the compounds of interest were eluted with 400  $\mu$ L of MeOH+0.1% FA.

##### **HPLC-MS analysis**

Before the HPLC-MS analysis in triplicates, all samples were reconstituted in 150  $\mu$ L 5% ACN. Siderophores and mycotoxins were separated using a Dionex UltiMate 3000 HPLC system (Thermo Scientific, MA, USA). Reconstituted urine and serum samples were injected into an Acquity HSS C18/1.8-mm, 2.1 by 5-mm VanGuard precolumn connected to an Acquity HSS T3/1.8-mm, 1.0 by 150-mm analytical column (both from Waters, Prague, Czechia). Analytes were eluted at a 50- $\mu$ L/min flow rate using the following gradient of buffers A and B: 1% B at 1 min followed by linear increases to 60% B at 20 min and 99% B at 23 min and then a 3-min hold at 99% B, with a 2-min linear fall to 1% B and a 12-min hold before the next injection. Here, buffer A was 5% ACN with 0.1% aqueous FA, and buffer B was 95% ACN with 0.1% aqueous FA. Previously reported MS settings (**section 4.2**) were applied to quantify analytes.

##### **Data processing**

All acquired data were processed similarly to mentioned parameters in **section 4.2**. The urine concentrations of siderophores (Fc, TafC, and TafB) and Gtx were further normalized to the urine creatinine concentration to obtain creatinine index values [139] using the following formula: siderophore or secondary metabolite concentration (ng/mL)/creatinine concentration (mg/dL x 100).

## **Statistical analysis**

The clinical samples were statistically analyzed using GraphPad Prism 8.0.1 software (GraphPad, San Diego, CA, USA). The reported descriptive statistics include means, medians, interquartile ranges, SDs, standard errors of the means, and coefficients of variation. The Gaussian distribution of the data was tested using the D'Agostino-Pearson normality test, and as the normality test did not meet the requirements for parametric tests, nonparametric tests were used. The urine and serum samples were considered positive if at least one of the urine creatinine-indexed fungal metabolite or serum concentrations (TafC, TafB, Fc, or Gtx) were higher than an LC-MS method-defined LOD for a particular marker.

### **4.3.2 Diagnosis of equine aspergillosis**

Materials presented in this section have been published in ref. [140].

#### **Metabolite extraction**

Metabolites were extracted from serum and BALF samples using our previously reported two-step liquid-liquid extraction protocol (**section 4.2**). The samples were spiked with FoxE and Leucine-enkephalin internal standards to final concentrations of 50 and 25 ng/mL, respectively. The control horse group serum and BALF samples were used to prepare matrix-matched calibration curves for Fc, TafC, and Gtx based on solutions with final concentrations of 1, 5, 10, 50, 100, and 250 ng/mL.

To extract metabolites from tissue samples, whole lungs were lyophilized and homogenized with a mortar and pestle. A 25 mg sample of the resulting homogenized powder was then dissolved in (400  $\mu$ L) 15% LC-MS grade ACN followed by extraction as **section 4.1** and quantification by the standard addition method.

#### **HPLC-MS analysis**

Pooled samples of serum and BALF or lung homogenates were re-suspended in 150 or 200  $\mu$ L of 15% ACN, respectively and analysed in triplicates using similar LC-MS settings as in **sections 4.1** and **4.2**.

#### **Data processing**

Qualitative and quantitative data analysis was conducted using the in-house CycloBranch version 2.0.19 software [135] and Data Analysis 5.0 (Bruker Daltonik, Bremen, Germany).

## 5 RESULTS AND DISCUSSION

The goal of the first section of this thesis is to introduce infection metallomics a mass spectrometry platform we designed based on the central concept that microbial metallophores are specific, sensitive, non-invasive, and promising biomarkers of invasive infectious diseases. The second section of this thesis includes fungal pathogen *R. microsporus* *in vitro* cultivation, followed by LC-MS analysis of its siderophores. The third section involves *in vitro* cultivation of fungal pathogen *A. fumigatus* with subsequent growth stage-specific siderophore and mycotoxin quantification to distinguish between colonization and invasive infection. In addition, the time course quantification of *A. fumigatus* secondary metabolites during its interaction with neutrophils, bacterial pathogen *P. aeruginosa* and polymycovirus was performed. The fourth and last part is then focused on the application of infection metallomics-based diagnosis in human IPA and equine aspergillosis.

### 5.1 Introduction to infection metallomics

The results of this section have been published in the following article:  
R.H. Patil, D. Luptakova V. Havlicek, Infection metallomics for critical care in the post-COVID era. *Mass Spectrom Rev* (2023) [141].

In response to WHO alerts, we recognized an urgent need to improve diagnostics of the most clinically significant pathogens, and established infection metallomics, a MS-based platform utilizing microbial and mammalian metallophores in functional and diagnostic applications. Both host cells and pathogens rely on metals such as iron, zinc, nickel, manganese or copper to carry out their essential functions. Thus, infection metallomics exclusively focuses on the analysis of metal-containing infection biomarkers called metallophores using a combination of elemental and molecular MS. In this work, we summarized ESKAPEc nosocomial bacterial pathogens standing for *Enterococcus faecium*, *Staphylococcus aureus*, *Klebsiella pneumoniae*, *Acinetobacter baumannii*, *P. aeruginosa*, *Enterobacter* spp., *Escherichia coli* and mycobacteria as well as fungal pathogens such as *Candida* spp. and *A. fumigatus* metallophores, followed by the non-invasive application of metallophores from a historical perspective (**Fig. 5.1**).

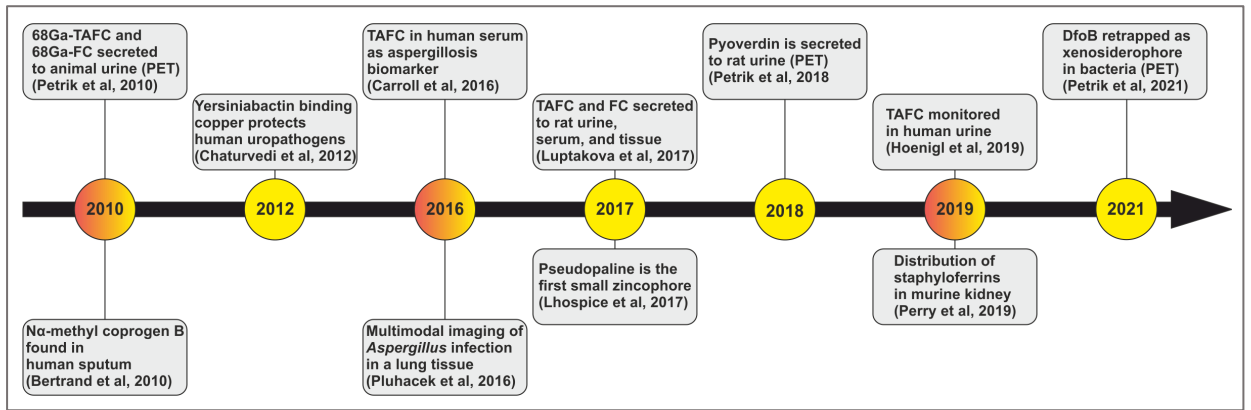


**Figure 5.1** A historical perspective on non-invasive applications of metallophores. Unmarked entries are associated with MS detection. DfoB, desferrioxamine B; FC, ferricrocin; Ga, gallium; PET, positron emission tomography; TAFC, triacetylfulsarinine C

We then described a strategy of infection metallomics for detecting the onset of pathogenic infection in critically ill patients (**Fig. 5.2**). Either non-invasive such as breath condensate or urine, or invasive sampling (serum, BAL, endotracheal aspirate, sputum, or biopsy analysis) from critically ill patients can be used for detection of virulence factors secreted by infecting microbe. Rapid analysis with pathogen identification is crucial to initiate smart combination anti-microbial treatment during the window of opportunity, which exists when the pathogen consortium is transitioning from colonization to causing infection to the host.

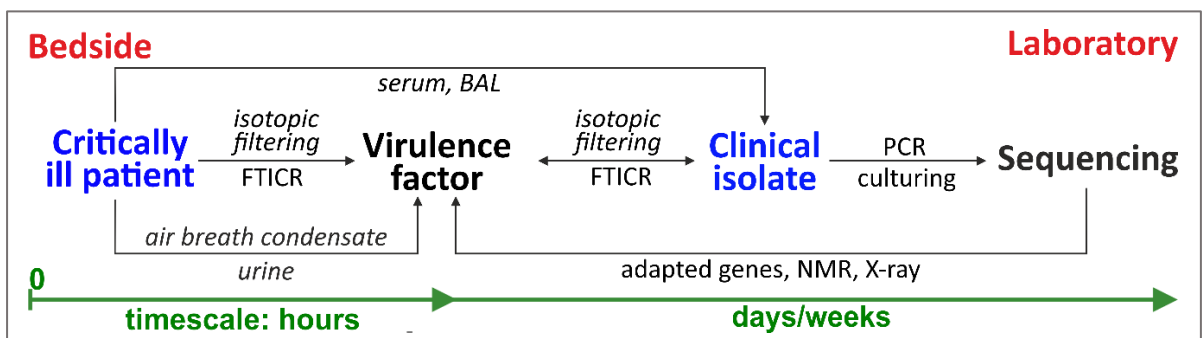


**Figure 5.2** The concept of infection metallomics from bedside to laboratory. BAL, bronchoalveolar lavage; FTICR, Fourier-transform ion cyclotron resonance; NMR, nuclear magnetic resonance; PCR, polymerase chain reaction.

At the bedside, the rapid analysis of non-invasively collected samples is achieved using MS, where isotopic data filtering can specifically detect metal-containing infection biomarkers at the pathogen-host interface within the time scale of hours. Alternatively, culturing clinical specimens, such as urine, serum, sputum, or aspirates, together with molecular tools, including PCR and gene sequencing, can be used for the characterization of less common pathogens. Further *de novo* approaches allow the isolation of new virulence factors from fermentation broths by preparative chromatography, followed by absolute structure determination using X-ray diffraction and nuclear magnetic resonance techniques.

We defined sample flow and key MS instruments (**Fig. 5.3**) used to directly monitor microbial Fe-, Co-, Zn-, Mn-, or Cu-containing virulence factors, detected at concentrations of ng/L to  $\mu\text{g/mL}$  in humans or animal models. The suitable extraction protocols depend on the structure of these analytes [142].

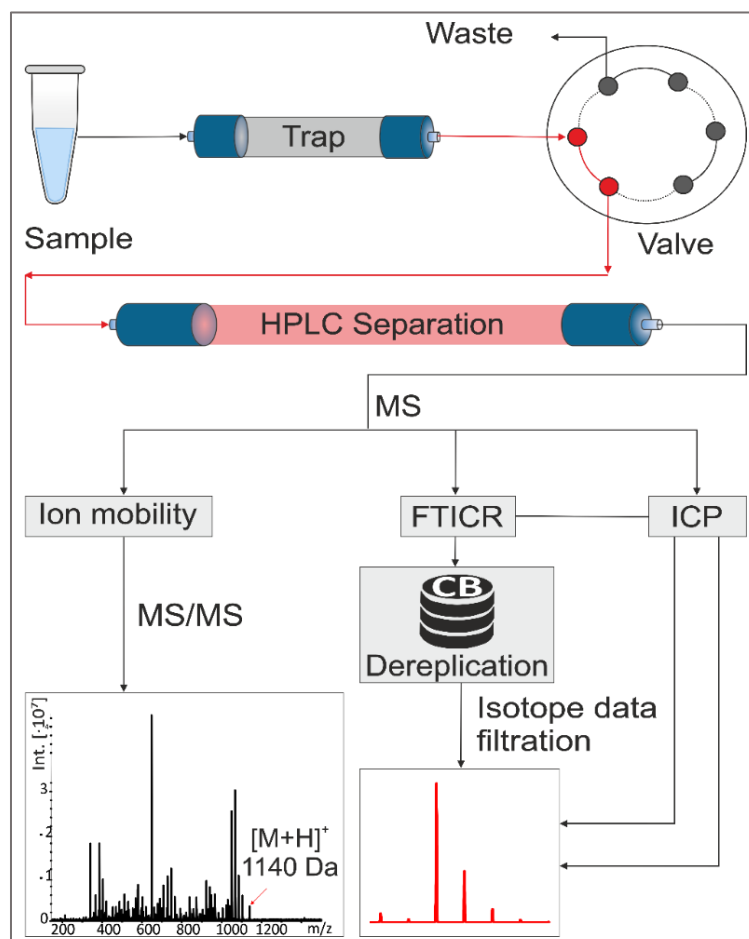


**Figure 5.3** Sample flow and key MS instruments for infection metallomics with isotope data filtering. CB, CycloBranch software; FTICR, Fourier-transform ion cyclotron resonance; HPLC, high-performance liquid chromatography; ICP, inductively coupled plasma; MS, mass spectrometry



The analytical process initiates with LC followed by applying one of three MS techniques. An ESI or ion mobility spectrometry with a quadrupole/time-of-flight (TOF) instrument can provide excellent MS/MS data on metal-containing compounds that might otherwise be difficult to dissociate. An even more powerful approach is to apply high-resolution FTICR-MS which enables unambiguous identification of metallophores in bodily fluid and tissue samples. Finally, inductively coupled plasma (ICP) MS is routinely used for metal quantitation, for instance, analysis of urine samples to detect uropathogenic strains.

Metallophores can be analysed via targeted using a microbial siderophore database [143] and *de novo* approaches [144]. Moreover, CycloBranch is an explicitly designed software for infection metallomics where one can quickly identify all compounds exhibiting predefined isotopic features in a chromatographic or imzML data set [145]. Application of this tool involves both elemental (ICP MS) and molecular ESI or MALDI MS datasets (**Fig. 5.4**) with a bonus of *de novo* sequencing features [146].

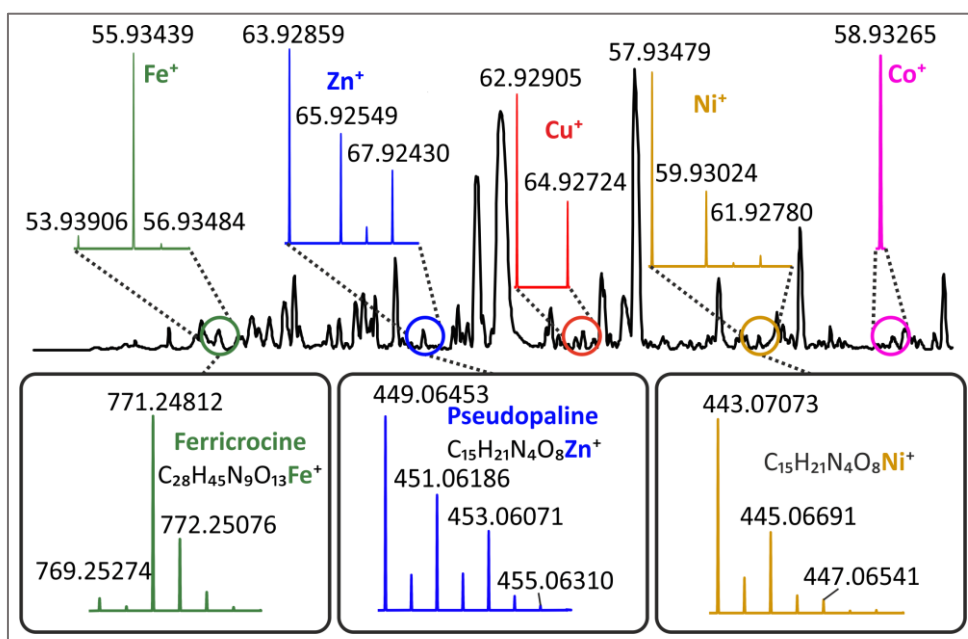


**Figure 5.4** In silico modelling of siderophores ferri-ferricrocin and zinc-pseudopaline isotopic profiles. Note that the mass defects of specific nuclides (in this case, 68/66Zn 1.99881, 66/64Zn 1.9969, and 56/54Fe 1.99533) are used to identify metal-containing species in both elemental and molecular mass spectrometry datasets.

Further, MS-based analysis of lung, urinary tract and central nervous system (CNS) infections is elaborated. In lung infections, the airways represent a common entry point for fungal spores (**Fig. 5.5**). Inoculation of rat model with *Aspergillus* conidia was found to

induce secretion of TafC and Fc siderophores into the urine, serum, and lung tissue where the site of infection was investigated by positron emission tomography (PET) [147]. Another study demonstrated the use of MS imaging to visualize the distribution of microbial siderophores in infected rat lungs to detect the site of infection [148]. The fungal burden in rat lung tissue was determined by combining ICP-MS and scanning electron microscopy. This revealed a noticeable increase in the iron concentration in infected areas, attributing to both severe haemorrhage and secretion of fungal siderophores. The experiments with inoculation of variable conidial loads were conducted in immunocompromised rats to understand the difference in siderophore biomarker levels in neutropenic and non-neutropenic hosts. With higher inoculation with  $10^8$  *Aspergillus* conidia, the first *A. fumigatus* siderophore biomarkers (TafC and Fc) were detected in host urine as early as 4h postinfection [149]. However, with a lower inoculation dose of  $10^4$  conidia to mimic the situation in immunocompetent hosts, a detectable MS signal was first observed 30 h after inoculation. Animal model studies have revealed that infectious fungal species exhibit high biological diversity, and MS methods can be used to monitor the distribution and metabolism of fungal siderophores *in vivo*. Moreover, *A. fumigatus* siderophore TafC has soon reported in human serum [150] and urine samples [139]. In mixed infection rat models and critically ill patients, mixed bacterial and fungal secondary metabolites were detected in the urine, indicating a distant lung infection. Similarly, analysis of breath condensate revealed an early infection by *P. aeruginosa* [151].

The application of infection metallomics in uropathogen characterization is another well-developed field of clinical MS. *E. coli* is the most frequent pathogen, followed by *Klebsiella*, *Enterobacter*, *Proteus* spp., and *Citrobacter* isolated from urine in hospital settings [152]. *E. coli* is known to secrete siderophores, enterobactin and aerobactin, as well as the secondary metabolites dihydroxy-benzoylserine, its dimer and trimer, and dihydroxybenzoic acid (Hider & Kong, 2010). Enterobactin production has also been reported in urinary isolates of *Klebsiella*, *Enterobacter*, and *Citrobacter*. Siderocalin, a soluble protein with high ferric ion affinity, can starve *E. coli* for iron during urinary tract infections. Another uropathogen *Staphylococcus aureus* producing metallophores, staphylopin with binding affinity to Co, Ni, Zn, and Cu [153] and staphyloferrins A, B [154], which were found to be heterogeneously distributed within infectious foci [155]. Several uropathogenic strains, such as *Yernia* spp. *Enterobacter* spp. and *Klebsiella* spp. secrete the common biomarker yersiniabactin which binds iron, copper, and some other metals. The fungal pathogens *Candida* spp. and *Aspergillus* spp. are often associated with

nosocomial infections in critically ill patients, including the CNS. Due to the blood-brain barrier, diagnosing and treating CNS infections in neonates, children, and adults is particularly challenging. The meningitis-causing microbe *Neisseria* spp. use heterologous siderophores secreted by other bacteria like *E. coli* [156]. Additionally, it was revealed that *L. monocytogenes* utilizes iron-bound transferrin as its sole source of iron and also uses epinephrine and 3,4-dihydroxyphenylalanine as well as xenosiderophores produced by other bacterial and fungal pathogens such as pyoverdine and ferrioxamine B [157]. Infection metallomics using MS imaging could play a key role in describing pathogen routing pathways and mechanisms in CNS infections by visualizing the metallophores secreted by invading pathogens overlaid with the molecular signals of host defense molecules.

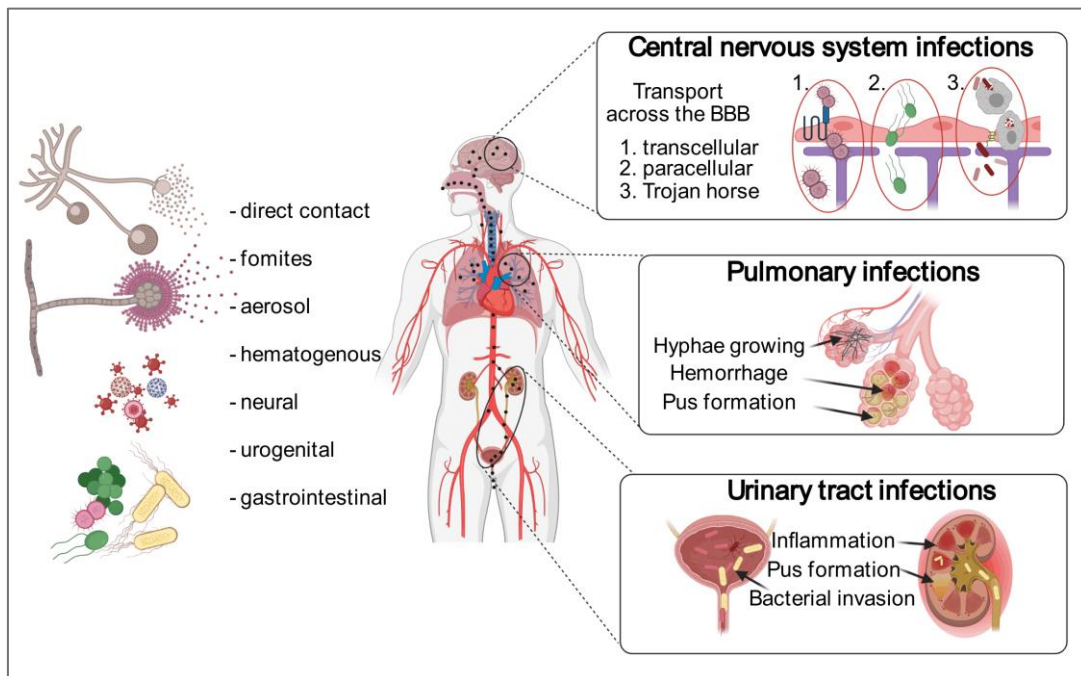


**Figure 5.5** Entry of pathogens into a critically ill patient. Around 70% of all intensive care unit cases are related to bacterial infections predominated with Gram-negative bacteria, whereas viral, fungal, and mixed infections account for around 20% of cases [158, 159].

Lastly, we compared the performance of infection metallomics-based diagnosis to routinely used clinical approaches, mainly culturing, microscopy and PCR in IPA (**Fig. 5.6**). Infection metallomics either outperformed or matched all existing diagnostic methods to four critical parameters such as sensitivity, specificity, invasivity and timeliness. Maximizing analytical dynamic range is the key technical challenge to

overcome while developing any diagnostic tool. Infection metallomics combined with isotopic data filtration can achieve a wide dynamic range by utilising microbes' tremendous capacity to secrete biomarker molecules into a host. For instance, *P. aeruginosa* is known to secrete  $10^{11}$  pyoverdine molecules per cell per time point [160]. This vast production of virulence factors could be why the metabolomic approach outperformed other omics strategies in terms of sensitivity except for PCR.

Method	Sensitivity	Specificity	Invasivity	Timeliness
sCulturing	Yellow	Green	Red	Red
sGM/sPCR	Yellow	Green	Red	Green
bGM/bPCR	Green	Green	Red	Green
bMicroscopy	Yellow	Yellow	Red	Green
<i>Infection metallomics</i>	Green	Green	Green	Green

**Figure 5.6** Performance of infection metallomics and four other techniques for diagnosing *Aspergillus* infections concerning four key criteria. sGM denotes galactomannan serology. bGM denotes galactomannan in bronchoalveolar lavage fluid. Performance is indicated using the following colour code: **excellent**, **fair**, and **poor**. Data presented from [151, 161] and [139]. b, bronchoalveolar lavage; PCR, polymerase chain reaction; s, serum.

Alike every other new technique, infection metallomics also has some limitations. Although the clinical analysis of metallophores is attractive due to its non-invasivity, original site of certain infections, such as pulmonary and CNS infections, cannot be determined using non-invasive sampling. However, by combining infection metallomics with PET imaging also being non-invasive, it becomes possible to observe the specific accumulation of radioactive  $^{68}\text{Ga}$ -siderophores in animals infected by bacteria or fungi. On the other hand, invasive sampling involving BALF and cerebrospinal fluid can reflect infection sites in pulmonary and CNS infections. Currently, no tools can describe the interplay between viral, bacterial, and fungal infections. However, at minimum, infection metallomics can assess and quantify the interplay between bacterial and fungal pathogen interaction in a host and monitor the microbiome's dynamic response to antibiotic, antiviral, and antimycotic therapies. Combined analysis of metallophores and their dynamics can determine how the infected pathogens are infiltrating into and proliferating within specific tissues and shed light on coinfections where eliminating one pathogen may lead to

increased activity by another. This study shows that infection metallomics can potentially improve outcomes in intensive care medicine by allowing safe sampling of highly infective patients with fungal, bacterial, and mycobacterial infections with minimal risk of disease transmission and reducing the financial and technical burden in hospital settings. Infection metallomics may thus advance medical MS, like the introduction of the MALDI Biotyper in 2009.

## 5.2 LC-MS based characterization of *R. microsporus* siderophores

The results of this section have been published in the following article:

A. Škríba, R.H. Patil, P. Hubáček, R. Dobiáš, A. Palyzová, H. Marešová, T. Pluháček V. Havlíček, Rhizoferrin glycosylation in *Rhizopus microsporus*. *J Fungi* 6(2020)89 [130].

Metabolomic studies of *R. microsporus* are scarce; as a result, the metabolome of a *R. microsporus* patient isolate was reported in this study. The urinal and *in vitro* metabolic profiles of the same patient with proven *R. microsporus* invasive infection were compared. Additionally, a new chromatographic method for the separation of carboxylate siderophore was developed. Initially, for chromatographic method development for RHF, a standard Waters Acquity HSS T3 (1.0 × 150 mm, 1.8 μm) column was used. The stationary phase revealed significant adsorption of desferri- RHF. Therefore, the ferri form of RHF was utilised for better separation of molecules. Positive and negative ion modes were tested for the detection of RHF and its analogues. Further, the desolvation temperature and ion transfer optic parameters were optimized to decrease the in-source fragmentation. Using developed chromatography and MS method, *R. microsporus* cultivation under iron-limited conditions and D-glucose as a carbon source provided RHF (345.3 ± 13.5 mg/g) and imido-RHF (1.2 ± 0.03 mg/g) as two dominant products in continuous accumulation of selected ions (CASI) 200-700 mass window (**Fig. 5.7**). The RHF trace was visible with a deteriorated peak shape of the protonated molecules at  $m/z$  437.140 while imido-RHF trace was detected for protonated molecules at  $m/z$  419.130 (**Fig. 5.7 E, D**). Further, we found that storage of samples, even in a lyophilized state for up to five months at room temperature, caused extensive RHF decomposition to the imido- and bis-imido-RHF forms (**Fig. 5.7 B**). The citryl-RHF intermediate with an elution time of 2.36 min was characterized by the accurate mass of the protonated molecule at  $m/z$  263.124 (263.124

calculated for  $C_{10}H_{18}N_2O_6$ ). For the first time in this study, we report the production of glycosylated RHF analogues in directed cultivation (**Fig. 5.7 G–I**).

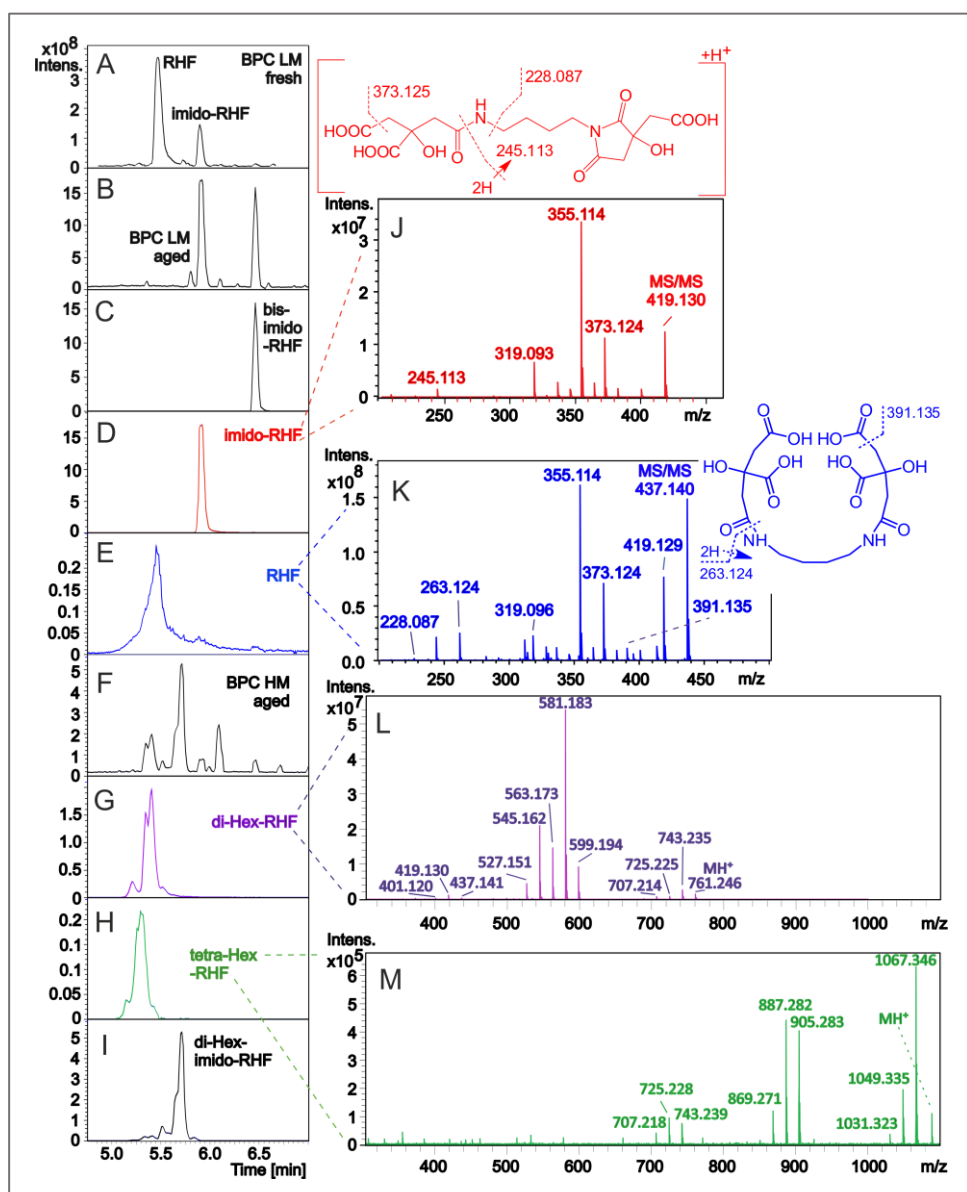


**Figure 5.7** Chromatographic separation and tandem mass spectrometry of *R. microsporus* secondary metabolites. BPC: base peak chromatogram, Hex: hexose. (**A**, **B**), BPC in the 200–700 Daltons mass range of fresh or aged (5 months) lyophilizates; (**C–E**), extracted ion chromatograms corresponding to bis-imido-RHF, imido-RHF, and RHF, respectively (0.005 Dalton window), (**F–I**) BPC and selected ion chromatograms of di-Hex-RHF, tetra-Hex-RHF, and di-Heximido-RHF, respectively. (**J–M**) refer to the product ion mass spectra (10 eV collisional energy) of imido-RHF, RHF, di-Hex-RHF, and tetra-Hex-RHF, respectively. The structure on the top indicates the intrinsic fragmentation in the RHF.

Compared to parent molecules (RHF and imido-RHF), both di- and tetra-Hex- RHF had a mutually different and slightly lower affinity to the stationary phase. The positive-ion ESI mass spectra provided clusters of protonated and cationized species. Ion signals of the putative mono- and tri-Hex-RHFs co-eluted with the corresponding di- and tetra-analogues. Although the formation of mono- and tri-Hex-RHFs cannot be excluded, we concluded that the corresponding ionic species represent fragments rather than biosynthetic intermediates. Alternatively, di-Hex-imido-RHF was well separated (**Fig. 5.7I**). The tandem MS of the di- and tetra-Hex analogues revealed the consecutive losses of Hex units from the protonated molecules (**Fig. 5.7 L, M**) and the intrinsic fragmentations in the RHF (**Fig. 5.7 J, K**). The fragmentation pattern indicated in **Fig. 5.7** correlated with the ion compositions derived from exact mass measurements. Moreover, CycloBranch software directly annotated other metabolites summarized in this study.

Glycosylation of RHF provided more polar and possibly more enzymatically stable products. We speculated that RHF glycosylation could benefit the producer; e.g., *R. microsporus* converted zearalenone to its more soluble 4- $\beta$ -D-glucopyranoside [162]. Our results suggested that RHF is an analytically complex molecule for direct detection in patients with invasive mucormycosis, and its metabolic fate in the host body remains uncertain. Aged lyophilized samples exhibited considerable RHF and imido-RHF instabilities (**Fig. 5.7 B**). This instability in human serum or urine is expected to be even more compromised owing to enzymatic processes in those matrices. Hence, bis-imido-RHF or its metabolic products should be among the few *R. microsporus* biomarkers remaining in bodily fluids for targeted metabolomics. Our experiments for detecting RHF analogues directly in patient urine or serum samples were also inconclusive. The reason was the antifungal treatment which most likely stopped siderophore production before sampling. However, analysis of patient urine suffering from pulmonary mucormycosis revealed the detection of the antifungal drug posaconazole along with all its major metabolites, including hydroxyderivatives or glucuronides, in a single LC-MS run. Nevertheless, RHF is the dominant product of *R. microsporus* cultivation under iron-restricted conditions. Although RHF and its analogues could serve as potential candidates for zygomycete diagnostics, future studies are required to determine the biotransformations of RHF in the host and to reveal its chemical stability and protein binding precisely.

### 5.3 LC-MS-based *A. fumigatus* growth-specific siderophore and mycotoxin quantitation to distinguish between colonization and invasive infection

The results of this section have been published in the following article:

D. Luptakova, R.H. Patil, R. Dobias, D.A. Stevens, T. Pluhacek, A. Palyzova, M. Kanova, M. Navratil, Z. Vrba, P. Hubacek V. Havlicek, Siderophore-Based Noninvasive Differentiation of *Aspergillus fumigatus* Colonization and Invasion in Pulmonary Aspergillosis. *Microbiol Spectr.* 11(2023) [132].

Distinguishing invasive disease from benign colonization is a crucial biological challenge in clinical settings. Overdiagnosis and unnecessary treatment can occur if colonization is mistaken for infection. The importance of this study lies in demonstrating that siderophore analysis can distinguish between asymptomatic colonization and invasive pulmonary aspergillosis. We reported clear associations between fungal development phases, from conidial germination to the proliferative stage of invasive aspergillosis, and changes in secondary metabolite secretion.

In order to analyze siderophore production during growth of *A. fumigatus* we first observed key stages of conidial germination using bright field microscopy. The conidia from the clinical isolate of *A. fumigatus* were incubated at 37°C in an iron-limited medium with glucose as a carbon source for 72 h. During the first 3 h of incubation, no morphological changes were observed in conidia, indicating conidial dormancy. Isotropic growth was observed between 3 and 6 h post-inoculation, wherein at 6 h, most conidia began swelling and doubled in size. Polarized growth began 6 h after inoculation. By 8 h, the majority of conidia had germ tubes growing from one side of the cell (**Fig. 5.8**). All these processes are asynchronous. As a result, the growth curves have broader distribution. The results summarized in **Fig. 5.8 B** and **Fig. 5.9** revealed evident germination phase-dependent variations in the abundances of *A. fumigatus* siderophores involved in iron homeostasis, quantified by HPLC-MS-based infection metallomics. Intracellular Hfc was mainly detected in dormant conidia. Further, its reappearance in residual fungal mass after 48 h indicated the formation of asexual conidiophores at the air-glass interface, which cannot be eliminated in shaken cultures.



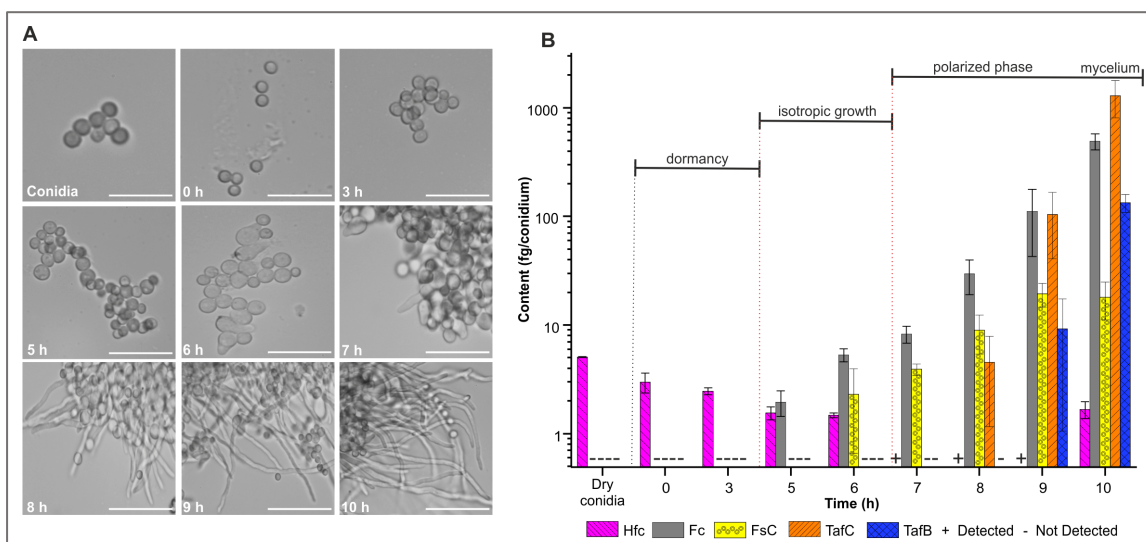


**Figure 5.8** A) Transition of *A. fumigatus* conidia during germination, observed by bright-field microscopy. Bar represents 10  $\mu\text{m}$ . Top row- dormancy, middle row- isotropic growth and bottom row- polarised growth. B) Levels of intra and extracellular siderophores during *A. fumigatus* conidial germination. Data are presented as means  $\pm$  standard deviations. Hfc, hydroxyferricrocin; Fc, ferricrocin; FsC, fusarinine C; TafC, triacetylfusarinine C; TafB, triacetylfusarinine B.

Predominantly intracellular Fc marked the onset of isotropic growth, exhibited by the swelling of conidia. There was an exponential increase in its content, up to the constant level in the residual fungal mass, reflecting the need for iron accumulation necessary for hyphal growth and further conidiation. Fc reported to be transcellular [46], was also detected in the supernatant in this study. The gradual increase in FsC secretion was already detected at the beginning of the isotropic phase. It was followed by the secretion of TafC and its hydrolytic derivative TafB during the fungal transition to polarized growth. An inverse relationship of the abundances of TafC and TafB at the stationary phase of growth reflected the iron capture, release, or storage steps managed by *Aspergillus*. Moreover, the detection of mycotoxins, including fumigaclavine A, fumiquinazoline C, fumiquinazoline D, 3-hydroxy-fumiquinazoline A, and tryptoquivaline F/J, exclusively in conidia, demonstrated the ability of *A. fumigatus* to adapt to environmental conditions.

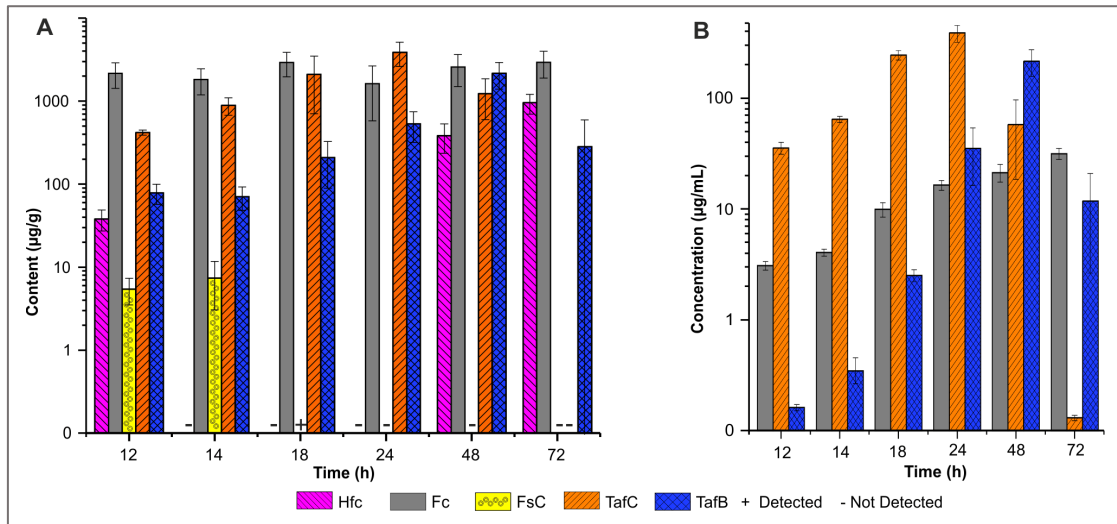


**Figure 5.9** Time-related quantitative siderophore analysis in *A. fumigatus* in **A)** residual fungal mass and **B)** supernatant from 12 to 72 h postinoculation. Data are presented as means  $\pm$  standard deviations. Hfc, hydroxyferricrocin; Fc, ferricrocin; FsC, fusarinine C; TafC, triacetylfulvarinine C; TafB, triacetylfulvarinine B.

In this study, each *A. fumigatus* morphotype demonstrated both qualitatively and quantitatively different profiles of siderophores. The results showed that Hfc and Fc indicated the beginning of germination and isotropic growth of *A. fumigatus*, respectively, whereas TafC and TafB produced during later stages of germination marked the phase of proliferation.

### 5.3.1. *A. fumigatus* siderophores and mycotoxins production during interaction with neutrophils and *P. aeruginosa*

As mentioned earlier, siderophore and mycotoxins play a crucial role in *A. fumigatus* virulence, we sought to describe the dynamics of these metabolite's production during *A. fumigatus* interaction *in vitro*. The interaction between *Aspergillus* and host cells is crucial for successful invasion. Moreover, *Aspergillus* co-exists with other pathogens in nature and the host. Based on this, we designed an interaction experiment with innate immune cells, mainly blood-derived neutrophils, since they are part of the primary line of defence and with bacterial pathogen *P. aeruginosa*, which is most commonly found to cohabit with *A. fumigatus*.

Firstly, we developed a new extraction protocol for sensitive and simultaneous detection of both Gtx and BmGtx using LC-MS, thereby avoiding suppression by enormous siderophore secretion. SPE involving washing in a double volume of 60% MeOH +0.1FA followed by elution in 100% MeOH+0.1FA provided the best results for improved detection of Gtx and BmGtx with reduced carry over of siderophores.

The analysis of co-culture supernatant with *A. fumigatus* and *P. aeruginosa* showed that Fc secretion was significantly suppressed in the presence of *P. aeruginosa* over 72 h of incubation (**Fig. 5.10 A**). TafC was first detected at 12 h in only single *A. fumigatus* culture with significantly lower production from the stationary phase of bacterial growth, i.e., from 18h in dual culture samples (**Fig. 5.10 B**). Conversely, TafB secretion was detected at 24h, only in dual culture; however, further growth from 36h resulted in reduced TafB secretion in contrast to single culture (**Fig. 5.10 C**).

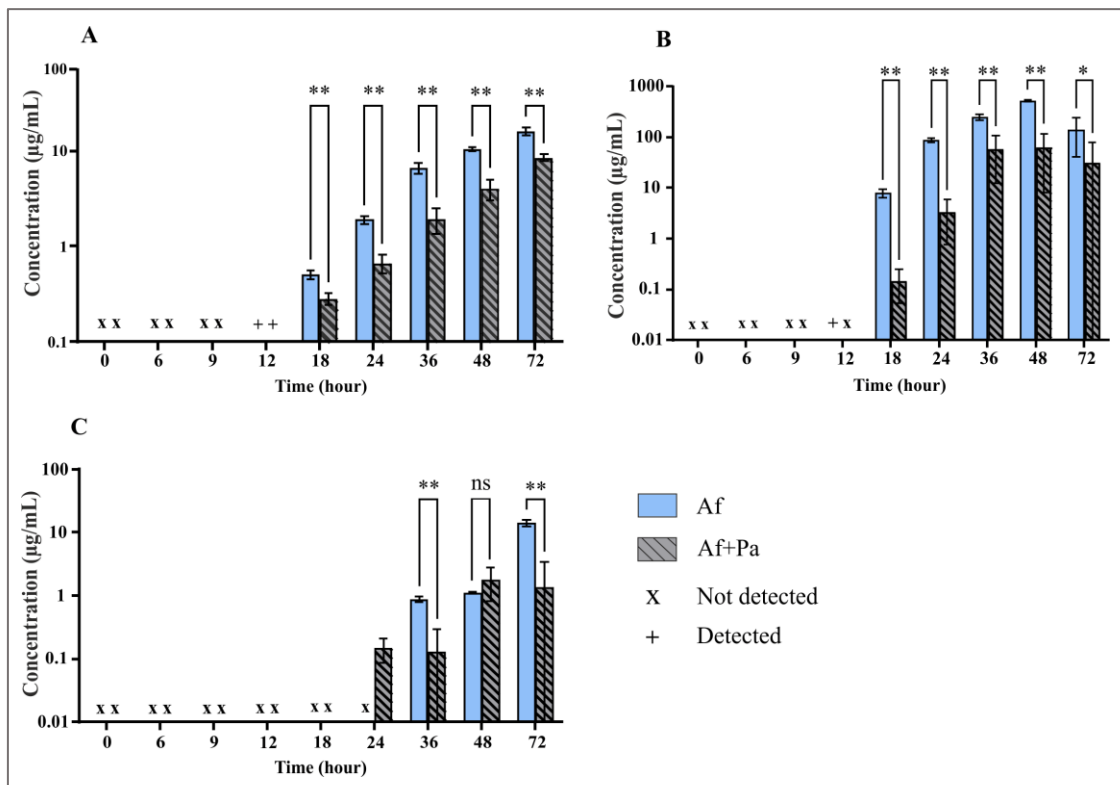


**Figure 5.10** Kinetics of siderophore production in *A. fumigatus* and *P. aeruginosa* during co-culture. Secretion of **A)** Fc and **B)** TafC was significantly higher in single culture of *A. fumigatus* than during co-culture with *P. aeruginosa* over 72 h. **C)** TafB was first quantified at 24h only in co-culture samples with further decreased in its production compared to single *A. fumigatus* culture. Data are presented as means  $\pm$  SDs. The statistical significance (Mann-Whitney test) is indicated by ns (not significant), \* ( $P < 0.05$ ), \*\* ( $P < 0.01$ ). Af, *A. fumigatus*; Pa, *P. aeruginosa*

Our results indicated that during the competition for iron in a shared environment, *P. aeruginosa* dominates *A. fumigatus* by modulating iron acquisition strategies. Nevertheless, we could not detect Gtx or its metabolites in this study, even using a developed extraction protocol. This contradicts the other findings [163, 164]; however, given that the growth conditions used in those two studies differ than this study could have implications on Gtx secretion.

Further, we determined siderophore and mycotoxins production in the interaction processes between neutrophil and *A. fumigatus*. Neutrophils are reported to respond specifically to hyphal forms of *A. fumigatus* [165] as a result, the experiment was carried out using neutrophils ( $1 \times 10^6$  cells/mL) and *A. fumigatus* hyphae (100  $\mu$ g/mL). The results summarized in **Fig. 5.11** showed that Fc, TafC and TafB content was significantly higher during the incubation of *A. fumigatus* with neutrophils until 36 h. The higher content of Fc and TafC was also detected at 48 h in *A. fumigatus* infected neutrophil samples; however, due to biological variation observed between replicates, it was statistically insignificant. Interestingly TafB was continuously detected till 48 h with neutrophil incubation, while single *A. fumigatus* culture showed detection till 18 h (**Fig. 5.11 C**). None of these siderophores was detected in control neutrophil supernatant or pellet samples. The more siderophore content detected from the beginning of the experiment was mainly due to the incubation of neutrophils with lyophilized *A. fumigatus* hyphae. From these results, we concluded that an experiment involving incubating *A. fumigatus* germinating conidia with neutrophils is necessary to study the kinetics of siderophore production during host-cell interaction.

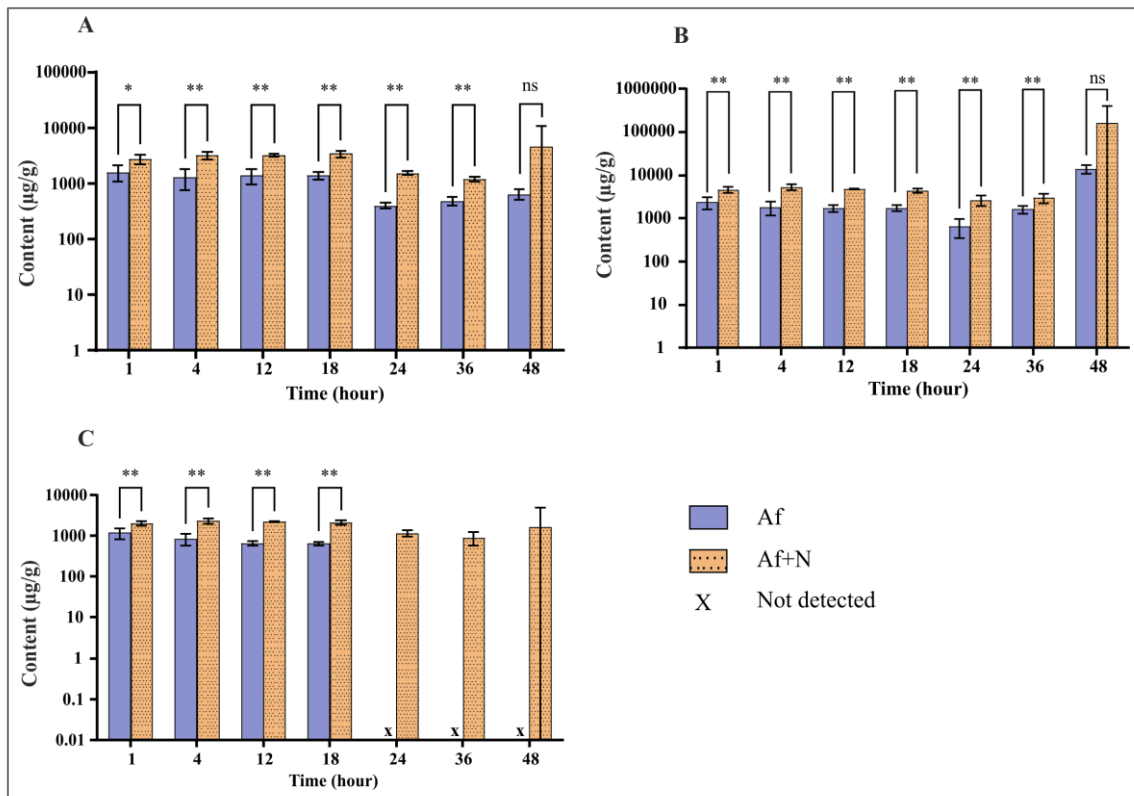


**Figure 5.11** *A. fumigatus* siderophore production upon incubation of hyphae with neutrophils over time. All siderophores content, **A)** Fc, **B)** TafC and **C)** TafB, was elevated during interaction with neutrophils than single *A. fumigatus* culture. Data are presented as means  $\pm$  standard deviations. The statistical significance (Mann-Whitney test) is indicated by ns (not significant), \* ( $P < 0.05$ ), \*\* ( $P < 0.01$ ). Af, *A. fumigatus*; N, neutrophils

Regarding mycotoxins, we mainly targeted the detection of Gtx and its metabolites due to their immunosuppressive properties, as mentioned earlier. We quantified both Gtx and BmGtx in supernatant samples at 48h (**Fig. 5.12**). The detection of Gtx only at 48h could be a result of a possible defence strategy used by *A. fumigatus* against neutrophils. On the other hand, low zinc concentration, reported to play an essential role in Gtx regulation (in this case 4.2  $\mu$ M), could also trigger Gtx production.

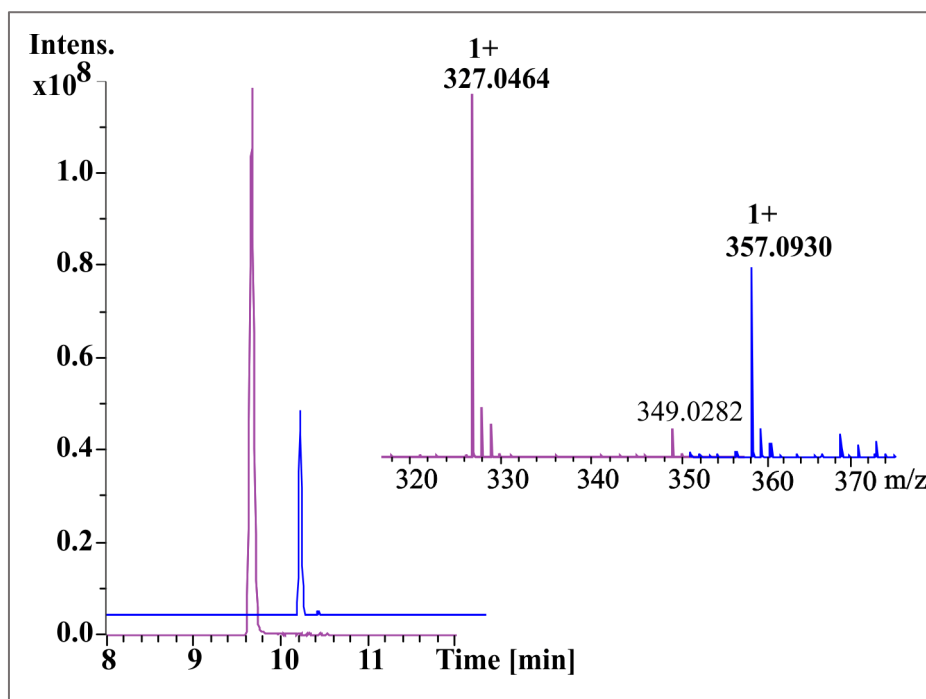


**Figure 5.12** Extraction of Gtx (M+H)<sup>1+</sup>(pink) and BmGtx (M+H)<sup>1+</sup>(blue) with their annotation in *A. fumigatus* incubated neutrophil supernatant at 48h. Gtx, gliotoxin; BmGtx, bismethylgliotoxin

Our results indicated that siderophores, Fc, TafC, TafB and mycotoxins Gtx and BmGtx were the main molecules detected during an exposure of *A. fumigatus* hyphae to neutrophil cells. However, further experiments to overcome the mentioned limitations are necessary to confirm the findings.

### 5.3.2 *A. fumigatus* siderophores and mycotoxins production during interaction with polmycovirus

The results of one part of this section have been published in the following article: R.H. Patil, I. Kotta-Loizou, A. Palyzová, T. Pluháček, D.A. Stevens, V. Havlíček, Freeing *Aspergillus fumigatus* of the polmycovirus makes it more resistant in the competition with *Pseudomonas aeruginosa* due to altered iron-acquiring tactics (2021) [136].

Mycoviruses can affect a range of host phenotypes, including virulence and toxin production. One of our colleagues reported that mycovirus (AfuPmV-1) infection weakened *A. fumigatus* in competition with *P. aeruginosa* via altering fungal stress responses by a mechanism somehow linked to iron metabolism [103]. As a result, in this study, *A. fumigatus* iron-acquiring tactics are described during *A. fumigatus* polymycovirus-1 (AfuPmV-1) infection. Moreover, the effect of mycovirus on *A. fumigatus* mycotoxins (Gtx and BmGtx) production is also described. The results summarized in **Fig. 5.13** revealed differential secretion kinetics of siderophores in virus-free (VF) and virus-infected (VI) strains. The differences in the secretion rate of extracellular TafC between the VF and the VI strains were statistically significant (Kruskal–Wallis,  $p < 0.01$ ) in the early (24 and 31 h) and stationary growth phase (48, 54, 72 h) (**Fig. 5.13**). Similar secretion kinetics was observed for Fc detection in the supernatant. As Hfc and Fc are siderophores involved in iron storage, we also determined their content in conidia and fungal pellets in the stationary growth phase. However, the sum of Fc and Hfc content ( $\mu\text{g}$  per g of a pellet) was similar in VF and VI strains in the pellet and conidia.

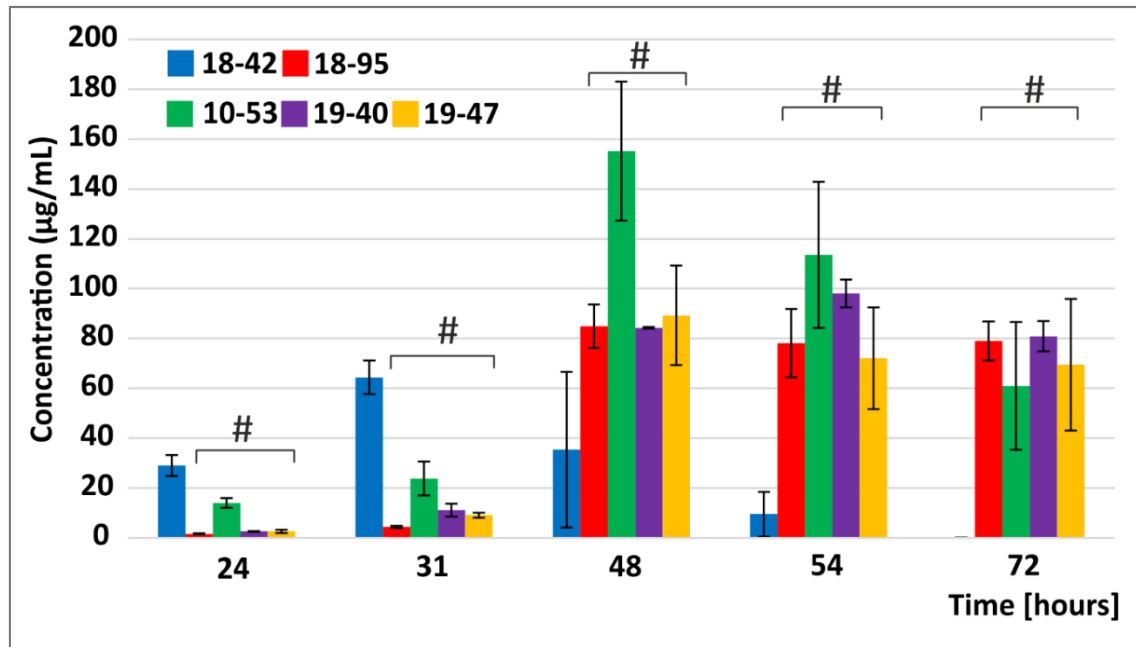


**Figure 5.13** TafC secretion in *A. fumigatus* supernatant. TafC production was earlier in VF than in the VI strains, indicated by an # symbol. The error bars show a standard error of mean  $n=9$ .

Our study showed that polmycovirus infection altered the iron-acquiring tactics of *A. fumigatus* supported by rapid secretion of siderophores by VF than VI strains in the exponential growth of *A. fumigatus*. Thus, the VF strain was more resistant in iron competition against *P. aeruginosa*. Notably, we would like to state that rather than only selected time points, a study of a whole time course is essential, as the data could have been interpreted differently if only selected time points had been used for reaching conclusions (**Fig. 5.13**) (TafC secretion at 31 versus 72 h).

Pigment production was another phenotype that we checked upon mycovirus infection. No differences in colouration between the five strains were visible on solid media of malt extract agar. Conversely, in an iron-limited liquid medium, green colour pigment secretion was visible only in VI strains. As mentioned earlier, *A. fumigatus* secretes different forms of melanin; as a result, this observation was verified using MALDI-MS for melanin detection in VI samples. None of the melanin or its precursors was detectable in our culture; therefore, we concluded that pigments secreted in VI strains were not associated with melanin production. Our data suggested that the presence of the virus in the infected fungal cell represents a substantial metabolic burden where AfuPmV-1 proteins or RNA interfered with fungal siderophore synthesis and iron metabolism. As a result, fungal virulence attenuation through transfection of *Aspergillus* with mycoviruses could represent a promising experimental approach analogous to antibacterial phage therapy.

As a next step, we have investigated whether AfuPmV-1 influences the production of mycotoxins in *A. fumigatus*. Gtx production is dependent on the presence of nutrients; therefore, this experiment was performed in a media containing all nutrients and trace elements, keeping AfuPmV-1 as a sole source of a stress factor. The analysis of the supernatants in this kinetic study revealed that Gtx and BmGtx were first detected at 36 h of incubation in VI strains (except for BmGtx in 19-40 detected at 24h) (**Fig. 5.14**). Gtx secretion was mainly observed in the stationary phase of fungal growth (36, 48 and 60 h) in all VI strains (**Fig. 5.14 A**).



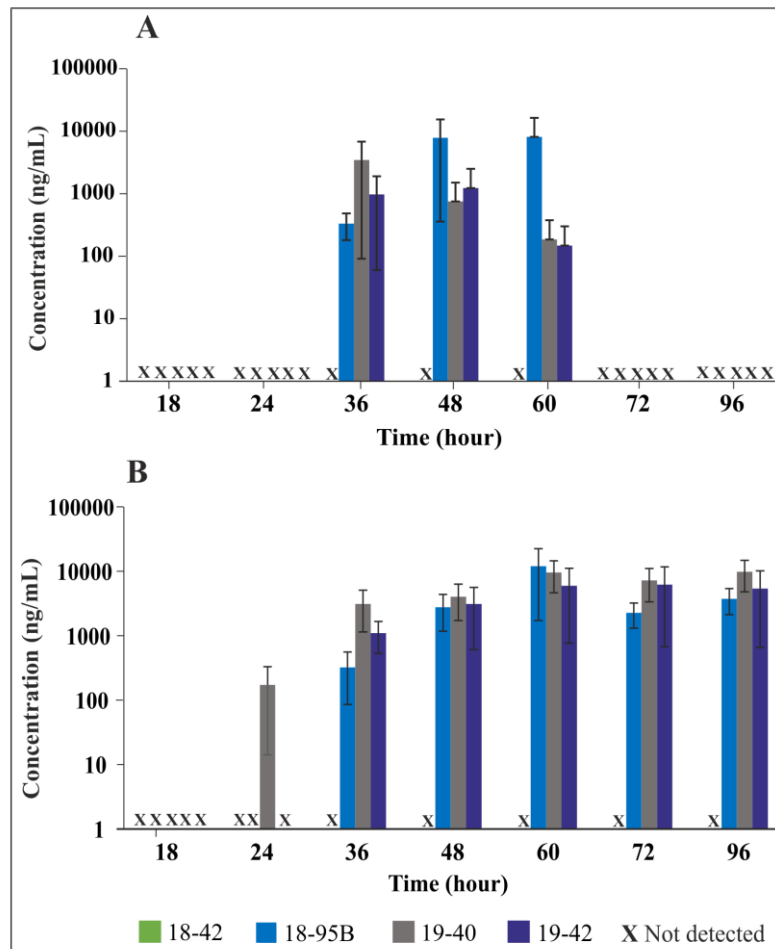


**Figure 5.14** A) Gtx and B) BmGtx production in supernatant over the time course of 96 h in VI strains.

On the other hand, BmGtx production was continuously detected over the complete time course of the study till 96 h in VI strains (**Fig. 5.14 B**). No Gtx nor BmGtx were detected in the VF strain at any time in our study. Moreover, increased levels of BmGtx after 60 h appear to correlate with a decrease in Gtx levels since BmGtx is a negative regulator of Gtx biosynthesis upon an increase in Gtx levels [62]. Our results support the hypothesis that Gtx thiomethylation is a potential *A. fumigatus* protection mechanism against Gtx toxicity. Results in this work indicated that AfuPmV-1 infection is a stress factor for *A. fumigatus* supported by differential secretion of *A. fumigatus* antibacterial mycotoxins, particularly Gtx and its derivative BmGtx.

Among several nutrients, Gtx production is inversely related to zinc availability. Based on this observation and to further confirm previous LC-MS results, we performed gene expression analysis targeting Gtx biosynthesis genes, mainly *gliG*, *gliN*, *gliT*, *gliA*

and BmGtx gene *gtmA*. Here similar VF and VI strains were grown under zinc-depleted media for 48 h. Initially, we confirmed the presence and content of AfuPmV-1 in all strains (**Fig. 5.15 A**). Our results indicated that expression of all the Gtx biosynthesis genes tested, i.e., *gliG*, *gliN*, *gliT* and *gliA*, were upregulated in VI strains than VF (**Fig. 5.15 B**). *gtmA* involved in BmGtx synthesis was also found to be expressed more in VI strains. As stated previously the study of the whole time course is essential, which is a limitation of this experiment. However, these results proved that zinc availability plays a vital role in Gtx production, supported by two studies indicating the upregulation of Gtx genes in zinc depletion and no detection of Gtx in the zinc-containing media in the VF strain.

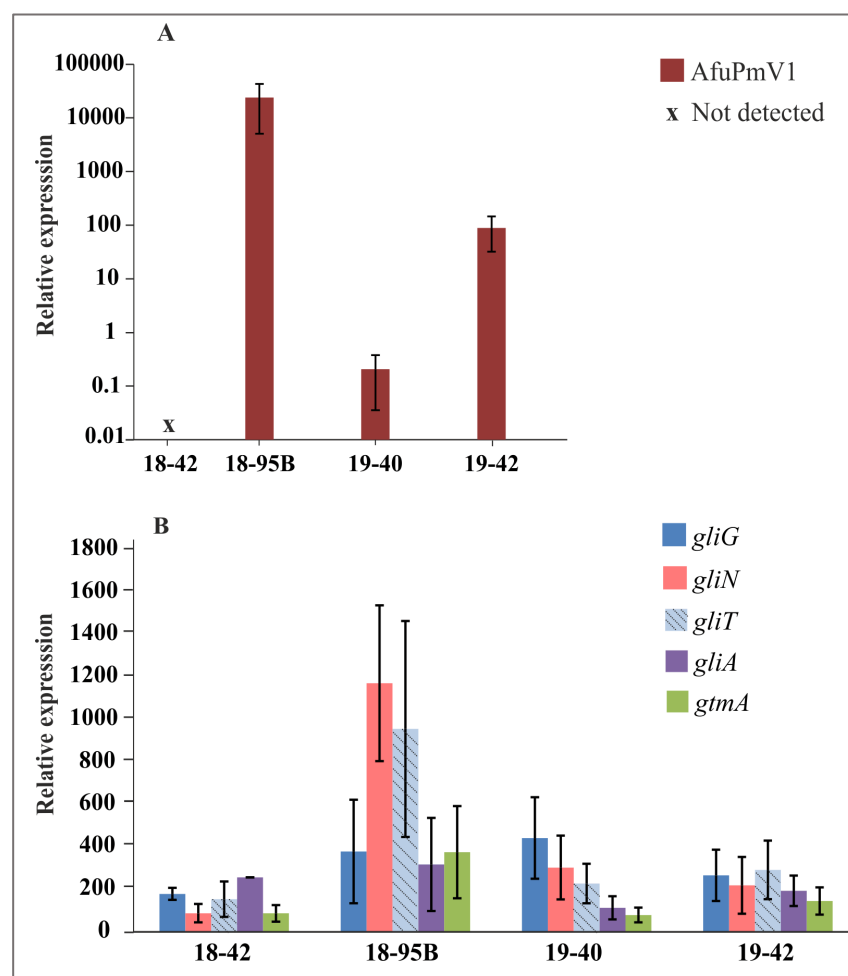


**Figure 5.15** Relative expression of **A)** AfuPmV-1 in VI strains **B)** *gli* biosynthetic cluster including *gliG*, *gliN*, *gliT* and *gliA* together with *gtmA* in VF and VI strains in zinc-depleted media at 48h.

## 5.4 Infection metallomics-based diagnosis

All the knowledge obtained throughout the preparation of section 5.1 and 5.3 was utilized to demonstrate the potential utility of infection metallomics for diagnosing aspergillosis. *Aspergillus* spp. infections are frequent in both humans and animals; therefore, we conducted this study in the diagnosis of aspergillosis in humans as well as horses.

Results shown in this section have been published in the following articles:

D. Luptakova, R.H. Patil, R. Dobias, D.A. Stevens, T. Pluhacek, A. Palyzova, M. Kanova, M. Navratil, Z. Vrba, P. Hubacek V. Havlicek, Siderophore-Based Noninvasive Differentiation of *Aspergillus fumigatus* Colonization and Invasion in Pulmonary Aspergillosis. *Microbiol Spectr.* 11(2023) [132].

R. Dobias, P. Jahn, K. Tothova, O. Dobesova, D. Visnovska, R. Patil, A. Skriba, P. Jaworska, M. Skoric, L. Podojil, M. Kantorova, J. Mrazek, E. Krejci, D.A. Stevens V. Havlicek, Diagnosis of Aspergillosis in Horses. *J Fungi* 9(2023) [140].

### 5.4.1 Human invasive pulmonary aspergillosis

The whole idea behind this work is based on the hypothesis that fungal growth-dependent production of siderophores can allow differentiation of colonization and invasive infection in critically ill patients. Depending on the host's status, once a conidial niche is established, with subsequent germination, tissue invasion, and angioinvasion, fungal virulence factors are disseminated via the bloodstream to other organs (**Fig. 5.15**). *A. fumigatus* excreted siderophores are, distributed from the site of infection to the circulation system from where they are filtered into the urine (**Fig. 5.15 C**). On the top, their concentrations could be affected by viability of the pathogen in response to host factors or antifungal treatment (**Fig. 5.15 B**).

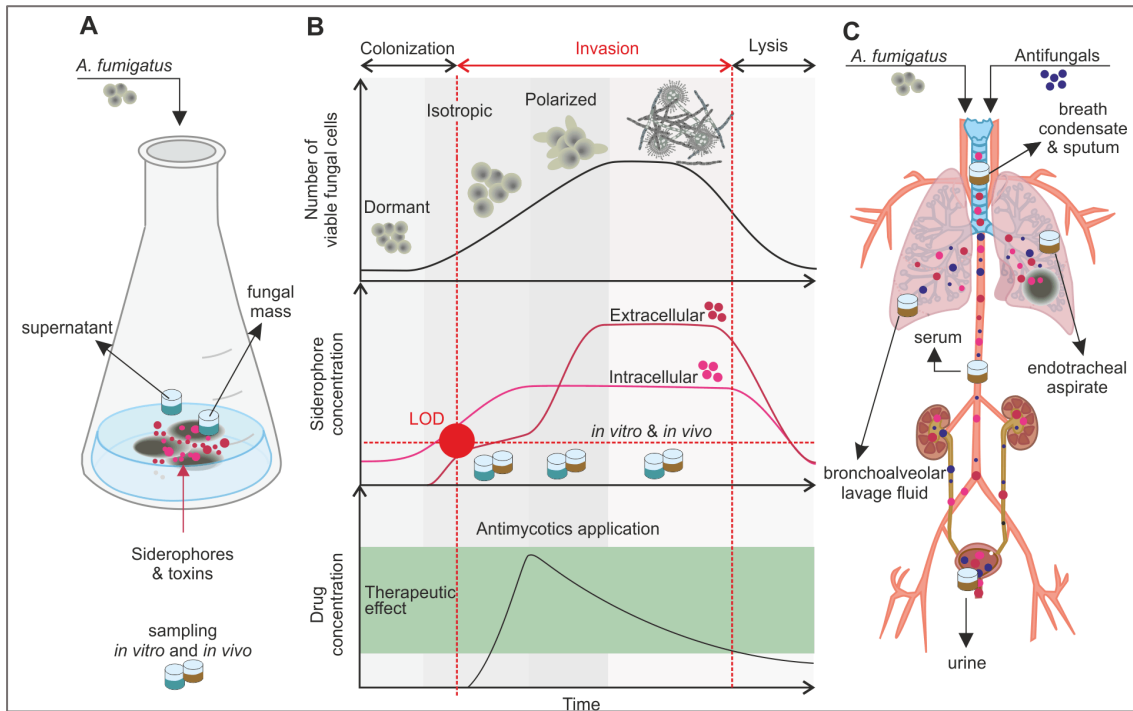


**Figure 5.15** Conceptual overview for characterization of *A. fumigatus* colonization and invasion in critically ill patients. The *in vitro* observations were transferred to human diagnostics.

Therefore, the results from *in vitro* *A. fumigatus* germination study were applied to diagnosing IPA *in vivo*. In this 3-year observational, retrospective, noninterventional clinical study, 35 patients were enrolled, of which 22 patients with non-IPA infections served controls and 13 patients were diagnosed with probable IPA [166]. Applying our infection metallomics strategy, the characteristic *A. fumigatus* siderophores identified from *in vitro* study (section 5.3) were screened in urine and serum samples of all patients. Fc, TafC, TafB, and Gtx were the primary, secondary metabolites detected in IPA patients (**Fig. 5.16**). Importantly, none of these metabolites were detected in the controls. For urine analysis, biological variability in patients with diverse renal functions was partly compensated by applying a creatinine index.

Underlying disease	Risk factor(s)	uGtx/Crea index	Infection metallomics (mean value $\pm$ SD) <sup>b</sup>				Conventional biomarker		Death
			uFc/Crea index	uTafC/Crea index	uTafB/Crea index	sGM (ODI)	sBDG (pg/mL)		
Multiple myeloma	Neutropenia, IST	15.8 $\pm$ 1.0	Det	17.2 $\pm$ 0.2	ND	1.56	501	No	
Non-Hodgkin lymphoma	Neutropenia, IST	Det	ND	32.1 $\pm$ 0.4	ND	3.14	115	No	
Multiple myeloma	Neutropenia, IST	ND	ND	Det	ND	0.17	ND	Yes	
Bronchopneumonia	Flu (H1N1)	85.2 $\pm$ 3.7	8.3 $\pm$ 0.7	82.9 $\pm$ 1.5	5.4 $\pm$ 0.1	5.9	276	Yes	
COPD	Steroids	ND	11.9 $\pm$ 2.7	35.7 $\pm$ 0.4	11.5 $\pm$ 0.4	0.89	>523	Yes	
COPD	Flu (H1N1)	ND	ND	Det	ND	0.1	161	No	
DM II	Ketoacidosis	33.8 $\pm$ 1.4	4.2 $\pm$ 0.5	2.3 $\pm$ 0.1	ND	0.26	155	No	
Bronchopneumonia	Flu (H1N1), steroids	67.9 $\pm$ 6.6	40.6 $\pm$ 2.2	3,117.4 $\pm$ 78.2	59.6 $\pm$ 3.0	7.9	>523	Yes	
Liver transplant	Steroids, IST	ND	ND	27.6 $\pm$ 0.3	4.7 $\pm$ 0.3	0.06	221	No	
Bronchopneumonia	Steroids	ND	ND	12.9 $\pm$ 0.3	ND	0.56	>523	No	
Polytrauma		ND	ND	ND	ND	0.24	75	No	
COPD	DC	596.3 $\pm$ 13.1	505.1 $\pm$ 8.0	1,071.1 $\pm$ 5.6	250.4 $\pm$ 2.2	0.126	>523	No	
Burns		ND	ND	Det	ND	0.121	ND	No	

<sup>a</sup>All cases (13 in total) were classified as "probable aspergillosis" (26, 27). uFc, ferricrocin in urine; uTafC, triacetylfusarinine C in urine; uTafB, triacetylfusarinine B in urine; uGtx, gliotoxin in urine; sGM, galactomannan in serum; sBDG,  $\beta$ -D-glucan in serum; ND, not detected; Det, detected; Crea, creatinine; ODI, optical density index; COPD, chronic obstructive pulmonary disease; DM II, diabetes mellitus type II; IST, immunosuppressants; DC, decompensated cirrhosis; Flu, influenza.

<sup>b</sup>For creatinine indexing, see reference 21.

**Figure 5.16** Non-invasive detection of IPA in human urine of immunocompromised and immunocompetent patients.

The results summarized in **Fig. 5.17** indicated that the TafC/creatinine index provided the highest detection sensitivity of 92.3% (95% confidence interval [CI], 64.0 to 99.8%) and specificity of 100% (95% CI, 84.6 to 100%), substantially better than the indications provided by GM and BDG serology. The serum GM and BDG sensitivities were 46.2 and 76.9%, respectively, and their specificities were 86.4 and 63.6% for the same patient cohort. Interestingly, we obtained poor sensitivity for TafC in serum (2 of 13 patients with IPA).

Biomarker	LOD threshold	Sensitivity (%) (95% CI)	Specificity (%) (95% CI)
<b>Infection metallomics<sup>b</sup></b>			
uGtx/Crea index	$\geq 2.7$ ng/mL	46.2 (19.2–74.9)	100 (84.6–100)
uFc/Crea index	$\geq 0.9$ ng/ml	46.2 (19.2–74.9)	100 (84.6–100)
uTafC/Crea index	$\geq 0.6$ ng/mL	92.3 (64.0–99.8)	100 (84.6–100)
uTafB/Crea index	$\geq 0.6$ ng/mL	38.5 (13.9–68.4)	100 (84.6–100)
<b>Conventional approaches</b>			
sGM	$\geq 0.5$ ODI	46.2 (19.2–74.9)	86.4 (65.1–97.1)
sBDG	$\geq 80$ pg/mL	76.9 (46.2–95.0)	63.6 (40.7–82.8)

<sup>a</sup>All cases (13 in total) were classified as "probable aspergillosis" (26, 27). uFc, ferricrocin in urine; uTafC, triacetylfusarinine C in urine; uTafB, triacetylfusarinine B in urine; uGtx, gliotoxin in urine; sGM, galactomannan in serum; sBDG,  $\beta$ -D-glucan in serum; Crea, creatinine; CI, confidence interval.

<sup>b</sup>For creatinine indexing, see reference 21.

**Figure 5.17** Comparison of infection metallomics-based urine diagnosis with conventional serology indicating LOD, sensitivity, and specificity values for patients with IPA

Besides, this work is the first report of TafB and Gtx detection in human urine samples. However, our study is subject to certain limitations, including the low clinical sample size hence, prospective cohort studies are needed to validate our approach for routine clinical diagnosis. Nevertheless, we demonstrated the potential utility of infection metallomics by non-invasive determination of an array of biomarkers such as TafC, Fc, TafB and Gtx in a single analysis for reliable diagnosis of IPA. We presented clear links between germination or infection phase-dependent siderophore production and observations in critically ill patients.

#### 5.4.2 Equine aspergillosis

*A. fumigatus*, *A. niger*, *A. flavus*, *A. nidulans*, and *A. versicolor* are the dominating species in equine aspergillosis [167]. In horses, *aspergilli* are known to cause guttural pouch mycosis [168] and rare equine invasive pulmonary aspergillosis with almost 100% mortality [169]. Similar to humans, diagnosis of IPA is challenging in veterinary medicine also. In this study, we combined PCR, GM and BDG serology and infection metallomics-based metabolites detection.

The study involved BALF and serum samples collected from 18 horses suffering from IPA (n=1), equine asthma (n=12), and five healthy controls. In this study, measurement of GM levels in BALF provided sensitivity and specificity close to 100% and 94%, respectively, in the diagnosis of IPA (**Fig. 5.18**), consistent with the results obtained for the same approach in human intensive care [170]. Moreover, only Gtx was detected in the BALF and lung tissue samples, confirming the ongoing IPA. However, *Aspergillus*-DNA offered lower specificities due to the presence of *Aspergillus spp.* in the BALF of the healthy control horses.

	bGM (PI = 2.56)	b <i>Aspergillus</i> -DNA	bGtx (86 ng/mL)	sGM (PI = 0.409)	sBDG (1142 pg/mL)
Sensitivity (95% CI)	100% (0.02–1)	100% (0.02–1)	100% (0.02–1)	100% (0.16–1)	100% (0.16–1)
Specificity (95% CI)	94% (0.71–1)	88% (0.64–0.99)	100% (0.8–1)	55% (0.32–0.77)	92% (0.62–1)
PPV	18% (0.01–0.99)	33% (0.01–0.91)	100% (0.02–1)	18% (0.02–0.52)	67% (0.09–0.99)
NPV	100% (0.79–1)	100% (0.78–1)	100% (0.8–1)	100% (0.72–1)	92% (0.72–1)
AUC	0.941	0.941	1	0.625	0.95

GM, galactomannan; b, bronchoalveolar lavage fluid; PPV, Positive Predictive Value; NPV, Negative Predictive Value; AUC, Area under the Curve; Gtx, gliotoxin; s, serum; BDG, 1,3-β-D-glucan; PI, Positivity Index.

**Figure 5.18** Equine serum and BALF analysis for aspergillus biomarkers of invasive aspergillosis

In the same study, for the horses with guttural pouch mycoses (GPM) (n=2), the presence of *A. fumigatus* was confirmed by culture, DNA, and microscopy on tissue samples in case report 1 on day one sampling. In biomarker analysis, intracellular fungal components, i.e., GM and Fc, were positively detected; however, the extracellular fungal markers TafC and Gtx were not detected, specifying the presence of a non-proliferating localized fungal ball. However, the repeated sampling on day 7 revealed *A. nidulans* by culture with GM and Fc biomarkers.

In case report 2 on GPM, the elevated Fc and GM levels were attributed to *A. nidulans* based on culture, *Aspergillus*-DNA, and microscopic analysis (**Fig. 5.19**). *A. nidulans* was the dominant species involved in both equine GPM cases examined in this work; as a result, panfungal biomarker Fc was detected. More extensive clinical studies are required for better inference, though our results indicate that combining two techniques could be helpful in the early equine IPA diagnosis.

GP	Day	Tool			Biomarker		
		Culture	<i>Aspergillus</i> -DNA	Microscopy (BSH)	GM (PI $\geq$ 0.5)	Fc (ng/mL)	Sampling
GPM1 associated with nasopharyngeal dysphagia							
Left	1	<i>A. fumigatus</i>	<i>A. fumigatus</i>	Positive	9.72	492	BAT
Left	7	<i>A. nidulans</i>	<i>Aspergillus</i> spp.	Positive	10.4	1364	AS
GPM2 associated with oral dysphagia							
Left	1	<i>A. nidulans</i>	<i>Aspergillus</i> spp.	Positive	8.64	597	BAT
Right	1	<i>A. nidulans</i>	<i>Aspergillus</i> spp.	Positive	8.63	3574	BAT
Left	15	<i>A. nidulans</i>	Negative	Negative	7.54	496	AS
Right	15	Negative	Negative	Negative	7.65	ND	AS

GP, guttural pouch; GPM, guttural pouch mycosis; BSH, branching septated hyphae; GM, galactomannan; Fc, ferrirocinn; BAT, before antifungal therapy; AS, after surgery; PI, positivity index; ND, not detected.

**Figure 5.19** *A. fumigatus* diagnostic tools and biomarkers detection in equine guttural pouch debridement.

## 6 CONCLUSION

This work introduced infection metallomics, a MS platform for detecting microbial metallophores, which are specific, sensitive, noninvasive, and promising biomarkers of invasive infectious diseases. This diagnostic minimises false positivity as mammalian cells do not synthesize microbial siderophores or mycotoxin molecules. Instrumentally, the concept was built on isotopically-filtered MS data (LC-MS and imzML formats with fine isotope structure resolution), which enabled untargeted metallophore analysis in microbes with understudied metabolomes or limited molecular studies. Specific isotopic profiles in  $\text{Fe}^{3+}$ ,  $\text{Zn}^{2+}$ ,  $\text{Cu}^{2+}$ ,  $\text{Ni}^{2+}$ , and other elements made it possible to design new functional studies tools involving extra and intracellular metallophores relevant to lung, CNS, or urogenital tract infections.

The metabolome mainly targeting siderophores was characterized for *R. microsporus* causing mucormycosis and *A. fumigatus* responsible for IPA using LC-MS. For the first time, the glycosylation of RHF, a siderophore of *R. microsporus* was described in a clinical isolate by LC-MS and accurate tandem MS. The stage-specific germination of *A. fumigatus* conidia and production of siderophores, mainly HfC, Fc, TafC, and FsC, was characterised for each *A. fumigatus* morphotype. This study showed that both qualitatively and quantitatively different profiles of siderophores could distinguish asymptomatic colonization and invasive infection. The role of siderophores and mycotoxins was further monitored to study the interplay among microbes involving *A. fumigatus* interaction with *P. aeruginosa* and polymycovirus as well as with host neutrophils *in vitro*. The data indicated that *P. aeruginosa* took the upper hand in co-culture with *A. fumigatus*, suppressing *A. fumigatus* siderophore production. Incubation of *A. fumigatus* with neutrophils indicated elevated siderophores levels and immunosuppressive Gtx and BmGtx detection. The AfuPmV-1 modified the expression of genes involved in Gtx biosynthesis, leading to upregulation of Gtx and BmGtx production in VI strains over VF strain demonstrated using qRT-PCR and LC-MS analysis. The AfuPmV-1 infection also interfered with the iron uptake strategies of *A. fumigatus* showed by the slowest onset of siderophore synthesis in VI strains than VF over the time course.

The application of next-generation infection diagnostics was then documented in human and equine aspergillosis. The *in vitro* results from *A. fumigatus* germination were



translated to the bedside, where detection of fungal siderophores in urine (a clinical specimen distant from a deep infection site) enabled early, specific, and non-invasive diagnosing of patients suffering from IPA. This work is also the first report on the secretion of TafB and Gtx into human urine samples. In the one-health concept, the diagnosis of aspergillosis was elaborated in horses. Along with routine diagnostic methods such as BDG and GM detection, Gtx was found in the lung tissue and BALF in the fatal invasive aspergillosis case. However, in guttural pouch aspergillosis cases, two horses positively responded to antimycotic therapies; as a result drop in the concentration of intracellular and panfungal *Aspergillus* siderophore, Fc was detected in the debridement.

In the near future, infection metallomics may expand to new application fields. Until now, primarily inter-cellular phenomena were interpreted and upgraded into the next generation infection diagnostics. Although initially developed with FTICR-MS, transfer to widely spread MALDI TOF instruments is feasible. The concept can be used in intracellular pathogens and may shift from infection metallomics to functional metallomics. Defining emerging metallophore targets in the host cells, investigating new chemical structures of metal-bound chelators, discoveries of NRPS systems coding metallophores in understudied species, and stating new treatment intervention sites represent just a few lists of areas in which infection metallomics might be of help.

## REFERENCES

- [1] J. Shankar, S. Tiwari, S.K. Shishodia, M. Gangwar, S. Hoda, R. Thakur P. Vijayaraghavan, Molecular Insights Into Development and Virulence Determinants of Aspergilli: A Proteomic Perspective. *Front Cell Infect Microbiol.* 8 (2018) 180.
- [2] V. EspinosaA. Rivera, First Line of Defense: Innate Cell-Mediated Control of Pulmonary Aspergillosis. *Front Microbiol.* 7 (2016) 272.
- [3] F. Bongomin, S. Gago, R.O. Oladele D.W. Denning, Global and Multi-National Prevalence of Fungal Diseases-Estimate Precision. *Journal of Fungi.* 3 (2017) 10.3390/jof3040057.
- [4] E.M. Negm, M.S. Mohamed, R.A. Rabie, W.S. Fouad, A. Beniamen, A. Mosallem, A.E. Tawfik H.M. Salama, Fungal infection profile in critically ill COVID-19 patients: a prospective study at a large teaching hospital in a middle-income country. *BMC Infect Dis.* 23 (2023) 246.
- [5] World Health Organization. Fungal Priority Pathogens List to Guide Research, Development and Public Health Action. (2022).
- [6] B. Mousavi, M.T. Hedayati, N. Hedayati, M. Ilkit S. Syedmousavi, Aspergillus species in indoor environments and their possible occupational and public health hazards. *Curr Med Mycol.* 2 (2016) 36-42.
- [7] I. Valsecchi, V. Dupres, E. Stephen-Victor, J.I. Guijarro, J. Gibbons, R. Beau, J. Bayry, J.Y. Coppee, F. Lafont, J.P. Latge A. Beauvais, Role of Hydrophobins in *Aspergillus fumigatus*. *J Fungi (Basel).* 4 (2017).
- [8] S.E. Cagas, M.R. Jain, H. Li D.S. Perlin, The proteomic signature of *Aspergillus fumigatus* during early development. *Mol Cell Proteomics.* 10 (2011) M111 010108.
- [9] T. Fontaine, C. Simenel, G. Dubreucq, O. Adam, M. Delepierre, J. Lemoine, C.E. Vorgias, M. Diaquin J.P. Latge, Molecular organization of the alkali-insoluble fraction of *Aspergillus fumigatus* cell wall. *J Biol Chem.* 275 (2000) 27594-27607.
- [10] E. Mowat, S. Lang, C. Williams, E. McCulloch, B. Jones G. Ramage, Phase-dependent antifungal activity against *Aspergillus fumigatus* developing multicellular filamentous biofilms. *J Antimicrob Chemother.* 62 (2008) 1281-1284.
- [11] N.L. SmithD.W. Denning, Underlying conditions in chronic pulmonary aspergillosis including simple aspergilloma. *Eur Respir J.* 37 (2011) 865-872.

- [12] D.W. Denning, K. Riniotis, R. Dobrashian H. Sambatakou, Chronic cavitary and fibrosing pulmonary and pleural aspergillosis: case series, proposed nomenclature change, and review. *Clin Infect Dis.* 37 Suppl 3 (2003) S265-280.
- [13] R. Agarwal, A.N. Aggarwal, D. Gupta S.K. Jindal, Aspergillus hypersensitivity and allergic bronchopulmonary aspergillosis in patients with bronchial asthma: systematic review and meta-analysis. *Int J Tuberc Lung Dis.* 13 (2009) 936-944.
- [14] A.P. Knutsen R.G. Slavin, Allergic bronchopulmonary aspergillosis in asthma and cystic fibrosis. *Clin Dev Immunol.* 2011 (2011) 843763.
- [15] D.W. Denning, A. Pleuvry D.C. Cole, Global burden of allergic bronchopulmonary aspergillosis with asthma and its complication chronic pulmonary aspergillosis in adults. *Med Mycol.* 51 (2013) 361-370.
- [16] R. Agarwal, D. Maskey, A.N. Aggarwal, B. Saikia, M. Garg, D. Gupta A. Chakrabarti, Diagnostic performance of various tests and criteria employed in allergic bronchopulmonary aspergillosis: a latent class analysis. *PLoS One.* 8 (2013) e61105.
- [17] J. Pfister, Summer, D., Petrik, M., Khoylou, M., Lichius, A., Kaeopookum, P., Kochinke, L., Orasch, T., Haas, H. and Decristoforo, C, Hybrid imaging of *Aspergillus fumigatus* pulmonary infection with fluorescent, <sup>68</sup>Ga-labelled siderophores. *Biomolecules.* (2020).
- [18] A. Cornillet, C. Camus, S. Nimubona, V. Gandemer, P. Tattevin, C. Belleguic, S. Chevrier, C. Meunier, C. Lebert, M. Aupee, S. Caulet-Maugendre, M. Faucheux, B. Lelong, E. Leray, C. Guiguen J.P. Gangneux, Comparison of epidemiological, clinical, and biological features of invasive aspergillosis in neutropenic and nonneutropenic patients: a 6-year survey. *Clin Infect Dis.* 43 (2006) 577-584.
- [19] A.F.A.D. Schauwvlieghe, R. Verwijs, B.J.A. Rijnders, N. Philips, J. Wauters, L. Vanderbeke, T.C. Van, K. Lagrou, P.E. Verweij, d.V.F.L. Van, D. Gommers, P. Spronk, D.C.J.J. Bergmans, A. Hoedemaekers, E.-R. Andrinopoulou, d.B.C.H.S.B. van, N.P. Juffermans, C.J. Hodiamont, A.G. Vonk, P. Depuydt J. Boelens, Invasive aspergillosis in patients admitted to the intensive care unit with severe influenza: a retrospective cohort study. *Lancet Resp Med.* 6 (2018) 782-792.
- [20] D. Armstrong-James, J. Youngs, T. Bicanic, A. Abdolrasouli, D.W. Denning, E. Johnson, V. Mehra, T. Pagliuca, B. Patel, J. Rhodes, S. Schelenz, A. Shah, F.L. van de Veerdonk, P.E. Verweij, P.L. White M.C. Fisher, Confronting and mitigating the risk of COVID-19 associated pulmonary aspergillosis. *Eur Respir J.* 56 (2020).

- [21] J. Jung, H.L. Hong, S.O. Lee, S.H. Choi, Y.S. Kim, J.H. Woo S.H. Kim, Immune reconstitution inflammatory syndrome in neutropenic patients with invasive pulmonary aspergillosis. *J Infect.* 70 (2015) 659-667.
- [22] R. Dobias, D.A. Stevens V. Havlicek, Current and Future Pathways in Aspergillus Diagnosis. *Antibiotics (Basel).* 12 (2023).
- [23] M. Bassetti E. Bouza, Invasive mould infections in the ICU setting: complexities and solutions. *J Antimicrob Chemother.* 72 (2017) i39-i47.
- [24] J. D'Haese, K. Theunissen, E. Vermeulen, H. Schoemans, G. De Vlieger, L. Lammertijn, P. Meersseman, W. Meersseman, K. Lagrou J. Maertens, Detection of galactomannan in bronchoalveolar lavage fluid samples of patients at risk for invasive pulmonary aspergillosis: analytical and clinical validity. *J Clin Microbiol.* 50 (2012) 1258-1263.
- [25] X.J. Cao, Y.P. Li, L.M. Xie, H.L. Zhang, Y.S. Qin X.G. Guo, Diagnostic Accuracy of Bronchoalveolar Lavage Fluid Galactomannan for Invasive Aspergillosis. *Biomed Res Int.* 2020 (2020) 5434589.
- [26] D. Farmakiotis, A. Le, Z. Weiss, N. Ismail, D.W. Kubiak S. Koo, False positive bronchoalveolar lavage galactomannan: Effect of host and cut-off value. *Mycoses.* 62 (2019) 204-213.
- [27] C. Pazos, J. Ponton A. Del Palacio, Contribution of (1->3)-beta-D-glucan chromogenic assay to diagnosis and therapeutic monitoring of invasive aspergillosis in neutropenic adult patients: a comparison with serial screening for circulating galactomannan. *J Clin Microbiol.* 43 (2005) 299-305.
- [28] M. Mikulska, E. Furfaro, S. Dettori, D.R. Giacobbe, L. Magnasco, C. Dentone, L. Ball, C. Russo, L. Taramasso, A. Vena, E. Angelucci, P. Pelosi M. Bassetti, Aspergillus-PCR in bronchoalveolar lavage - diagnostic accuracy for invasive pulmonary aspergillosis in critically ill patients. *Mycoses.* 65 (2022) 411-418.
- [29] D. Buchheidt, C. Baust, H. Skladny, J. Ritter, T. Suedhoff, M. Baldus, W. Seifarth, C. Leib-Moesch R. Hehlmann, Detection of Aspergillus species in blood and bronchoalveolar lavage samples from immunocompromised patients by means of 2-step polymerase chain reaction: clinical results. *Clin Infect Dis.* 33 (2001) 428-435.
- [30] C. Halliday, R. Hoile, T. Sorrell, G. James, S. Yadav, P. Shaw, M. Bleakley, K. Bradstock S. Chen, Role of prospective screening of blood for invasive aspergillosis by polymerase chain reaction in febrile neutropenic recipients of

- haematopoietic stem cell transplants and patients with acute leukaemia. *Br J Haematol.* 132 (2006) 478-486.
- [31] M. Mikulska, E. Furfaro, E. De Carolis, E. Drago, I. Pulzato, M.L. Borghesi, E. Zappulo, A.M. Raiola, C.D. Grazia, V. Del Bono, G. Cittadini, E. Angelucci, M. Sanguinetti C. Viscoli, Use of *Aspergillus fumigatus* real-time PCR in bronchoalveolar lavage samples (BAL) for diagnosis of invasive aspergillosis, including azole-resistant cases, in high risk haematology patients: the need for a combined use with galactomannan. *Med Mycol.* 57 (2019) 987-996.
- [32] Z. Pan, M. Fu, J. Zhang, H. Zhou, Y. Fu J. Zhou, Diagnostic accuracy of a novel lateral-flow device in invasive aspergillosis: a meta-analysis. *J Med Microbiol.* 64 (2015) 702-707.
- [33] S. HeldtM. Hoenigl, Lateral Flow Assays for the Diagnosis of Invasive Aspergillosis: Current Status. *Curr Fungal Infect Rep.* 11 (2017) 45-51.
- [34] G.L. Johnson, S.J. Sarker, F. Nannini, A. Ferrini, E. Taylor, C. Lass-Florl, W. Mutschlechner, S.A. Bustin S.G. Agrawal, *Aspergillus*-Specific Lateral-Flow Device and Real-Time PCR Testing of Bronchoalveolar Lavage Fluid: a Combination Biomarker Approach for Clinical Diagnosis of Invasive Pulmonary Aspergillosis. *J Clin Microbiol.* 53 (2015) 2103-2108.
- [35] J. Houšť, J. Spížek V. Havlíček, Antifungal drugs. *Metabolites.* 10 (2020) 106.
- [36] B.H. Segal, L.A. Barnhart, V.L. Anderson, T.J. Walsh, H.L. Malech S.M. Holland, Posaconazole as salvage therapy in patients with chronic granulomatous disease and invasive filamentous fungal infection. *Clin Infect Dis.* 40 (2005) 1684-1688.
- [37] H. Sambatakou, B. Dupont, H. Lode D.W. Denning, Voriconazole treatment for subacute invasive and chronic pulmonary aspergillosis. *Am J Med.* 119 (2006) 527 e517-524.
- [38] J.A. Maertens, Raad, II, K.A. Marr, T.F. Patterson, D.P. Kontoyiannis, O.A. Cornely, E.J. Bow, G. Rahav, D. Neofytos, M. Aoun, J.W. Baddley, M. Giladi, W.J. Heinz, R. Herbrecht, W. Hope, M. Karthaus, D.G. Lee, O. Lortholary, V.A. Morrison, I. Oren, D. Selleslag, S. Shoham, G.R. Thompson, 3rd, M. Lee, R.M. Maher, A.H. Schmitt-Hoffmann, B. Zeiher A.J. Ullmann, Isavuconazole versus voriconazole for primary treatment of invasive mould disease caused by *Aspergillus* and other filamentous fungi (SECURE): a phase 3, randomised-controlled, non-inferiority trial. *Lancet.* 387 (2016) 760-769.

- [39] J. Maertens, A. Glasmacher, R. Herbrecht, A. Thiebaut, C. Cordonnier, B.H. Segal, J. Killar, A. Taylor, N. Kartsonis, T.F. Patterson, M. Aoun, D. Caillot, C. Sable G. Caspofungin Combination Therapy Study, Multicenter, noncomparative study of caspofungin in combination with other antifungals as salvage therapy in adults with invasive aspergillosis. *Cancer*. 107 (2006) 2888-2897.
- [40] M.C. Fisher, N.J. Hawkins, D. Sanglard S.J. Gurr, Worldwide emergence of resistance to antifungal drugs challenges human health and food security. *Science*. 360 (2018) 739-742.
- [41] K.a.H. Haynes, H., Siderophore biosynthesis but not reductive iron assimilation is essential for *Aspergillus fumigatus* virulence. *J Exp Med*, (2004).
- [42] A. Skriba, R.H. Patil, P. Hubacek, R. Dobias, A. Palyzova, H. Maresova, T. Pluhacek V. Havlicek, Rhizoferrin Glycosylation in *Rhizopus microsporus*. *J Fungi (Basel)*. 6 (2020) 89.
- [43] B. Holinsworth J.D. Martin, Siderophore production by marine-derived fungi. *Biometals*. 22 (2009) 625-632.
- [44] M. Schrettl, E. Bignell, C. Kragl, Y. Sabiha, O. Loss, M. Eisendle, A. Wallner, H.N. Arst, Jr., K. Haynes H. Haas, Distinct roles for intra- and extracellular siderophores during *Aspergillus fumigatus* infection. *PLoS Pathog*. 3 (2007) 1195-1207.
- [45] I. Raymond-Bouchard, C.S. Carroll, J.R. Nesbitt, K.A. Henry, L.J. Pinto, M. Moinzadeh, J.K. Scott M.M. Moore, Structural requirements for the activity of the MirB ferrisiderophore transporter of *Aspergillus fumigatus*. *Eukaryot Cell*. 11 (2012) 1333-1344.
- [46] I. Happacher, M. Aguiar, M. Alilou, B. Abt, T.J.H. Baltussen, C. Decristoforo, W.J.G. Melchers H. Haas, The Siderophore Ferricrocin Mediates Iron Acquisition in *Aspergillus fumigatus*. *Microbiol Spectr*. 11 (2023) e0049623.
- [47] C. Kragl, M. Schrettl, B. Abt, B. Sarg, H.H. Lindner H. Haas, EstB-mediated hydrolysis of the siderophore triacetylfusarinine C optimizes iron uptake of *Aspergillus fumigatus*. *Eukaryot Cell*. 6 (2007) 1278-1285.
- [48] H. Tamiya, E. Ochiai, K. Kikuchi, M. Yahiro, T. Toyotome, A. Watanabe, T. Yaguchi K. Kamei, Secondary metabolite profiles and antifungal drug susceptibility of *Aspergillus fumigatus* and closely related species, *Aspergillus lentulus*, *Aspergillus udagawae*, and *Aspergillus viridinutans*. *J Infect Chemother*. 21 (2015) 385-391.

- [49] M.A. Mehedi MA, Khondkar PR, Sultana S, Islam MA, Rashid MA, Chowdhury R., Pseurotin A: an antibacterial secondary metabolite from *Aspergillus fumigatus*. (2010).
- [50] X.J. Li, Q. Zhang, A.L. Zhang J.M. Gao, Metabolites from *Aspergillus fumigatus*, an endophytic fungus associated with *Melia azedarach*, and their antifungal, antifeedant, and toxic activities. *J Agric Food Chem.* 60 (2012) 3424-3431.
- [51] R.H. Du, E.G. Li, Y. Cao, Y.C. Song R.X. Tan, Fumigaclavine C inhibits tumor necrosis factor alpha production via suppression of toll-like receptor 4 and nuclear factor kappaB activation in macrophages. *Life Sci.* 89 (2011) 235-240.
- [52] H.S. Choi, J.S. Shim, J.A. Kim, S.W. Kang H.J. Kwon, Discovery of gliotoxin as a new small molecule targeting thioredoxin redox system. *Biochem Biophys Res Commun.* 359 (2007) 523-528.
- [53] D.M. Gardiner B.J. Howlett, Bioinformatic and expression analysis of the putative gliotoxin biosynthetic gene cluster of *Aspergillus fumigatus*. *FEMS Microbiol Lett.* 248 (2005) 241-248.
- [54] J.W. Bok, D. Chung, S.A. Balajee, K.A. Marr, D. Andes, K.F. Nielsen, J.C. Frisvad, K.A. Kirby N.P. Keller, GliZ, a transcriptional regulator of gliotoxin biosynthesis, contributes to *Aspergillus fumigatus* virulence. *Infect Immun.* 74 (2006) 6761-6768.
- [55] J.W. Bok, S.A. Balajee, K.A. Marr, D. Andes, K.F. Nielsen, J.C. Frisvad N.P. Keller, LaeA, a regulator of morphogenetic fungal virulence factors. *Eukaryot Cell.* 4 (2005) 1574-1582.
- [56] O. Bayram, S. Krappmann, M. Ni, J.W. Bok, K. Helmstaedt, O. Valerius, S. Braus-Stromeyer, N.J. Kwon, N.P. Keller, J.H. Yu G.H. Braus, VelB/VeA/LaeA complex coordinates light signal with fungal development and secondary metabolism. *Science.* 320 (2008) 1504-1506.
- [57] Y.K. Suen, K.P. Fung, C.Y. Lee S.K. Kong, Gliotoxin induces apoptosis in cultured macrophages via production of reactive oxygen species and cytochrome c release without mitochondrial depolarization. *Free Radic Res.* 35 (2001) 1-10.
- [58] H.L. Pahl, B. Krauss, K. Schulze-Osthoff, T. Decker, E.B. Traenckner, M. Vogt, C. Myers, T. Parks, P. Warring, A. Muhlbacher, A.P. Czernilofsky P.A. Baeuerle, The immunosuppressive fungal metabolite gliotoxin specifically inhibits transcription factor NF-kappaB. *J Exp Med.* 183 (1996) 1829-1840.

- [59] S. Tsunawaki, L.S. Yoshida, S. Nishida, T. Kobayashi T. Shimoyama, Fungal metabolite gliotoxin inhibits assembly of the human respiratory burst NADPH oxidase. *Infect Immun.* 72 (2004) 3373-3382.
- [60] M. Stanzani, E. Orciuolo, R. Lewis, D.P. Kontoyiannis, S.L. Martins, L.S. St John K.V. Komanduri, *Aspergillus fumigatus* suppresses the human cellular immune response via gliotoxin-mediated apoptosis of monocytes. *Blood.* 105 (2005) 2258-2265.
- [61] S.K. Dolan, G. O’Keeffe, G.W. Jones S. Doyle, Resistance is not futile: gliotoxin biosynthesis, functionality and utility. *Trends in Microbiology.* 23 (2015) 419-428.
- [62] S.K. Dolan, R.A. Owens, G. O’Keeffe, S. Hammel, D.A. Fitzpatrick, G.W. Jones S. Doyle, Regulation of nonribosomal peptide synthesis: bis-thiomethylation attenuates gliotoxin biosynthesis in *Aspergillus fumigatus*. *Chem Biol.* 21 (2014) 999-1012.
- [63] A. Gomez-Lopez, C. Rueda, R. Pando Pozo L.M. Sanchez Gonzalez, Dynamics of gliotoxin and bis(methylthio)gliotoxin production during the course of *Aspergillus fumigatus* infection. *Med Mycol.* 60 (2022).
- [64] M.P. Domingo, C. Colmenarejo, L. Martinez-Lostao, A. Mullbacher, C. Jarne, M.J. Revillo, P. Delgado, L. Roc, J.F. Meis, A. Rezusta, J. Pardo E.M. Galvez, Bis(methyl)gliotoxin proves to be a more stable and reliable marker for invasive aspergillosis than gliotoxin and suitable for use in diagnosis. *Diagn Microbiol Infect Dis.* 73 (2012) 57-64.
- [65] S.C. Kerr, G.J. Fischer, M. Sinha, O. McCabe, J.M. Palmer, T. Choera, F.Y. Lim, M. Wimmerova, S.D. Carrington, S. Yuan, C.A. Lowell, S. Oscarson, N.P. Keller J.V. Fahy, FleA Expression in *Aspergillus fumigatus* Is Recognized by Fucosylated Structures on Mucins and Macrophages to Prevent Lung Infection. *PLoS Pathog.* 12 (2016) e1005555.
- [66] G. Weiss, Iron and immunity: a double-edged sword. *Eur J Clin Invest.* 32 Suppl 1 (2002) 70-78.
- [67] P.R. Taylor, L. Martinez-Pomares, M. Stacey, H.H. Lin, G.D. Brown S. Gordon, Macrophage receptors and immune recognition. *Annu Rev Immunol.* 23 (2005) 901-944.
- [68] G.M. Gersuk, D.M. Underhill, L. Zhu K.A. Marr, Dectin-1 and TLRs permit macrophages to distinguish between different *Aspergillus fumigatus* cellular states. *J Immunol.* 176 (2006) 3717-3724.



- [69] K. Luther, A. Torosantucci, A.A. Brakhage, J. Heesemann F. Ebel, Phagocytosis of *Aspergillus fumigatus* conidia by murine macrophages involves recognition by the dectin-1 beta-glucan receptor and Toll-like receptor 2. *Cell Microbiol.* 9 (2007) 368-381.
- [70] H. Sun, X.Y. Xu, H.T. Shao, X. Su, X.D. Wu, Q. Wang Y. Shi, Dectin-2 is predominately macrophage restricted and exhibits conspicuous expression during *Aspergillus fumigatus* invasion in human lung. *Cell Immunol.* 284 (2013) 60-67.
- [71] M.M. Mircescu, L. Lipuma, N. van Rooijen, E.G. Pamer T.M. Hohl, Essential role for neutrophils but not alveolar macrophages at early time points following *Aspergillus fumigatus* infection. *J Infect Dis.* 200 (2009) 647-656.
- [72] A.D. Kennedy, J.A. Willment, D.W. Dorward, D.L. Williams, G.D. Brown F.R. DeLeo, Dectin-1 promotes fungicidal activity of human neutrophils. *Eur J Immunol.* 37 (2007) 467-478.
- [73] M. Feldmesser, Role of neutrophils in invasive aspergillosis. *Infect Immun.* 74 (2006) 6514-6516.
- [74] C. Auvynet Y. Rosenstein, Multifunctional host defense peptides: antimicrobial peptides, the small yet big players in innate and adaptive immunity. *FEBS J.* 276 (2009) 6497-6508.
- [75] C. Garlanda, E. Hirsch, S. Bozza, A. Salustri, M. De Acetis, R. Nota, A. Maccagno, F. Riva, B. Bottazzi, G. Peri, A. Doni, L. Vago, M. Botto, R. De Santis, P. Carminati, G. Siracusa, F. Altruda, A. Vecchi, L. Romani A. Mantovani, Non-redundant role of the long pentraxin PTX3 in anti-fungal innate immune response. *Nature.* 420 (2002) 182-186.
- [76] R.P. Gazendam, J.L. van Hamme, A.T. Tool, M. Hoogenboezem, J.M. van den Berg, J.M. Prins, L. Vitkov, F.L. van de Veerdonk, T.K. van den Berg, D. Roos T.W. Kuijpers, Human Neutrophils Use Different Mechanisms To Kill *Aspergillus fumigatus* Conidia and Hyphae: Evidence from Phagocyte Defects. *J Immunol.* 196 (2016) 1272-1283.
- [77] K.A. Zarembek, J.A. Sugui, Y.C. Chang, K.J. Kwon-Chung J.I. Gallin, Human polymorphonuclear leukocytes inhibit *Aspergillus fumigatus* conidial growth by lactoferrin-mediated iron depletion. *J Immunol.* 178 (2007) 6367-6373.
- [78] A.H. Hissen, J.M. Chow, L.J. Pinto M.M. Moore, Survival of *Aspergillus fumigatus* in serum involves removal of iron from transferrin: the role of siderophores. *Infect Immun.* 72 (2004) 1402-1408.

- [79] R. Amin, A. Dupuis, S.D. Aaron F. Ratjen, The effect of chronic infection with *Aspergillus fumigatus* on lung function and hospitalization in patients with cystic fibrosis. *Chest*. 137 (2010) 171-176.
- [80] D.A. Stevens, Moss, R.B., Kurup, V.P., Knutsen, A.P., Greenberger, P., Judson, M.A., Denning, D.W., Cramer, R., Brody, A.S., Light, M. and Skov, M, Allergic bronchopulmonary aspergillosis in cystic fibrosis – state of the art: Cystic Fibrosis Foundation Consensus Conference. (2003).
- [81] J. Zhao, W. Cheng, X. He Y. Liu, The co-colonization prevalence of *Pseudomonas aeruginosa* and *Aspergillus fumigatus* in cystic fibrosis: A systematic review and meta-analysis. *Microb Pathog*. 125 (2018) 122-128.
- [82] K. Duan, C. Dammel, J. Stein, H. Rabin M.G. Surette, Modulation of *Pseudomonas aeruginosa* gene expression by host microflora through interspecies communication. *Mol Microbiol*. 50 (2003) 1477-1491.
- [83] A. Korgaonkar, U. Trivedi, K.P. Rumbaugh M. Whiteley, Community surveillance enhances *Pseudomonas aeruginosa* virulence during polymicrobial infection. *Proc Natl Acad Sci U S A*. 110 (2013) 1059-1064.
- [84] J.P. Pearson, M. Feldman, B.H. Iglewski A. Prince, *Pseudomonas aeruginosa* cell-to-cell signaling is required for virulence in a model of acute pulmonary infection. *Infect Immun*. 68 (2000) 4331-4334.
- [85] G. Sass, H. Nazik, J. Penner, H. Shah, S.R. Ansari, K.V. Clemons, M.C. Groleau, A.M. Dietl, P. Visca, H. Haas, E. Deziel D.A. Stevens, *Aspergillus-Pseudomonas* interaction, relevant to competition in airways. *Med Mycol*. 57 (2019) S228-S232.
- [86] E. Mowat, R. Rajendran, C. Williams, E. McCulloch, B. Jones, S. Lang G. Ramage, *Pseudomonas aeruginosa* and their small diffusible extracellular molecules inhibit *Aspergillus fumigatus* biofilm formation. *FEMS Microbiol Lett*. 313 (2010) 96-102.
- [87] F.J. Reen, J.P. Phelan, D.F. Woods, R. Shanahan, R. Cano, S. Clarke, G.P. McGlacken F. O'Gara, Harnessing Bacterial Signals for Suppression of Biofilm Formation in the Nosocomial Fungal Pathogen *Aspergillus fumigatus*. *Front Microbiol*. 7 (2016) 2074.
- [88] B. Briard, P. Bomme, B.E. Lechner, G.L. Mislin, V. Lair, M.C. Prevost, J.P. Latge, H. Haas A. Beauvais, *Pseudomonas aeruginosa* manipulates redox and iron homeostasis of its microbiota partner *Aspergillus fumigatus* via phenazines. *Sci Rep*. 5 (2015) 8220.

- [89] B. Briard, V. Rasoldier, P. Bomme, N. ElAouad, C. Guerreiro, P. Chassagne, L. Muszkieta, J.P. Latge, L. Mulard A. Beauvais, Dirhamnolipids secreted from *Pseudomonas aeruginosa* modify anjpeungal susceptibility of *Aspergillus fumigatus* by inhibiting beta1,3 glucan synthase activity. *ISME J.* 11 (2017) 1578-1591.
- [90] N.H. sass G, Penner J, Shah H, Ansari SR, Clemons KV, Groleau MC, Dietl AM, Visca P, Haas H, Déziel E, Stevens DA, Studies of *Pseudomonas aeruginosa* mutants indicate pyoverdine as the central factor in inhibition of *Aspergillus fumigatus* biofilm. (2018).
- [91] J.C. Penner, J.A.G. Ferreira, P.R. Secor, J.M. Sweere, M.K. Birukova, L.M. Joubert, J.A.J. Haagensen, O. Garcia, A.V. Malkovskiy, G. Kaber, H. Nazik, R. Manasherob, A.M. Spormann, K.V. Clemons, D.A. Stevens P.L. Bollyky, Pf4 bacteriophage produced by *Pseudomonas aeruginosa* inhibits *Aspergillus fumigatus* metabolism via iron sequestration. *Microbiology (Reading)*. 162 (2016) 1583-1594.
- [92] J.A. Ferreira, J.C. Penner, R.B. Moss, J.A. Haagensen, K.V. Clemons, A.M. Spormann, H. Nazik, K. Cohen, N. Banaei, E. Carolino D.A. Stevens, Inhibition of *Aspergillus fumigatus* and Its Biofilm by *Pseudomonas aeruginosa* Is Dependent on the Source, Phenotype and Growth Conditions of the Bacterium. *PLoS One*. 10 (2015) e0134692.
- [93] R.W. Bastos, D. Akiyama, T.F. Dos Reis, A.C. Colabardini, R.S. Luperini, P.A. de Castro, R.L. Baldini, T. Fill G.H. Goldman, Secondary Metabolites Produced during *Aspergillus fumigatus* and *Pseudomonas aeruginosa* Biofilm Formation. *mBio*. 13 (2022) e0185022.
- [94] E. Reece, S. Doyle, P. Grealley, J. Renwick S. McClean, *Aspergillus fumigatus* Inhibits *Pseudomonas aeruginosa* in Co-culture: Implications of a Mutually Antagonistic Relationship on Virulence and Inflammation in the CF Airway. *Front Microbiol*. 9 (2018) 1205.
- [95] G. Sass, S.R. Ansari, A.M. Dietl, E. Deziel, H. Haas D.A. Stevens, Intermicrobial interaction: *Aspergillus fumigatus* siderophores protect against competition by *Pseudomonas aeruginosa*. *PLoS One*. 14 (2019) e0216085.
- [96] W.J. Moree, V.V. Phelan, C.H. Wu, N. Bandeira, D.S. Cornett, B.M. Duggan P.C. Dorrestein, Interkingdom metabolic transformations captured by microbial imaging mass spectrometry. *Proc Natl Acad Sci U S A*. 109 (2012) 13811-13816.

- [97] I. Kotta-Loizou R.H.A. Coutts, Mycoviruses in Aspergilli: A Comprehensive Review. *Frontiers in Microbiology*. 8 (2017).
- [98] M.J. Schmitt F. Breinig, The viral killer system in yeast: from molecular biology to application. *FEMS Microbiol Rev*. 26 (2002) 257-276.
- [99] F.R. Schmidt, P.A. Lemke K. Esser, Viral influences on aflatoxin formation by *Aspergillus flavus*. *Applied Microbiology and Biotechnology*. 24 (1986) 248-252.
- [100] A. Ninomiya, S.I. Urayama, R. Suo, S. Itoi, S.I. Fuji, H. Moriyama D. Hagiwara, Mycovirus-Induced Tenuazonic Acid Production in a Rice Blast Fungus *Magnaporthe oryzae*. *Front Microbiol*. 11 (2020) 1641.
- [101] L. Nerva, W. Chitarra, I. Siciliano, F. Gaiotti, M. Ciuffo, M. Forgia, G.C. Varese M. Turina, Mycoviruses mediate mycotoxin regulation in *Aspergillus ochraceus*. *Environ Microbiol*. 21 (2019) 1957-1968.
- [102] M.F. Bhatti, A. Jamal, E.M. Bignell, M.A. Petrou R.H. Coutts, Incidence of dsRNA mycoviruses in a collection of *Aspergillus fumigatus* isolates. *Mycopathologia*. 174 (2012) 323-326.
- [103] H. Nazik, I. Kotta-Loizou, G. Sass, R.H.A. Coutts D.A. Stevens, Virus Infection of *Aspergillus fumigatus* Compromises the Fungus in Intermicrobial Competition. *Viruses*. 13 (2021).
- [104] L. Kanhayuwa, I. Kotta-Loizou, S. Ozkan, A.P. Gunning R.H. Coutts, A novel mycovirus from *Aspergillus fumigatus* contains four unique dsRNAs as its genome and is infectious as dsRNA. *Proc Natl Acad Sci U S A*. 112 (2015) 9100-9105.
- [105] G. Sass, I. Kotta-Loizou, M. Martinez, D.J. Larwood D.A. Stevens, Polymycovirus Infection Sensitizes *Aspergillus fumigatus* for Antifungal Effects of Nikkomycin Z. *Viruses*. 15 (2023).
- [106] D.A. Stevens, I. Kotta-Loizou, M. Martinez, R.H.A. Coutts G. Sass, Virus Infection Impairs Fungal Response to Stress: Effect of Salt. *Viruses*. 15 (2023).
- [107] A. Takahashi-Nakaguchi, E. Shishido, M. Yahara, S.-i. Urayama, A. Ninomiya, Y. Chiba, K. Sakai, D. Hagiwara, H. Chibana, H. Moriyama T. Gono, Phenotypic and Molecular Biological Analysis of Polymycovirus AfuPmV-1M From *Aspergillus fumigatus*: Reduced Fungal Virulence in a Mouse Infection Model. *Frontiers in Microbiology*. 11 (2020).
- [108] S. Ozkan R.H. Coutts, *Aspergillus fumigatus* mycovirus causes mild hypervirulent effect on pathogenicity when tested on *Galleria mellonella*. *Fungal Genet Biol*. 76 (2015) 20-26.

- [109] J. Jennessen, J. Schnurer, J. Olsson, R.A. Samson J. Dijksterhuis, Morphological characteristics of sporangiospores of the tempe fungus *Rhizopus oligosporus* differentiate it from other taxa of the *R. microsporus* group. *Mycol Res.* 112 (2008) 547-563.
- [110] Y. Ogawa, S. Tokumasu K. Tubaki, An original habitat of tempeh molds. *Mycoscience.* 45 (2004) 271-276.
- [111] M.M. Roden, T.E. Zaoutis, W.L. Buchanan, T.A. Knudsen, T.A. Sarkisova, R.L. Schaufele, M. Sein, T. Sein, C.C. Chiou, J.H. Chu, D.P. Kontoyiannis T.J. Walsh, Epidemiology and Outcome of Zygomycosis: A Review of 929 Reported Cases. *Clinical Infectious Diseases.* 41 (2005) 634-653.
- [112] E. Alvarez, D.A. Sutton, J. Cano, A.W. Fothergill, A. Stchigel, M.G. Rinaldi J. Guarro, Spectrum of zygomycete species identified in clinically significant specimens in the United States. *J Clin Microbiol.* 47 (2009) 1650-1656.
- [113] H. Prakash, A.K. Ghosh, S.M. Rudramurthy, P. Singh, I. Xess, J. Savio, U. Pamidimukkala, J. Jillwin, S. Varma, A. Das, N.K. Panda, S. Singh, A. Bal A. Chakrabarti, A prospective multicenter study on mucormycosis in India: Epidemiology, diagnosis, and treatment. *Med Mycol.* 57 (2019) 395-402.
- [114] M. Slavin, S. van Hal, T.C. Sorrell, A. Lee, D.J. Marriott, K. Daveson, K. Kennedy, K. Hajkovicz, C. Halliday, E. Athan, N. Bak, E. Cheong, C.H. Heath, C. Orla Morrissey, S. Kidd, R. Beresford, C. Blyth, T.M. Korman, J. Owen Robinson, W. Meyer, S.C. Chen, Australia G. New Zealand Mycoses Interest, Invasive infections due to filamentous fungi other than *Aspergillus*: epidemiology and determinants of mortality. *Clin Microbiol Infect.* 21 (2015) 490 e491-410.
- [115] A. Chakrabarti, S.S. Chatterjee, A. Das, N. Panda, M.R. Shivaprakash, A. Kaur, S.C. Varma, S. Singhi, A. Bhansali V. Sakhuja, Invasive zygomycosis in India: experience in a tertiary care hospital. *Postgrad Med J.* 85 (2009) 573-581.
- [116] H. PrakashA. Chakrabarti, Global Epidemiology of Mucormycosis. *J Fungi (Basel).* 5 (2019).
- [117] T.J. Walsh, M.N. Gamaletsou, M.R. McGinnis, R.T. Hayden D.P. Kontoyiannis, Early clinical and laboratory diagnosis of invasive pulmonary, extrapulmonary, and disseminated mucormycosis (zygomycosis). *Clin Infect Dis.* 54 Suppl 1 (2012) S55-60.
- [118] J. Larche, M. Machouart, K. Burton, J. Collomb, M.F. Biava, A. Gerard B. Fortier, Diagnosis of cutaneous mucormycosis due to *Rhizopus microsporus* by an

- innovative PCR-restriction fragment-length polymorphism method. *Clin Infect Dis.* 41 (2005) 1362-1365.
- [119] K. Nagao, T. Ota, A. Tanikawa, Y. Takae, T. Mori, S. Udagawa T. Nishikawa, Genetic identification and detection of human pathogenic *Rhizopus* species, a major mucormycosis agent, by multiplex PCR based on internal transcribed spacer region of rRNA gene. *J Dermatol Sci.* 39 (2005) 23-31.
- [120] A. Kyvernitakis, H.A. Torres, Y. Jiang, G. Chamilos, R.E. Lewis D.P. Kontoyiannis, Initial use of combination treatment does not impact survival of 106 patients with haematologic malignancies and mucormycosis: a propensity score analysis. *Clin Microbiol Infect.* 22 (2016) 811 e811-811 e818.
- [121] K. Voigt, T. Wolf, K. Ochsenreiter, G. Nagy, K. Kaerger, E. Shelest T. Papp, 15 Genetic and Metabolic Aspects of Primary and Secondary Metabolism of the Zygomycetes, in *Biochemistry and Molecular Biology*, D. Hoffmeister, Editor. 2016, Springer International Publishing: Cham. p. 361-385.
- [122] W.M. Artis, J.A. Fountain, H.K. Delcher H.E. Jones, A mechanism of susceptibility to mucormycosis in diabetic ketoacidosis: transferrin and iron availability. *Diabetes.* 31 (1982) 1109-1114.
- [123] J.R. Boelaert, A.Z. Fenves J.W. Coburn, Deferoxamine therapy and mucormycosis in dialysis patients: report of an international registry. *Am J Kidney Dis.* 18 (1991) 660-667.
- [124] H.M. Drechsel, J.; Freund, S.; Jung, G.; Boelaert, J.R.; Winkelmann, G., Rhizoferrin—A novel siderophore from the fungus *Rhizopus microsporus* var. *rhizopodiformis*. (1991).
- [125] H. Drechsel, Tschierske, M., Thieken, A., Jung, G., Zähner, H. and Winkelmann, G, The carboxylate type siderophore rhizoferrin and its analogs produced by directed fermentation (1995).
- [126] C.S. Carroll, C.L. Grieve, I. Murugathasan, A.J. Bennet, C.M. Czekster, H. Lui, J. Naismith M.M. Moore, The rhizoferrin biosynthetic gene in the fungal pathogen *Rhizopus deleamar* is a novel member of the NIS gene family. *Int. J. Biochem. Cell Biol.* 89 (2017) 136-146.
- [127] M. de Locht, J.R. Boelaert Y.J. Schneider, Iron uptake from ferrioxamine and from ferrirhizoferrin by germinating spores of *Rhizopus microsporus*. *Biochem Pharmacol.* 47 (1994) 1843-1850.

- [128] M. Vanlandewijck, L. He, M.A. Mäe, J. Andrae, K. Ando, F. Del Gaudio, K. Nahar, T. Lebouvier, B. Laviña, L. Gouveia, Y. Sun, E. Raschperger, M. Räsänen, Y. Zarb, N. Mochizuki, A. Keller, U. Lendahl C. Betsholtz, A molecular atlas of cell types and zonation in the brain vasculature. *Nature*. 554 (2018) 475-480.
- [129] A.M. Collins, J. Rylance, D.G. Wootton, A.D. Wright, A.K. Wright, D.G. Fullerton S.B. Gordon, Bronchoalveolar lavage (BAL) for research; obtaining adequate sample yield. *J Vis Exp*, (2014).
- [130] A. Škríba, Patil, R.H., Hubáček, P., Dobiáš, R., Palyzová, A., Marešová, H., Pluháček, T. and Havlíček, V., Rhizoferrin Glycosylation in *Rhizopus microsporus*. (2020).
- [131] E. Layre, L. Sweet, S. Hong, C.A. Madigan, D. Desjardins, D.C. Young, T.-Y. Cheng, J.W. Annand, K. Kim I.C. Shamputa, A comparative lipidomics platform for chemotaxonomic analysis of *Mycobacterium tuberculosis*. *Chemistry & biology*. 18 (2011) 1537-1549.
- [132] D. Luptakova, R.H. Patil, R. Dobias, D.A. Stevens, T. Pluhacek, A. Palyzova, M. Kanova, M. Navratil, Z. Vrba, P. Hubacek V. Havlicek, Siderophore-Based Noninvasive Differentiation of *Aspergillus fumigatus* Colonization and Invasion in Pulmonary Aspergillosis. *Microbiol Spectr*. 11 (2023) e0406822.
- [133] J. Schindelin, I. Arganda-Carreras, E. Frise, V. Kaynig, M. Longair, T. Pietzsch, S. Preibisch, C. Rueden, S. Saalfeld B. Schmid, Fiji: an open-source platform for biological-image analysis. *Nature methods*. 9 (2012) 676-682.
- [134] Bioanalytical method validation: guidance for industry. US Food and Drug Administration, Silver Spring, MD. (2018).
- [135] J. Novak, A. Skriba V. Havlicek, CycloBranch 2: Molecular Formula Annotations Applied to imzML Data Sets in Bimodal Fusion and LC-MS Data Files. *Anal Chem*. 92 (2020) 6844-6849.
- [136] R.H. Patil, I. Kotta-Loizou, A. Palyzova, T. Pluhacek, R.H.A. Coutts, D.A. Stevens V. Havlicek, Freeing *Aspergillus fumigatus* of Polymycovirus Infection Renders It More Resistant to Competition with *Pseudomonas aeruginosa* Due to Altered Iron-Acquiring Tactics. *J Fungi (Basel)*. 7 (2021).
- [137] R.H. Patil, I. Kotta-Loizou, A. Palyzova, T. Pluhacek, R.H.A. Coutts, D.A. Stevens V. Havlicek, Correction: Patil et al. Freeing *Aspergillus fumigatus* of Polymycovirus Infection Renders It More Resistant to Competition with

- Pseudomonas aeruginosa* Due to Altered Iron-Acquiring Tactics. *J. Fungi* 2021, 7, 497. *J Fungi (Basel)*. 8 (2022).
- [138] E.J. Want, I.D. Wilson, H. Gika, G. Theodoridis, R.S. Plumb, J. Shockcor, E. Holmes J.K. Nicholson, Global metabolic profiling procedures for urine using UPLC-MS. *Nat Protoc.* 5 (2010) 1005-1018.
- [139] M. Hoenigl, T. Orasch, K. Faserl, J. Prattes, J. Loeffler, J. Springer, F. Gsaller, F. Reischies, W. Duettmann, R.B. Raggam, H. Lindner H. Haas, Triacetylfusarinine C: a urine biomarker for diagnosis of invasive aspergillosis. *J Infection.* 78 (2019) 150-157.
- [140] R. Dobias, P. Jahn, K. Tothova, O. Dobesova, D. Visnovska, R. Patil, A. Skriba, P. Jaworska, M. Skoric, L. Podojil, M. Kantorova, J. Mrazek, E. Krejci, D.A. Stevens V. Havlicek, Diagnosis of Aspergillosis in Horses. *J Fungi (Basel)*. 9 (2023).
- [141] R.H. Patil, D. Luptakova V. Havlicek, Infection metallomics for critical care in the post-COVID era. *Mass Spectrom Rev.* 42 (2023) 1221-1243.
- [142] T. Pluháček, A. Škríba, J. Novák, D. Luptáková V. Havlíček, Analysis of microbial siderophores by mass spectrometry, in *Methods in Molecular Biology*, S.K. Bhattacharya, Editor. 2019, Springer Nature.
- [143] T. Pluháček, K. Lemr, D. Ghosh, D. Milde, J. Novák V. Havlíček, Characterization of microbial siderophores by mass spectrometry. *Mass Spectrometry Reviews.* 35 (2016) 35-47.
- [144] J. Novák, A. Škríba, J. Zápál, M. Kuzma V. Havlíček, CycloBranch: An open tool for fine isotope structures in conventional and product ion mass spectra. *J Mass Spectrom.* 53 (2018) 1097-1103.
- [145] J. Novák, A. Škríba V. Havlíček, CycloBranch 2: molecular formula annotations applied to imzML data sets in bimodal fusion and LC-MS data files. *Anal Chem.* 92 (2020) 6844-6849.
- [146] J. PrivratskyJ. Novak, MassSpecBlocks: a web-based tool to create building blocks and sequences of nonribosomal peptides and polyketides for tandem mass spectra analysis. *J Cheminform.* 13 (2021) 51.
- [147] D. Luptáková, T. Pluháček, M. Petřík, J. Novák, A. Palyzová, L. Sokolová, A. Škríba, B. Šedivá, K. Lemr V. Havlíček, Non-invasive and invasive diagnoses of aspergillosis in a rat model by mass spectrometry. *Sci Rep.* 7 (2017) 16523.



- [148] T. Pluháček, M. Petřík, D. Luptáková, O. Benada, A. Palyzová, K. Lemr V. Havlíček, *Aspergillus* infection monitored by multimodal imaging in a rat model. *Proteomics*. 16 (2016) 1785-1792.
- [149] A. Škríba, T. Pluháček, A. Palyzová, Z. Novy, K. Lemr, M. Hajduch, M. Petřík V. Havlíček, Early and non-invasive diagnosis of aspergillosis revealed by infection kinetics monitored in a rat model. *Front Microbiol*. 9 (2018) 2356.
- [150] C.S. Carroll, L.N. Amankwa, L.J. Pinto, J.D. Fuller M.M. Moore, Detection of a serum siderophore by LC-MS/MS as a potential biomarker of invasive aspergillosis. *PLoS One*. 11 (2016) e0151260.
- [151] R. Dobias, A. Skriba, T. Pluhacek, M. Petrik, A. Palyzova, M. Kanova, E. Cubova, J. Houst, J. Novak, D.A. Stevens, G. Mitulovic, E. Krejci, P. Hubacek V. Havlicek, Noninvasive Combined Diagnosis and Monitoring of Aspergillus and Pseudomonas Infections: Proof of Concept. *J Fungi (Basel)*. 7 (2021).
- [152] K. Gupta, L. Grigoryan B. Trautner, Urinary tract infection. *Ann Intern Med*. 167 (2017) ITC49-ITC64.
- [153] G. Ghseini, C. Brutesco, L. Ouerdane, C. Fojcik, A. Izaute, S. Wang, C. Hajjar, R. Lobinski, D. Lemaire, P. Richaud, R. Voulhoux, A. Espaillat, F. Cava, D. Pignol, E. Borezée-Durant P. Arnoux, Biosynthesis of a broad-spectrum nicotianamine-like metallophore in *Staphylococcus aureus*. *Science*. 352 (2016) 1105-1109.
- [154] J.L. Cotton, J. Tao C.J. Balibar, Identification and characterization of the *Staphylococcus aureus* gene cluster coding for staphyloferrin A. *Biochemistry*. 48 (2009) 1025-1035.
- [155] W.J. Perry, J.M. Spraggins, J.R. Sheldon, C.M. Grunenwald, D.E. Heinrichs, J.E. Cassat, E.P. Skaar R.M. Caprioli, *Staphylococcus aureus* exhibits heterogeneous siderophore production within the vertebrate host. *Proc Natl Acad Sci USA*. 116 (2019) 21980-21982.
- [156] D. Perkins-Balding, M. Ratliff-Griffin I. Stojiljkovic, Iron transport systems in *Neisseria meningitidis*. *Microbiol Mol Biol Rev*. 68 (2004) 154-171.
- [157] N. Simon, V. Coulanges, P. Andre D.J. Vidon, Utilization of exogenous siderophores and natural catechols by *Listeria monocytogenes*. *Appl Environ Microb*. 61 (1995) 1643-1645.
- [158] J.L. Vincent, J. Rello, J. Marshall, E. Silva, A. Anzueto, C.D. Martin, R. Moreno, J. Lipman, C. Gomersall, Y. Sakr, K. Reinhart E.I.G.o. Investigators, International

- study of the prevalence and outcomes of infection in intensive care units. *JAMA*. 302 (2009) 2323-2329.
- [159] J.L. Vincent, Y. Sakr, M. Singer, I. Martin-Loeches, F.R. Machado, J.C. Marshall, S. Finfer, P. Pelosi, L. Brazzi, D. Aditjaningsih, J.F. Timsit, B. Du, X. Wittebole, J. Maca, S. Kannan, L.A. Gorordo-Delsol, J.J. De Waele, Y. Mehta, M.J.M. Bonten, A.K. Khanna, M. Kollef, M. Human, D.C. Angus E.I. Investigators, Prevalence and Outcomes of Infection Among Patients in Intensive Care Units in 2017. *JAMA*. 323 (2020) 1478-1487.
- [160] A. Johnová, M. Dobišová, M.A. Abdallah P. Kyslík, Overproduction of pyoverdins by Fur mutants of *Pseudomonas aeruginosa* strains PAO1 and Fe10 in stirred bioreactors. *Biotechnol Lett*. 23 (2001) 1759-1763.
- [161] R. DobiášV. Havlíček, Microbial siderophores: markers of infectious diseases, in *Microbial and natural macromolecules: synthesis and applications*, S. Das and H.R. Das, Editors. 2021, Academic Press, Elsevier, USA.
- [162] H. Kamimura, Conversion of zearalenone to zearalenone glycoside by *Rhizopus* sp. *Appl Environ Microbiol*. 52 (1986) 515-519.
- [163] A. Margalit, D. Sheehan, J.C. Carolan K. Kavanagh, Exposure to the *Pseudomonas aeruginosa* secretome alters the proteome and secondary metabolite production of *Aspergillus fumigatus*. *Microbiology (Reading)*. 168 (2022).
- [164] E.K. Manavathu, D.L. Vager J.A. Vazquez, Development and antimicrobial susceptibility studies of in vitro monomicrobial and polymicrobial biofilm models with *Aspergillus fumigatus* and *Pseudomonas aeruginosa*. *BMC Microbiol*. 14 (2014) 53.
- [165] B.P. Knox, Q. Deng, M. Rood, J.C. Eickhoff, N.P. Keller A. Huttenlocher, Distinct innate immune phagocyte responses to *Aspergillus fumigatus* conidia and hyphae in zebrafish larvae. *Eukaryot Cell*. 13 (2014) 1266-1277.
- [166] M. Bassetti, E. Azoulay, B.-J. Kullberg, M. Ruhnke, S. Shoham, J. Vazquez, D.R. Giacobbe T. Calandra, EORTC/MSGERC definitions of invasive fungal diseases: summary of activities of the intensive care unit working group. *Clin Infect Dis*. 72 (2021) S121-S127.
- [167] C. Cafarchia, L.A. Figueredo D. Otranto, Fungal diseases of horses. *Vet Microbiol*. 167 (2013) 215-234.
- [168] O. Dobesova, B. Schwarz, K. Velde, P. Jahn, Z. Zert B. Bezdekova, Guttural pouch mycosis in horses: a retrospective study of 28 cases. *Vet Rec*. 171 (2012) 561.

- [169] L.W. Pace, N.R. Wirth, R.R. Foss W.H. Fales, Endocarditis and pulmonary aspergillosis in a horse. *J Vet Diagn Invest.* 6 (1994) 504-506.
- [170] J.P. Donnelly, S.C. Chen, C.A. Kauffman, W.J. Steinbach, J.W. Baddley, P.E. Verweij, C.J. Clancy, J.R. Wingard, S.R. Lockhart, A.H. Groll, T.C. Sorrell, M. Bassetti, H. Akan, B.D. Alexander, D. Andes, E. Azoulay, R. Bialek, R.W. Bradsher, Jr, S. Bretagne, T. Calandra, A.M. Caliendo, E. Castagnola, M. Cruciani, M. Cuenca-Estrella, C.F. Decker, S.R. Desai, B. Fisher, T. Harrison, C.P. Heussel, H.E. Jensen, C.C. Kibbler, D.P. Kontoyiannis, B.-J. Kullberg, K. Lagrou, F. Lamoth, T. Lehrnbecher, J. Loeffler, O. Lortholary, J. Maertens, O. Marchetti, K.A. Marr, H. Masur, J.F. Meis, C.O. Morrissey, M. Nucci, L. Ostrosky-Zeichner, L. Pagano, T.F. Patterson, J.R. Perfect, Z. Racil, E. Roilides, M. Ruhnke, C.S. Prokop, S. Shoham, M.A. Slavin, D.A. Stevens, G.R. Thompson, III, J.A. Vazquez, C. Viscoli, T.J. Walsh, A. Warris, L.J. Wheat, P.L. White, T.E. Zaoutis P.G. Pappas, Revision and update of the consensus definitions of invasive fungal disease from the European organization for research and treatment of cancer and the mycoses study group education and research consortium. *Clin Infect Dis*, (2019).

## LIST OF ABBREVIATIONS

<b>1-HP</b>	1-hydroxyphenazine
<b>ABPA</b>	Allergic bronchopulmonary aspergillosis
<b>ACN</b>	Acetonitrile
<b>AfuPmV-1</b>	<i>A.fumigatus</i> polymycovirus 1
<b>BALF</b>	bronchoalveolar lavage fluid
<b>BDG</b>	$\beta$ -1,3-glucan
<b>BmGtx</b>	bisdethiobis(methylthio)-gliotoxin
<b>CCPA</b>	chronic cavitary pulmonary aspergillosis
<b>CF</b>	cystic fibrosis
<b>CPA</b>	chronic pulmonary aspergillosis
<b>CNS</b>	central nervous system
<b>COPD</b>	chronic obstructive pulmonary disease
<b>DHN</b>	dihydroxy naphthalene
<b>FA</b>	formic acid
<b>Fc</b>	ferricrocin
<b>FoxE</b>	ferrioxamine E
<b>FsC</b>	fusarinine C
<b>FTICR</b>	fourier transform ion cyclotron resonance
<b>GM</b>	galactomannan
<b>GPM</b>	guttural pouch mycoses
<b>Gtx</b>	gliotoxin
<b>Hfc</b>	hydroxyferricrocin
<b>IgE</b>	immunoglobulin E
<b>ICP</b>	inductively coupled plasma
<b>IPA</b>	invasive pulmonary aspergillosis
<b>LFD</b>	lateral flow device
<b>LOD</b>	limit of detection
<b>LOQ</b>	limit of quantitation
<b>MeOH</b>	methanol
<b>NETs</b>	neutrophil extracellular traps
<b>NRPS</b>	non-ribosomal peptide synthetase

<b>PCA</b>	phenazine-1-carboxylic acid
<b>PCR</b>	polymerase chain reaction
<b>PET</b>	positron emission tomography
<b>PRRs</b>	pattern recognition receptors (PRRs)
<b>Ptx3</b>	pentraxin 3
<b>QS</b>	quorum sensing
<b>RHF</b>	rhizoferrin
<b>ROS</b>	reactive oxygen species
<b>SD</b>	standard deviation
<b>SPE</b>	solid phase extractions
<b>TafB</b>	triacylfusarinine B TafB
<b>TafC</b>	triacylfusarinine C
<b>TLRs</b>	toll-like receptors
<b>TOF</b>	time-of-flight

# CURRICULUM VITAE

**Name:** RUTUJA HIRAJI PATIL  
**Year and place of birth:** 1995, Maharashtra, India  
**E-mail:** rutuja.patil@biomed.cas.cz

## Education:

2013 - 2016 Bachelor of Science in Biotechnology, Maharashtra Education Society Abasaheb Garware College, Pune, India.

2016 - 2018 Master of Science in Biotechnology, Pondicherry University, India. Title: Standardization of inflammation induced sepsis in Sprague Dawley rats. (Supervisor: Prof. A. Hannah Rachel Vasanthi).

2018-2019 Advanced Post Graduate-Diploma in life science technologies, Sri Ramaswamy Memorial (SRM)- Department of Biotechnology Platform (DBT), SRM Institute of Science and Technology, Chennai, India. Topic: Urinary metabolomics analysis for biomarker identification in diabetic nephropathy. (Supervisor: Dr. M.Vairamani and Dr. K.M. Ramkumar).

2019 - Current PhD Student, Department of Analytical Chemistry, Faculty of Science, Palacký University, Olomouc, Czech Republic. Topic: Metabolomics of clinically important *Aspergillus fumigatus* and *Rhizopus microsporus* in diagnoses of invasive infections (Supervisor: Prof. Ing. Vladimír Havlíček).

## Internships:

2017 Research stay, School of life science, University of Hyderabad, India (3 months) Title: Cloning of dopamine receptors in *Clarias gariepinus* (Supervisor: Prof. B. Senthilkumaran).

2022-2023 PhD Research stay, Imperial College London, Department of Life Sciences, London, United Kingdom, (3 months) Title: Mycotoxin gene expression analysis in *A. fumigatus* polymycovirus strains (Supervision: Dr. Ioly Kotta-Loizou)

#### **Grants:**

- Principal investigator: Doctoral student grant competition at Palacký University Olomouc, grant no. DSGC-2021-0144 (2022), Title: Small molecular weight neutrophil secretome stimulated by *Aspergillus fumigatus*.
- Team member: Internal Grant Agency of Palacký University grant IGA\_PrF\_2022\_023.
- Team member: Czech Science Foundation, grant No. 21-17044S (2021-2023), Next Generation Infection Diagnostics.
- Team member: Czech Health Research Council, grant No. NU23-05-00095 (2023-2026), A prospective study on invasive pulmonary aspergillosis.

#### **Publications:**

- Škríba, A., Patil, R.H., Hubáček, P., Dobiáš, R., Palyzová, A., Marešová, H., Pluháček, T. and Havlíček, V., 2020. Rhizoferrin glycosylation in *Rhizopus microsporus*. *Journal of Fungi*, 6, p.89. DOI: 10.3390/jof6020089.
- Patil, R.H., Kotta-Loizou, I., Palyzová, A., Pluháček, T., Coutts, R.H., Stevens, D.A. and Havlíček, V., 2021. Freeing *Aspergillus fumigatus* of polymycovirus infection renders it more resistant to competition with *Pseudomonas aeruginosa* due to altered iron-acquiring tactics. *Journal of Fungi*, 7, p.497. DOI: 10.3390/jof7070497.
- Dobiáš, R., Jahn, P., Tóthová, K., Dobešová, O., Višňovská, D., Patil, R., Škríba, A., Jaworská, P., Škorič, M., Podojil, L. and Kantorová, M., 2023. Diagnosis of Aspergillosis in Horses. *Journal of Fungi*, 9, p.161. DOI: 10.3390/jof9020161
- Luptáková, D., Patil, R.H., Dobiáš, R., Stevens, D.A., Pluháček, T., Palyzová, A., Káňová, M., Navrátil, M., Vrba, Z., Hubáček, P. and Havlíček, V., 2023. Siderophore-based noninvasive differentiation of *Aspergillus fumigatus*

colonization and invasion in pulmonary aspergillosis. *Microbiology Spectrum*, 11, pp.e04068-22. DOI: 10.1128/spectrum.04068-22.

- Patil, R.H., Luptáková, D. and Havlíček, V., 2023. Infection metallomics for critical care in the post-COVID era. *Mass Spectrometry Reviews*. DOI: 10.1002/mas.21755.

#### **Conference poster presentations:**

- Patil, R.H., Kotta-Loizou, I., Palyzová, A., Pluháček, T., Stevens D.A., Havlíček, V., Freeing the *Aspergillus fumigatus* of the polynuclease makes it more resistant in the competition with *Pseudomonas* due to the altered iron-acquiring tactics. European Congress of Clinical Microbiology and Infectious Diseases, online, July 9-12, 2021, Poster No. 04053.
- Patil, R.H., Kotta-Loizou, I., Palyzová, A., Pluháček, T., Coutts, R., Stevens, D.A., Havlíček, V., Mycotoxin secretion by *Aspergillus fumigatus* as a response to mycovirus infection. The Advances against Aspergillosis and Mucormycosis virtual conference, Feb 2-3, 2022, Poster No. 42. One of the outstanding posters presented at the conference.
- Patil, R. H., Luptáková, D., Havlíček, V., Infection metallomics based functional studies in *Aspergillus fumigatus*. Proceedings of Advances in Chromatography and Electrophoresis & Chiranal, Olomouc June 13-16, 2022, Czech Republic.

#### **Conference oral presentations:**

- Patil, R.H., Dobiáš, R., Škríba, A., Pluháček, T., Luptáková, D., Palyzová, A., Havlíček, V., On the threshold between *Aspergillus fumigatus* colonization and proliferation in a host. The 31st MassSpec Forum, Feb 25-26, 2020, Vienna, Austria.
- Patil, R.H., Luptáková, D., Dobiáš, R., Pluháček, T., Palyzová, A., Havlíček, V., Extracellular secretome in polarized *Aspergillus fumigatus* growth triggers the invasive aspergillosis in a host. The Ninth Annual Conference of the Czech Society for Mass Spectrometry, Oct 11-12, 2021, Prague, Czech Republic.



- Patil, R.H., Kotta-Loizou, I., Palyzová, A., Pluháček, T., Coutts, R., Stevens D.A., Havlíček, V., Freeing *Aspergillus fumigatus* of Polymycovirus Infection Renders it More Resistant to Competition with *Pseudomonas aeruginosa* due to Altered Iron-Acquiring Tactics. Prague Meeting on Historical Perspectives of Mass Spectrometry & Opening of the Czech Mass Spectrometry Museum, Oct 13-14, 2021, Prague, Czech Republic.
- EU FT-ICR MS 2<sup>nd</sup> advanced user school Prague, Czech Republic (2021).
- Patil, R.H., Luptáková, D., Dobiáš, R., Stevens, D.A., Pluháček, T., Palyzová, A., A., Havlíček, V., Infection metallomics-based differentiation of *Aspergillus fumigatus* colonization and invasion. The 24th International Mass Spectrometry Conference, Maastricht, The Netherlands, 27 Aug-2 Sept 2022.
- Patil, R.H., Juříková T., Mácha H., Hrdý J., Marešová H., Palyzová A., Benada O. and Havlíček V., *Aspergillus fumigatus* and *Pseudomonas aeruginosa* interplay at a host interface. The Eleventh Annual Conference of the Czech Society for Mass Spectrometry, June 19-21, 2023, Brno, Czech Republic.

### **Scholarships and awards**

- J. L. Fisher scholarship, Olomouc, Czech Republic (2019 - Present).
- Nico Nibbering Student Travel Award to attend the 24th International Mass Spectrometry Conference, Maastricht, The Netherlands (2022).
- Austrian Proteomics & Metabolomics Association (APMA) travel grant for the 31st MassSpec Forum Vienna, Austria (2020).
- SRM-DBT fellowship, Chennai, India (2018 - 2019).
- Jawaharlal Nehru University (JNU-DBT) fellowship, Delhi, India (2016 - 2018).

## **Trainings**

- EU FT-ICR MS 2nd advanced user school Prague, Czech Republic (2021).
- A course in Mass Spectroscopy: “Fundamentals and Applications” organized by SRM-IST, Chennai, India (2018).
- Industrial training at Serum institute of India PVT. LTD. Pune India on large scale manufacturing of Diphtheria, Tetanus, Pertussis, Hib, BCG, r- Hepatitis B, Measles vaccines production and its quality control (2016).

**PALACKÝ UNIVERSITY IN OLOMOUC**

**Faculty of Science**

**Department of Analytical Chemistry**



**Metabolomics of clinically important *Aspergillus fumigatus* and *Rhizopus microsporus* in the diagnoses of invasive fungal infections**

**SUMMARY  
OF THE DOCTORAL THESIS**

Author:	Rutuja Hiraji Patil
Field of study:	Analytical Chemistry
Supervisor:	prof. Ing. Vladimír Havlíček, Dr.

**Olomouc 2023**

# SUMMARY

*Aspergillus fumigatus* and *Rhizopus microsporus* are globally distributed pathogenic fungi responsible for causing a wide spectrum of infections called aspergillosis and mucormycosis, respectively. The diagnosis of these infections still faces challenges due to various factors such as non-specific clinical symptoms, overlapping risk factors, non-discrimination between colonization and invasive infection and limited sensitivity to already existing diagnostic tools. Moreover, the increase in antifungal resistance and vaccine unavailability to these infections emphasizes the critical need for specific and timely diagnostics.

One area of research is using mycotoxins and microbial metallophores, specifically siderophores, which play crucial roles in fungal growth, survival, and pathogenesis; as a result, their complex structures could enable high diagnostic specificity. Liquid chromatography-mass spectrometry-based metabolomics can provide accurate and rapid detection of these fungal metabolites and can also specify a comprehensive overview of pathogen-induced changes to the host cells following infection.

Therefore, the main goal of this thesis is the liquid chromatography-mass spectrometry (MS) based characterization of *A. fumigatus* and *R. microsporus* siderophores and other metabolites. The thesis focuses on the following four topics: introduction of infection metallomics, characterization of *R. microsporus* siderophores, characterization of *A. fumigatus* siderophores and mycotoxins to distinguish between colonization and invasion, as well as during inter-kingdom interaction with bacterial pathogen *Pseudomonas aeruginosa*, host cells-neutrophils and polymycovirus and finally, infection metallomics based diagnosis of human and equine aspergillosis.

The theoretical part covers general information on *A. fumigatus* and *R. microsporus*, related infections, secondary metabolites, and specific knowledge about each mentioned topic. Experimental, results and discussion parts are divided into corresponding sections to each topic. The first section introduces infection metallomics, a MS platform based on the central concept that microbial metallophores are specific, sensitive, noninvasive, and promising biomarkers of invasive infectious diseases. The second section of this thesis includes *R. microsporus in vitro* cultivation, followed by liquid chromatography-mass spectrometry analysis of its siderophores. The third section involves *in vitro* cultivation of *A. fumigatus* with subsequent growth stage-specific siderophore and mycotoxin quantification to distinguish between colonization and invasive infection. Additionally, this section deals with the time course quantification of *A. fumigatus* secondary metabolites during its interaction with neutrophils, bacterial pathogen *P. aeruginosa* and polymycovirus. The analysis is performed using developed metabolite extraction protocol and mass spectrometry methods.

The fourth and last part focuses on applying infection metallomics-based diagnosis in human invasive pulmonary aspergillosis and equine aspergillosis.

Taken together, this thesis shows the performance of the non-invasive infection metallomics armoury and makes difference towards the standard serology, cultivation, microscopy, or nucleic acid analyses routinely used in invasive fungal infection diagnostics. The thesis documents why the innovative non-invasive approach based on mass spectrometry based microbial metallophores detection with benefit of isotope data filtration is inherently more sensitive and specific in selected applications than classical clinical standards.

# SOUHRN

*Aspergillus fumigatus* a *Rhizopus microsporus* jsou celosvětově rozšířené patogenní houby způsobující široké spektrum infekcí obecně nazývaných aspergilóza a mukormykóza. Diagnostika těchto infekcí stále čelí problémům kvůli nespecifickým klinickým příznakům, překrývajícím se rizikovým faktorům, neschopnosti rozlišit mezi kolonizací a invazí patogenu a omezené citlivosti současných diagnostických metod. Nárůst rezistence vůči antimykotikům a nedostupnost vakcín proti těmto infekcím podtrhuje kritickou potřebu specifické a včasné diagnostiky.

Jedna z oblastí výzkumu cílí na využití mikrobiálních metaloforů (konkrétně sideroforů) a mykotoxinů, které hrají klíčovou roli v růstu, přežívání a patogenezí hub. Metabolomika založená na kapalinové chromatografii a hmotnostní spektrometrii těchto biomarkerů může poskytnout rychlou, přesnou a specifickou detekci těchto patogenů. Zároveň může také reflektovat komplexní přehled změn vyvolaných patogenem v hostitelských buňkách po infekci.

Hlavním cílem této práce je charakterizace sideroforů a dalších metabolitů *A. fumigatus* a *R. microsporus* pomocí kapalinové chromatografie a hmotnostní spektrometrie. Práce je rozdělena do čtyř témat: představení infekční metalomiky, charakterizace sideroforů *R. microsporus*, charakterizace sideroforů a mykotoxinů *A. fumigatus* pro rozlišení kolonizace, invaze a mezidruhové interakce s bakteriálním patogenem *Pseudomonas aeruginosa*, hostitelskými neutrofilů a polymykovirem, a na závěr diagnostika aspergilózy u lidí a koní za využití infekční metalomiky.

Teoretická část zahrnuje obecné informace o houbách *A. fumigatus* a *R. microsporus*, o infekcích, které tyto patogeny způsobují a o konkrétních sekundárních metabolitech. Experimentální část, výsledky a diskuse jsou rozděleny do příslušných oddílů ke každému tématu. První oddíl představuje infekční metalomiku, hmotnostně spektrometrickou platformu založenou na ústředním konceptu, že mikrobiální metalofory jsou specifické, citlivé, neinvazivní a slibné biomarkery invazivních infekčních onemocnění. Druhá část této práce zahrnuje kultivaci *R. microsporus in vitro*, po níž následuje analýza jeho sideroforů pomocí kapalinové chromatografie a hmotnostní spektrometrie.

Třetí část zahrnuje kultivaci *A. fumigatus in vitro* s následnou kvantifikací sideroforů a mykotoxinů specifických pro daná růstová stádia s cílem rozlišit mezi kolonizací a invazivní infekcí. Dále se tato část zabývá kvantitativním popisem časového průběhu sekundárních metabolitů *A. fumigatus* při jeho interakci s neutrofily, bakteriálním patogenem *P. aeruginosa* a polymykovirem. Analýza se provádí pomocí námi vyvinutého protokolu extrakce metabolitů a metod hmotnostní spektrometrie. Čtvrtá a poslední část je zaměřena na aplikaci infekční metalomiky při diagnostice invazivní plicní aspergilózy u lidí a u koní.

Tato práce ukazuje výkonnost neinvazivního přístupu infekční metalomiky v porovnání s rutinně používanými diagnostickými metodami, jako je standardní sérologie, kultivace, mikroskopie nebo analýza nukleových kyselin. Práce dokumentuje inovativní a neinvazivní přístup založený na detekci mikrobiálních metaloforů pomocí hmotnostní spektrometrie s využitím izotopové datové filtrace, jež je ve vybraných aplikacích citlivější a specifitější metoda v porovnání s klasickými diagnostickými přístupy.

# TABLE OF CONTENTS

1	<b>INTRODUCTION</b> .....	6
2	<b>THEORETICAL PART</b> .....	7
2.1	<i>Aspergillus fumigatus</i> .....	7
2.2	Secondary metabolites of <i>A. fumigatus</i> .....	7
2.3	<i>A. fumigatus</i> in interaction studies <i>in vitro</i> .....	8
2.4	<i>Rhizopus microsporus</i> and mucromycosis.....	8
2.5	Secondary metabolites of <i>R. microsporus</i> .....	9
3	<b>AIMS OF THE THESIS</b> .....	10
4	<b>EXPERIMENTAL PART</b> .....	11
4.1	Liquid chromatography-mass spectrometry (LC-MS) based characterization of <i>R. microsporus</i> siderophores.....	11
4.2	LC-MS based <i>A. fumigatus</i> growth-specific siderophore and mycotoxin quantitation to distinguish between colonization and invasive infection.....	12
4.2.1	<i>A. fumigatus</i> siderophores and mycotoxins production during interaction with neutrophils and <i>P. aeruginosa</i> .....	14
4.2.2	<i>A. fumigatus</i> siderophores and mycotoxins production during interaction with polymycovirus.....	16
4.3	Infection metallomics-based diagnostics.....	18
4.3.1	Human invasive pulmonary aspergillosis.....	18
4.3.2	Equine aspergillosis.....	20
5	<b>RESULTS AND DISCUSSION</b> .....	21
5.1	Introduction to infection metallomics.....	21
5.2	LC-MS based characterization of <i>R. microsporus</i> siderophores.....	27
5.3	LC-MS based <i>A. fumigatus</i> growth-specific siderophore and mycotoxin quantitation to distinguish between colonization and invasive infection.....	30
5.3.1	<i>A. fumigatus</i> siderophores and mycotoxins production during interaction with neutrophils and <i>P. aeruginosa</i> .....	32
5.3.2	<i>A. fumigatus</i> siderophores and mycotoxins production during interaction with polymycovirus.....	36
5.4	Infection metallomics-based diagnosis.....	40
5.4.1	Human invasive pulmonary aspergillosis.....	40
5.4.2	Equine aspergillosis.....	42
6	<b>CONCLUSIONS</b> .....	44
	<b>REFERENCES</b> .....	46
	<b>CURRICULUM VITAE</b> .....	50



# 1 INTRODUCTION

Throughout history, infectious diseases caused by pathogenic bacteria, fungi, and viruses have afflicted humans. The recent COVID-19 (Coronavirus disease 2019) pandemic is a daunting reminder that this susceptibility continues even in the medically/scientifically enhanced world. Unfortunately, some of these microbial threats are still unrecognized or neglected, and fungi infecting billions of people yearly are examples of such overlooked threats. Fungal infections represent emerging global diseases, accounting for approximately 1.7 million deaths annually [1]. During the COVID-19 pandemic, invasive fungal infection incidence increased significantly among hospitalized patients [2]. Regardless of the high mortality, invasive fungal infections remain understudied and underdiagnosed compared to other infectious diseases. Most fungal infections lack rapid, sensitive and timely diagnostics. Additionally, the long-term prophylactic use of antifungal drugs in high-risk patients has stimulated multidrug resistance in fungi. With growing concern, World Health Organization recently released a fungal priority pathogen list wherein *Aspergillus fumigatus* belonging to the critical propriety group, and Mucorales from the high priority group will be mainly discussed in this thesis [3].

The need for high-throughput techniques capable of capturing diverse aspects of disease, such as definition and monitoring of changes in metabolites and proteins, has unlocked the door for mass spectrometry (MS)-based techniques in clinical diagnostics. MS with electrospray ionization (ESI) and matrix-assisted laser desorption/ionization (MALDI) were introduced in the late 1980s to detect large protein molecules. Moreover, coupling liquid chromatography (LC) with ESI-MS added another dimension for the analysis of the crude biological mixture in less time, and expanded the analytical dynamic range. MS technologies are constantly evolving by designing new ion sources, boosting resolution and sensitivity, and miniaturization to bench-top instruments. Though MS-based tools are still underused in some clinical settings, it can potentially extend the current capabilities of detecting disease markers or therapeutic drug levels with exceptional precision, accuracy, and reproducibility.

## 2 THEORETICAL PART

### 2.1 *Aspergillus fumigatus*

*A.fumigatus* is a ubiquitous saprotrophic mould with the ability to survive up to 70 °C through a vegetative mycelial lifecycle occurring in the soil, air or decaying organic material. *A. fumigatus* produces asexual conidia on specialized hyphal structures called conidiophores to survive in adverse conditions or for reproduction. These conidia are usually small (2 to 5µm) in size, metabolically less active and are the primary source of distribution of *Aspergilli* in the environment. A healthy human inhales 100-1000 conidia daily, which travel through the respiratory tract to the alveoli and begin the infection route [4]. In immunocompetent individuals, macrophages quickly clear inhaled conidia. However, if not eliminated by the immune system and with the help of a favourable environment such as water and nutrients, it starts germination leading to invasive hyphal growth, which can penetrate pulmonary tissue.

The germination of *A. fumigatus* conidia involves a specific morphological transition characterized by phases such as dormancy, isotropic growth, polarized growth and mycelium formation, critical for colonising *A. fumigatus* in the suitable host. The broad spectrum of disease caused by *Aspergillus* is dependent on the status of the host immune system. Among others, invasive pulmonary aspergillosis (IPA) is considered a life-threatening type of *Aspergillus*-related pulmonary infection with a mortality rate of 30% to 95% [5] which is involved in this work.

### 2.2 Secondary metabolites of *A. fumigatus*

Depending on growth conditions and for survival in hostile environments, *A. fumigatus* can produce a large number of secondary metabolites. Production of these metabolites benefits fungi during combat with host immune cells and increases competitiveness over other microbes, whereas some allow the fungus to acquire essential cofactors. One of the ways that *A. fumigatus* can thrive in the human body is through the production of secondary metabolites called siderophores. *A. fumigatus* produces two types of siderophores: fusarinine-type for iron uptake, including fusarinine C (FsC) and its derivative triacetylfusarinine C (TafC) as well as ferrichrome-type ferricrocin (Fc) and hydroxyferricrocin (Hfc) for iron storage and distribution in hyphae and conidia [6] respectively. Moreover, *A. fumigatus* secretes several mycotoxins, including, among others, fumiquinazolines, fumitremorgin, gliotoxin (Gtx) and fumagillin in response to environmental stimuli [7]. These mycotoxins exhibit antifungal (pseurotin) [8], (fumitremorgin B) [9] or anti-inflammatory (fumigaclavine C) [10] activity, while some provide competitive survival advantages. Moreover, mycotoxins such as fumagillin, melanins, trypacidin and Gtx are involved during interaction with the host immune system.

Even so, the production of these metabolites at specific stages of *A. fumigatus* growth and during its interaction with other microbes/cells is not well known. As a result, secondary metabolites, mainly siderophores and mycotoxins production, together with their potential role in diagnosis, is the main topic in this work.

### **2.3 *A. fumigatus* in interaction studies *in vitro***

*A. fumigatus* exists in diverse microbial communities, and studying its molecular interactions with other microorganisms in addition to the host can provide insights into its pathogenic as well as survival strategies. *A. fumigatus* and bacterial pathogen *P. aeruginosa* cohabit in nature and mainly in the airways of cystic fibrosis patients [11]. The potential of interspecies interactions could be vast and lead to both beneficial and antagonistic relationships, as a result, *A. fumigatus* interplay with *P. aeruginosa* and neutrophils is studied in this thesis.

*A. fumigatus* polymycovirus 1 (AfuPmV-1) [12], a member of the family Polymycoviridae, was initially uncovered in the *A. fumigatus* Af293 isolate. To date, no direct correlation between the presence of mycovirus and the quantitative or qualitative modulation of *A. fumigatus* siderophores and mycotoxins has been studied, which is reported in this thesis. Even though the clinical relevance of *A. fumigatus* virus infection is controversial, understanding of mycovirus–fungal host interactions could further illustrate their potential in the control of fungal infections.

### **2.4 *Rhizopus* species and mucromycosis**

After *Aspergillus*, Mucorales are the next common fungal pathogens in animals and humans. Mucorales are saprotrophic fungi comprising *Rhizopus* spp., *Mucor* spp., *Lichthiemia* spp., and with some others that represent a permanent part of the human environment, as commonly found in soil, animal excrements and decaying material. The genus *Rhizopus* is differentiated by the formation of pigmented sporangiophores, 3-11 µm in diameter, arising alone or in whorls bearing sporangia from horizontally growing aerial hyphae called stolons [13]. *Rhizopus* species have gained importance in both human health and industry as some species can act as plant pathogens causing spoilage of crops, while others are used in the fermentation of tempeh and ragi [14].

Mucormycosis is a life-threatening, angioinvasive disease caused by spore inhalation of fungi belonging to the order Mucorales. *R. oryzae* is the predominant agent identified, followed by *R. microsporus* and *R. homothallicus* associated with mucormycosis [15-17]. Invasive mucormycosis has mortality ranging from 23-80% in adult patients and up to 72.7% in paediatric patients [3]. Early diagnosis of mucormycosis is still challenging. The current diagnostic strategies rely on clinical findings, risk factor analysis, histopathology, and culture of specimens. The primary concern about these methods is that clinical

signs may vary with the form and stage of the infection. Moreover, low sensitivity and false negativity are reported in culture methods in 50% of mucormycosis cases [18]. As early diagnosis is the key factor for the successful management of the disease, diagnostic methods with more specific and sensitive molecular markers and secondary metabolite identification still need development in mucormycosis.

## **2.5 Secondary metabolites of *R. microsporus***

Recently polyketide synthase, non-ribosomal peptide synthetase (NRPS), and L-tryptophan dimethylallyl transferase encoding genes were identified in mucoromycota [19]. The availability of host iron plays a critical role in predisposing patients to mucormycosis. Clinical observation demonstrated that the level of available free iron in serum is a crucial factor affecting diabetic ketoacidosis patients to mucormycosis [20], while in other observation, dialysis patients treated with the iron chelator deferoxamine were found to be susceptible to a deadly form of mucormycosis [21]. *Rhizopus* is known to secrete polycarboxylate siderophore rhizoferrin (RHF) to supply iron through a receptor-mediated, energy-dependent process [22].

RHF production is reported in *R. delemar*, *Mucor circinelloides*, *Lichtheimia corymbifera*, *Syncephalastrum racemosum*, *Mucor heimalis*, *Rhizomucor pusillus* and *Cunninghamella echinulata*. Several RHF analogs have also been described by directed fermentation [23]. Recently, the RHF biosynthetic gene, a member of the NRPS-independent siderophore family, has been identified in *R. delemar* [24]. Moreover, RHF is inefficient in capturing iron from serum; however, *Rhizopus* can use xenosiderophores such as deferoxamine to obtain iron from the host [25]. To overcome the lack of knowledge on virulence factors and for further development of a new tool for non-invasive diagnosis, *R. microsporus* metabolome was studied using high-performance LC-MS in this thesis.

### 3 AIMS OF THE THESIS

The aim of this dissertation thesis is to comprehensively characterize *R. microsporus* and *A. fumigatus* siderophores and mycotoxins *in vitro* using LC-MS and demonstrate their utility in the diagnosis of invasive fungal infection in humans as well as animals.

The specific goals include:

- To design infection metallomics - a MS-based platform in a wide range of pathogen-related functional studies
- To analyze the siderophore production in *R. microsporus in vitro* using MS.
- To quantitatively assess *A. fumigatus* growth stage-specific siderophore and mycotoxin production to distinguish between colonization and invasive infection
- To explore *A. fumigatus* siderophores and mycotoxins production during interaction with immune cells (neutrophils), bacterial pathogen (*P. aeruginosa*) and AfuPmV-1.
- To demonstrate the application potential of infection metallomics to the invasive or non-invasive diagnoses of human IPA and equine aspergillosis.

## 4 EXPERIMENTAL PART

### 4.1 LC-MS-based characterization of *R. microsporus* siderophores

#### ***R. microsporus* identification and growth conditions**

*R. microsporus* isolate obtained from the sputum of an immunocompromised patient was grown in iron-depleted mineral medium (residual content 235.5 µg of Fe/L) containing 55 mM glucose, 50 mM NH<sub>4</sub>Cl, 11.2 mM KH<sub>2</sub>PO<sub>4</sub>, 7 mM KCl, 2.1 mM MgSO<sub>4</sub>·7H<sub>2</sub>O, 68 µM CaCl<sub>2</sub>·2H<sub>2</sub>O, and 20 µM ZnSO<sub>4</sub>·7H<sub>2</sub>O (pH 6.5). The medium was inoculated with spore suspension (10<sup>7</sup> spores/mL) and incubated for 48h at 30°C with shaking (190 rpm). The supernatant from the culture was separated by centrifugation (5,000× g, 4 °C, 15 min) and subsequently lyophilized.

#### **Metabolite extraction**

The lyophilized sample was re-dissolved in water, extracted two times with ethyl acetate and dried under reduced pressure. The remaining aqueous phase was mixed with four equivalents of methanol (MeOH) and incubated at -80 °C for 1 h. Precipitated proteins were removed by centrifugation (14,000×g, 4°C, 10 min), and the supernatant layer was transferred to a vial with the residual evaporated ethyl acetate fraction and concentrated under reduced pressure using a SpeedVac.

#### **HPLC-MS analysis**

The pooled extract was re-suspended in 5% LC-MS-grade acetonitrile (ACN) and injected onto an Acquity HSS T3 C18 analytical column (1.8 µm, 1.0 × 150 mm, Waters, Milford, MA, USA). Analytes were gradient-eluted with a 50 µL/min flow rate (A: 1% ACN with 0.1% formic acid (FA) in water, B: 95% ACN with 0.1% aqueous FA): 0 min, 2%; 2 min, 2%; 9 min, 60%; 11.0 min, 99%; 14 min, 99%; 14.5 min, 2%; and 20 min, 2% of B. The metabolites were quantified using HPLC-MS on a Dionex UltiMate 3000 Ultra HPLC system (Thermo Fisher Scientific, Waltham, MA, USA) connected to a Solarix 12T Fourier transform ion cyclotron resonance (FTICR) MS (Bruker Daltonics, Billerica, MA, USA) in electrospray positive-ion mode. A quadrupole filter to 200–700 and 500–1500 Daltons adjusted with two continuous accumulations of selected ion windows.

#### **Data processing**

All samples were measured in triplicates. Our in-house CycloBranch [40] version 2.0.8 and Bruker Data Analysis 5.0 software performed qualitative and quantitative data processing, respectively. RHF and bis-imido-RHF were quantified in fermentation broths by the standard addition method. The limit of

detection (LOD) and limit of quantitation (LOQ) were defined as the sum of the background average with 3 and 10 multiples of standard deviation [26] [26], respectively.

## **4.2 LC-MS based *A. fumigatus* growth-specific siderophore and mycotoxin quantitation to distinguish between colonization and invasive infection**

### ***A. fumigatus* identification and growth conditions**

*A. fumigatus* strain EI278 was isolated from a clinical sample received from the University Hospital in Motol (Prague, Czechia) and identified by phylogenetic analysis of the internal transcribed spacer regions 1 and 2. *A. fumigatus* conidia were harvested in phosphate-buffered saline (PBS) containing 0.01% Tween 80 from a culture grown at 37°C on malt extract agar (17, 3, and 20 g/L of malt extract, mycological peptone, and agar, respectively, adjusted to pH 5.4 before sterilization). The suspension was filtered using a 5- $\mu$ m SyringeStrainer (Pluriselect, San Diego, CA, USA). *A. fumigatus* conidia ( $10^8$ /mL) were inoculated into iron-limited minimal medium (pH 7) consisting of Na<sub>2</sub>HPO<sub>4</sub>·12H<sub>2</sub>O (14.62 g/L), KH<sub>2</sub>PO<sub>4</sub> (3 g/L), NaCl (0.5 g/L), NH<sub>4</sub>Cl (1 g/L); source of carbon: glucose (5 g/L); trace elements: MgSO<sub>4</sub>·7H<sub>2</sub>O (0.2 g/L), CaCl<sub>2</sub>·2H<sub>2</sub>O (0.05 g/L), ZnSO<sub>4</sub>·7H<sub>2</sub>O (0.01 g/L), MnSO<sub>4</sub>·H<sub>2</sub>O (0.017 g/L), CoCl<sub>2</sub>·6H<sub>2</sub>O (0.0048 g/L), CuSO<sub>4</sub>·5H<sub>2</sub>O (0.003 g/L), Na<sub>2</sub>MoO<sub>4</sub> (0.0045 g/L). The experiment with four biological replicates was performed with 10-mL cultures shaken in 50-mL Erlenmeyer flasks on an orbital shaker (190 rpm) at 37°C for 72 h. To detect fungal metabolites, samples of conidia, the residual fungal mass, and the supernatant were collected from each biological replicate at incubation times of 0 h, 3 h, 5 h, 6 h, 7 h, 8 h, 9 h, 10 h, 12 h, 14 h, 18 h, 24 h, 48 h, and 72 h. Before further sample processing, the supernatants were filtered through a Whatman membrane (5  $\mu$ m; VWR International, Stribrná Skalice, Czechia) using a sterile syringe. The residual fungal mass was washed three times with sterile water, centrifuged (14,000 x g for 2 min) at room temperature, and lyophilized.

### **Extraction and quantitation of metabolites**

Siderophores (Fc, Hfc, FsC, TafC, and triacetylfulsarine B (TafB)) and mycotoxins (Gtx, fumigaclavine A, fumiquinazoline C, fumiquinazoline D, 3-hydroxy-fumiquinazoline A, and tryptoquivaline F/J) were extracted from *A. fumigatus* as mentioned in **section 4.1** with some modifications. Briefly, samples (50  $\mu$ L of conidia, the residual fungal mass suspension, or the supernatant) were spiked with a ferrioxamine E (FoxE) (50 ng/mL) internal standard and ferrated with FeCl<sub>3</sub> (100  $\mu$ M) and were subjected to two-step liquid-liquid extraction using ethyl acetate (150  $\mu$ L) and MeOH (200  $\mu$ L). Calibration standards of Fc,

TafC, Gtx, fumigaclavine A, and fumiquinazoline D were prepared at final concentrations of 0.5, 1, 5, 10, 50, 100, 500, 750, and 1,000 ng/mL. The extracts were vacuum dried for 2 h at 35°C using a SpeedVac (catalog number SPD121P; Thermo Scientific, Pardubice, Czechia) and stored at -80°C until HPLC-MS analysis.

#### **HPLC-MS analysis**

Before the HPLC-MS analysis in triplicates, all samples were reconstituted in 150 µL of 15% ACN. Previously reported LC settings (**section 4.1**) were applied for the separation of analytes. Siderophores and mycotoxins were detected using a Solarix 12T (FT-ICR) MS (Bruker Daltonics, Billerica, MA, USA) with electrospray positive-ion mode. MS parameters were tuned and adjusted to optimize the signal intensity of the analytes of interest by applying a quadrupole filter to facilitate the continuous accumulation of the selected ions at 100 to 700 and 500 to 1,500  $m/z$  intervals for analyses of mycotoxins and siderophores, respectively.

#### **Data processing and method validation**

All acquired LC-MS data were processed using DataAnalysis v.5.0 software (Bruker Daltonics, Germany). Fumiquinazoline C, 3-hydroxy-fumiquinazoline A, and tryptoquivaline F/J were annotated from mass spectra by matching the exact  $m/z$  values and product ion mass spectra. The detected analytes were quantified using external calibration standards. Assuming similar ionization efficiencies, Hfc was semiquantified using the Fc calibration curve, and fumiquinazoline C, 3-hydroxy-fumiquinazoline A, and tryptoquivaline F/J were semiquantified using the fumiquinazoline D calibration curve, while FsC and TafB were semiquantified using the TafC calibration curve. The results were averaged from triplicates. The sample preparation methods were validated using control growth medium samples, according to U.S. Food and Drug Administration guidelines for validating bioanalytical methods [27], in terms of the calibration curve (linearity), LOD, LOQ, intra- and interday accuracy and precision, selectivity, specificity, sensitivity, carryover, and autosampler stability. Instrumental LOD and LOQ values were defined as the lowest concentrations for which the SD [26] of the intercept equaled 3.3 and 10, respectively.

#### **Statistical analysis**

The variations in the measured siderophores and mycotoxins from four biological replicates of *A. fumigatus* cultures at each stage of germination and subsequent growth were characterized in terms of means, SDs, standard errors of the means, and coefficients of variation using MS Excel 2016 and graphically visualized using OriginPro version 22 software (OriginLab



Corporation, Northampton, MA, USA). Data were presented as box plots displaying means  $\pm$  SD.

#### **4.2.1 *A. fumigatus* siderophores and mycotoxins production during interaction with neutrophils and *P. aeruginosa***

##### **Neutrophils isolation and *A. fumigatus* infection**

Neutrophils were isolated from anticoagulated blood using a neutrophil direct isolation kit employing (negative selection, StemCells; <https://www.stemcell.com/products/easysep-direct-human-neutrophil-isolation-kit.html>) based on manufacturer's instructions. Cells were counted using trypan blue and Turck solution (50 $\mu$ L of cell suspension + 950 $\mu$ L of diluted trypan blue or Turck solution) by light microscopy (Olympus) at the beginning of the experiment. At every time point, the viability of cells was visualized using trypan blue and determined by light microscopy (Olympus). For the infection experiment, neutrophils ( $1 \times 10^6$  cells/mL) were transferred to a complete growth medium (RPMI 1640, 10% fetal bovine serum) in 24-well plates and incubated with *A. fumigatus* strain EI278 hyphae at 37 °C for 48 h in 5% CO<sub>2</sub> atmosphere in triplicates. Entire plated neutrophils were transferred to a sterile tube and centrifuged for 300g for 10 min. Supernatants collected were immediately stored at -80°C until further processing. PBS was used to wash cell pellets, with successive centrifugation at 300g for 10 min.

##### ***A. fumigatus* and *P. aeruginosa* dual cultivation**

*A. fumigatus* (EI278) conidia ( $10^7$ conidia/mL) and *P. aeruginosa* (PAO1) cells ( $10^7$ cells/mL) were inoculated into iron-limited minimal medium (composition of the medium is similar to **section 4.2**). The experiment with three biological replicates was conducted as 100 mL culture into 500 mL Erlenmeyer flask shaken at 37°C on an orbital shaker (190 rpm). For metabolite analysis, supernatants were collected at 0 h, 6 h, 9 h, 12 h, 18 h, 24 h, 36 h, 48 h, and 72 h of incubation and immediately stored at -80 °C.

##### **Extraction of metabolites**

For siderophores (Fc, TafC and TafB), samples of supernatant were spiked with a FoxE (50 ng/mL) internal standard and ferrated with FeCl<sub>3</sub> (10 mM) and were subjected to previously reported liquid-liquid extraction protocol (**section 4.2**). For Gtx and its metabolites, several solvent and solid phase extractions (SPE) were tested to reduce dilution due to tremendous siderophore production and to improve mycotoxin detection sensitivity. Initially, liquid-liquid extraction using chloroform-MeOH and dichloromethane-MeOH was checked. Next, SPE (HLB and Sep-Pak, Waters, Milford, MA, USA) using appropriate elution solvent composition (50%, 60% and 100% MeOH+0.1% FA

and 50%, 60% and 100% ACN+0.1% FA) were examined. Based on the results, a protocol using SPE HLB 3cc (150 mg) cartridge was finalized. The samples of supernatant (50  $\mu$ L) were spiked with 2-heptyl-4(1H)-quinolone (10 ng/mL) as internal standard and were loaded on SPE cartridges preconditioned with 1mL MeOH +0.1% FA and equilibrated with 1mL 5% MeOH +0.1% FA. Polar impurities were removed with 1mL of 5%MeOH+0.1% FA, with the subsequent addition of 2mL of 60% MeOH +0.1% FA. The compounds of interest were eluted with 1 mL of MeOH+0.1% FA. The extracts were then vacuum dried for 2 h at 35°C and stored at -80°C until HPLC-MS analysis.

### HPLC-MS analysis

All the extracted samples from interaction with neutrophils and *P. aeruginosa* were reconstituted in 150  $\mu$ L of 15% ACN. Siderophores (Fc, TafC, TafB) were analyzed by an Acquity M-class HPLC system connected to a Synapt G2-Si Q-TOF MS (Waters Corporation, Manchester, UK). Each sample was loaded onto an Acquity HSS T3 C18 analytical column (1.8  $\mu$ m, 1.0  $\times$  150 mm, Waters Corporation, Manchester, UK). Gradient elution was performed at a 50  $\mu$ L/min flow rate: 0 min, 5%; 2 min, 5%; 10 min, 50%; 14 min, 95%; 16.5 min, 95%; 17 min, 5%; and 20 min, 5% of B. Solvent A contained 0.1% FA in the water, and solvent B contained 0.1% FA in ACN. The spectrometer was operated in electrospray positive-ion mode within 200–1200  $m/z$ .

Reconstituted samples for mycotoxins (Gtx and BmGtx) analysis were injected into an Acquity HSS C18/1.8-mm, 2.1 by 5-mm VanGuard precolumn connected to an Acquity HSS T3/1.8-mm, 1.0 x 150-mm analytical column (both from Waters, Prague, Czechia). Previously reported LC gradient conditions (**section 4.1**) were applied and detection was performed using a SolariX 12T (FT-ICR) MS (Bruker Daltonics, Billerica, MA, USA) with electrospray positive-ion mode. MS parameters were tuned and adjusted to optimize the signal intensity of the analytes of interest by applying a quadrupole filter for the continuous accumulation of the selected ions at 200 to 600  $m/z$  intervals.

### Data processing

Data for siderophores and mycotoxins were processed by MassLynx 4.1 software (Waters Corporation, Manchester, UK) and Cyclobranch [28] version 2.1.32, respectively. The detected analytes were quantified using external calibration standards in technical duplicates. Instrumental LOD and LOQ values were defined as the lowest concentrations for which the SDs of the intercept equalled 3.3 and 10, respectively.

### Statistical analysis

The obtained results were statistically analysed using GraphPad Prism 8.0.1 software (GraphPad, San Diego, CA, USA). A non-parametric Mann-Whitney test is used to compare between two groups for each time point where a *P* values of < 0.05 were considered statistically significant. The box plots are expressed as a mean ± SD.

### 4.2.2 *A. fumigatus* siderophores and mycotoxins production during interaction with the polymycovirus AfuPmV-1

#### Isolates

In a masked study, five *A. fumigatus* strains as mentioned below, were maintained on malt extract agar (1.7% malt extract, 0.3% mycological peptone, 3% Bacto agar, pH 5.4, for 10 days, at 37 °C.

Strain 18–42 (VF);	UK Af293 cured from AfuPmV-1
Strain 18–95 (VI);	UK Af293 with AfuPmV-1
Strain 10–53 (VI);	USA Af293 with AfuPmV-1
Strain 19–40 (VR);	18–42 re-infected with AfuPmV-1
Strain 19–47 (VR);	18–42 re-infected with AfuPmV-1

*A. fumigatus* UK AF293 strain (18–95) was cured using the protein synthesis inhibitor cycloheximide [29], producing a VF strain now designated 18–42. AfuPmV-1 was purified by differential polyethylene glycol precipitation and ultracentrifugation. Purified AfuPmV-1 was re-introduced in the VF *Aspergillus* by protoplast transfection, producing re-infected strains designated as 19–40 and 19–47. Strain 19-47 was misprinted, thereby corrected to 19-42 [30].

#### Fungal strains cultivation

For the detection of siderophores, strains 18-42, 18-95, 10-53, 19-40 and 19-42 ( $10^8$  conidia/mL) were grown in an iron-limited mineral medium with a similar composition mentioned in **section 4.2**. The samples of mycelia and supernatants were collected at 48, 52, or 24, 31, 48, 54, and 72 h, respectively.

For detection of mycotoxins, strains 18-42, 18-95 B, 19-40 and 19-42 ( $10^8$  conidia/mL) were inoculated into a minimal medium (composition is similar to **section 4.2**) along with  $\text{FeCl}_3 \cdot 6 \text{H}_2\text{O}$  (10  $\mu\text{M}$ ). The supernatant was collected at 18 h, 24 h, 36 h, 48 h, 72 h and 96 h of growth and immediately stored at -80 °C.

For gene expression analysis, conidia ( $10^7$  conidia/mL) were inoculated in media containing  $\text{Na}_2\text{HPO}_4 \cdot 12\text{H}_2\text{O}$  (14.62 g/L),  $\text{KH}_2\text{PO}_4$  (3 g/L),  $\text{NaCl}$  (0.5 g/L),  $\text{NH}_4\text{Cl}$  (1 g/L); source of carbon: glucose (5 g/L); trace elements:

MgSO<sub>4</sub>·7H<sub>2</sub>O (0.2 g/L), CaCl<sub>2</sub>·2H<sub>2</sub>O (0.05 g/L), FeCl<sub>3</sub>·6 H<sub>2</sub>O (10 μM). The cultures were shaken for 48 h in flasks, at 39 °C, on an orbital shaker (190 rpm). The experiment was carried out with three biological replicates, and mycelia were collected at 48 h. The mycelia were washed with sterile water and centrifuged twice at 14,000× g, 2 min, at room temperature before RNA extraction.

#### Extraction of metabolites

Previously mentioned liquid-liquid extraction (section 4.2) and SPE protocol (section 4.2.1) was applied for siderophores (Fc, TafC and TafB) and mycotoxins (Gtx and BmGtx) respectively.

#### HPLC-MS analysis

Before the HPLC-MS analysis in triplicates, all samples were reconstituted in 150 μL of 15% ACN. Previously reported LC-MS settings section 4.1 and section 4.2.1 were applied for quantification of siderophores and mycotoxins, respectively.

#### RNA extraction, complementary c-DNA synthesis and quantitative polymerase chain reaction (qPCR)

Total RNA was extracted from each strain 18-42, 18-95 B, 19-40 and 19-42 grown in three biological replicates for 48 h using the RNeasy mini kit (Qiagen). Following treatment with DNase I (Promega) and quantification by Nanodrop spectrophotometry, equal amounts of RNA were utilised as a template for cDNA synthesis using the SuperScript VI Reverse Transcriptase (Invitrogen). The qPCR assays were performed in the OneStepPlus Real-Time qPCR System (Applied Biosystems) utilizing the Power SYBR Green PCR Master Mix (Applied Biosystems) and the relative standard curve quantitation method. *A. fumigatus* β-tubulin sequence was used as an endogenous control. Target-specific primer pairs were designed using PrimerBlast and are listed in (Tab. 4.1).

Gene	Forward primer	Reverse primer
AfuPmV-1	ATAGGTCACGCCATAGCACG	CCCAGCACTGAGAAGAGGTG
β-tubulin	AATTGGTGCCCG TTTCTGG	CTATTCCGTCCCGACAAC
<i>gliG</i>	GCGACCTCCGATCTTGAG	TGACGGTGTGTGTGTGGA
<i>gliN</i>	ACTCCGAAAACGGCTACCTC	AGGACTCGCAGATTGGGTG
<i>gliA</i>	TACCTGCCGACCTACTTCCA	TCCAGGTCGAGGGTGTAGAG
<i>gliT</i>	CTTCGACTCTGGCGTCTACC	TCGAACAGCTGGTTGGTCTC
<i>gtmA</i>	TCCAGCGTACTCAACCACAC	GAAGACCGGTGTCTAACGCA

**Table 4.1** The list of forward and reverse primers used.

### **Statistical analysis**

Each sample was analysed in three technical replicates by MS, providing nine points for statistical analyses (3 x 3). The differences in the metabolite levels among *A. fumigatus* strains were presented as standard box plots with outliers plotted as individual points. The box plots were built using MS Excel 2016. Kruskal–Wallis One-Way ANOVA with Bonferroni (All-Pairwise) Multiple Comparison and Friedman’s Q Rank Test was used to compare the differences between the intra and extracellular metabolite levels in VF and VI *A. fumigatus* strains. Friedman’s Q Rank Test was explicitly used to test how the strain and growth-phase time affected siderophore levels. Statistical analysis was performed by NCSS 9 statistical software (NCSS, Kaysville, UT, USA).

For LC-MS-based mycotoxin analysis, each sample was analysed in two technical replicates. Data are presented as box plots displaying means  $\pm$  SD built using MS Excel 2016.

For gene expression analysis of mycotoxins, the results from three technical replicates were plotted as box plots displaying means  $\pm$  standard error of mean using MS Excel 2016.

## **4.3 Infection metallomics-based diagnosis**

### **4.3.1 Diagnosis of human invasive pulmonary aspergillosis**

#### **Extraction of metabolites**

According to a previously reported protocol, siderophores and mycotoxins were extracted from human urine and serum samples [31]. Briefly, urine and serum samples from patients and healthy individuals were centrifuged at 6,000 rpm for 30 s. All centrifuged samples (50  $\mu$ L) were spiked with the FoxE (100 ng/mL) internal standard. Urine and serum samples from healthy individuals were used to prepare calibration standards of Fc, TafC, and Gtx at final concentrations of 0.1, 0.5, 1, 5, 10, 50, 100, 500, 1,000, and 5,000 ng/mL. The samples were loaded onto Sep-Pak C18 1-mL Vac SPE cartridges (Waters, Prague, Czechia) preconditioned with MeOH+0.1% FA and equilibrated with H<sub>2</sub>O-0.1% FA. Impurities were removed with 200 $\mu$ L of 2%MeOH+0.1% FA, and the compounds of interest were eluted with 400 $\mu$ L of MeOH+0.1% FA.

### **HPLC-MS analysis**

Before the HPLC-MS analysis in triplicates, all samples were reconstituted in 150  $\mu$ L 5% ACN. Siderophores and mycotoxins were separated using a Dionex UltiMate 3000 HPLC system (Thermo Scientific, MA, USA). Reconstituted urine and serum samples were injected into an Acquity HSS C18/1.8-mm, 2.1 by 5-mm VanGuard precolumn connected to an Acquity HSS T3/1.8-mm, 1.0 by 150-mm analytical column (both from Waters, Prague, Czechia). Analytes were eluted at a 50- $\mu$ L/min flow rate using the following gradient of buffers A and B: 1% B at 1 min followed by linear increases to 60% B at 20 min and 99% B at 23 min and then a 3-min hold at 99% B, with a 2-min linear fall to 1% B and a 12-min hold before the next injection. Here, buffer A was 5% ACN with 0.1% aqueous FA, and buffer B was 95% ACN with 0.1% aqueous FA. Previously reported MS settings (**section 4.2**) were applied to quantify analytes.

### **Data processing**

All acquired data were processed similarly to mentioned parameters in **section 4.2**. The urine concentrations of siderophores (Fc, TafC, and TafB) and Gtx were further normalized to the urine creatinine concentration to obtain creatinine index values [32] using the following formula: siderophore or secondary metabolite concentration (ng/mL)/creatinine concentration (mg/dL x 100).

### **Statistical analysis**

The clinical samples were statistically analyzed using GraphPad Prism 8.0.1 software (GraphPad, San Diego, CA, USA). The reported descriptive statistics include means, medians, interquartile ranges, SDs, standard errors of the means, and coefficients of variation. The Gaussian distribution of the data was tested using the D'Agostino-Pearson normality test, and as the normality test did not meet the requirements for parametric tests, nonparametric tests were used. The urine and serum samples were considered positive if at least one of the urine creatinine-indexed fungal metabolite or serum concentrations (TafC, TafB, Fc, or Gtx) were higher than an LC-MS method-defined LOD for a particular marker.

### 4.3.2 Diagnosis of equine aspergillosis

#### Metabolite extraction

Metabolites were extracted from serum and BALF samples using our previously reported two-step liquid-liquid extraction protocol (**section 4.1**). The samples were spiked with FoxE and Leucine-enkephalin internal standards to final concentrations of 50 and 25 ng/mL, respectively. The control horse group serum and BALF samples were used to prepare matrix-matched calibration curves for Fc, TafC, and Gtx based on solutions with final concentrations of 1, 5, 10, 50, 100, and 250 ng/mL.

To extract metabolites from tissue samples, whole lungs were lyophilized and homogenized with a mortar and pestle. A 25 mg sample of the resulting homogenized powder was then dissolved in (400  $\mu$ L) 15% LC-MS grade ACN followed by extraction as **section 4.1** and quantification by the standard addition method.

#### HPLC-MS analysis

Pooled samples of serum and BALF or lung homogenates were re-suspended in 150 or 200  $\mu$ L of 15% ACN, respectively and analysed in triplicates using similar LC-MS settings as in **sections 4.1** and **4.2**.

#### Data processing

Qualitative and quantitative data analysis was conducted using the in-house CycloBranch version 2.0.19 software [28] and Data Analysis 5.0 (Bruker Daltonik, Bremen, Germany).

## 5 RESULTS AND DISCUSSION

The goal of the first section of this thesis is to introduce infection metallomics we designed as mass spectrometry platform based on the central concept that microbial metallophores are specific, sensitive, noninvasive, and promising biomarkers of invasive infectious diseases. The second section of this thesis includes fungal pathogen *R. microsporus* *in vitro* cultivation, followed by LC-MS analysis of its siderophores. The third section involves *in vitro* cultivation of fungal pathogen *A. fumigatus* with subsequent growth stage-specific siderophore and mycotoxin quantification to distinguish between colonization and invasive infection. In addition, the time course quantification of *A. fumigatus* secondary metabolites during its interaction with neutrophils, bacterial pathogen *P. aeruginosa* and polycytovirus was performed. The fourth and last part is then focused on the application of infection metallomics-based diagnosis in human IPA and equine aspergillosis.

### 5.1 Introduction to infection metallomics

The results of this section have been published in the following article: R.H. Patil, D. Luptakova V. Havlicek, Infection metallomics for critical care in the post-COVID era. *Mass Spectrom Rev* (2023) [33].

In response to WHO alerts, we recognized an urgent need to improve diagnostics of the most clinically significant pathogens, and established infection metallomics, a MS-based platform utilizing microbial and mammalian metallophores in functional and diagnostic applications. Both host cells and pathogens rely on metals such as iron, zinc, nickel, manganese or copper to carry out their essential functions. Thus, infection metallomics exclusively focuses on the analysis of metal-containing infection biomarkers called metallophores using a combination of elemental and molecular MS. In this work, we summarized ESKAPEc nosocomial bacterial pathogens standing for *Enterococcus faecium*, *Staphylococcus aureus*, *Klebsiella pneumoniae*, *Acinetobacter baumannii*, *P. aeruginosa*, *Enterobacter* spp., *Escherichia coli* and mycobacteria as well as fungal pathogens such as *Candida* spp. and *A. fumigatus* metallophores, followed by the non-invasive application of metallophores from a historical perspective (Fig. 5.1).



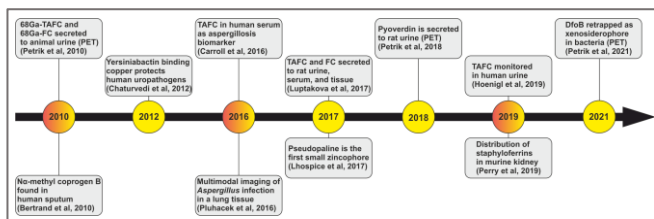


**Figure 5.1** A historical perspective on non-invasive applications of metallophores. Unmarked entries are associated with MS detection. DfoB, desferrioxamine B; FC, ferrirocinn; Ga, gallium; PET, positron emission tomography; TAFc, triacetylfulsarinine C

We then described a strategy of infection metallomics for detecting the onset of pathogenic infection in critically ill patients (**Fig. 5.2**). Either non-invasive such as breath condensate or urine, or invasive sampling (serum, BAL, endotracheal aspirate, sputum, or biopsy analysis) from critically ill patients can be used for detection of virulence factors secreted by infecting microbe. Rapid analysis with pathogen identification is crucial to initiate smart combination antimicrobial treatment during the window of opportunity, which exists when the pathogen consortium is transitioning from colonization to causing infection to the host.

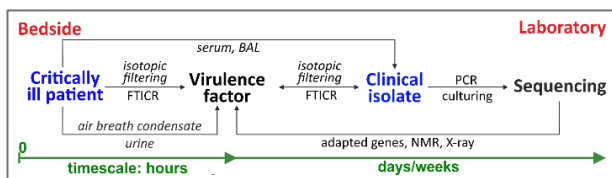


**Figure 5.2** The concept of infection metallomics from bedside to laboratory.

BAL, bronchoalveolar lavage; FTICR, Fourier-transform ion cyclotron resonance; NMR, nuclear magnetic resonance; PCR, polymerase chain reaction.

At the bedside, the rapid analysis of non-invasively collected samples is achieved using MS, where isotopic data filtering can specifically detect metal-containing infection biomarkers at the pathogen-host interface within the time scale of hours. Alternatively, culturing clinical specimens, such as urine, serum, sputum, or aspirates, together with molecular tools, including PCR and gene sequencing, can be used for the characterization of less common pathogens. Further *de novo* approaches allow the isolation of new virulence factors from fermentation broths by preparative chromatography, followed by absolute

structure determination using X-ray diffraction and nuclear magnetic resonance techniques.

We defined sample flow and key MS instruments (**Fig. 5.3**) used to directly monitor microbial Fe-, Co-, Zn-, Mn-, or Cu-containing virulence factors, detected at concentrations of ng/L to  $\mu\text{g/mL}$  in humans or animal models. The suitable extraction protocols depend on the structure of these analytes [34].

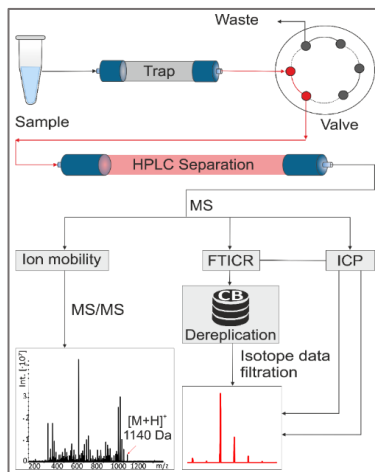


**Figure 5.3** Sample flow and key MS instruments for infection metallomics with isotope data filtering. CB, CycloBranch software; FTICR, Fourier-transform ion cyclotron resonance; HPLC, high-performance liquid chromatography; ICP, inductively coupled plasma; MS, mass spectrometry

The analytical process initiates with LC followed by applying one of three MS techniques. An ESI or ion mobility spectrometry with a quadrupole/time-of-flight (TOF) instrument can provide excellent MS/MS data on metal-containing compounds that might otherwise be difficult to dissociate. An even more powerful approach is to apply high-resolution FTICR-MS which enables unambiguous identification of metallophores in bodily fluid and tissue samples. Finally, inductively coupled plasma (ICP) MS is routinely used for metal quantitation, for instance, analysis of urine samples to detect uropathogenic strains.

Metallophores can be analysed via targeted using a microbial siderophore database [35] and *de novo* approaches [36]. Moreover, CycloBranch is an explicitly designed software for infection metallomics where one can quickly identify all compounds exhibiting predefined isotopic features in a

chromatographic or imzML data set [37]. Application of this tool involves both elemental (ICP MS) and molecular ESI or MALDI MS datasets (Fig. 5.4) with a bonus of *de novo* sequencing features [38].

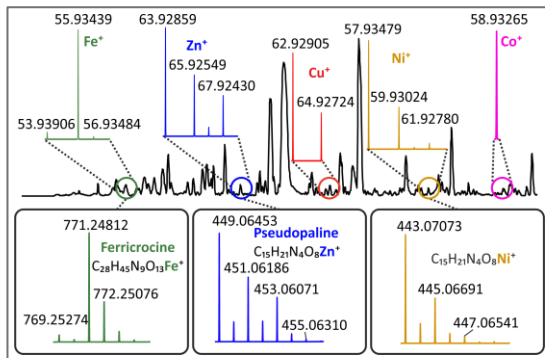


**Figure 5.4** In silico modeling of siderophores ferri-ferricrocin and zinc-pseudopaline isotopic profiles. Note that the mass defects of specific nuclides (in this case, 68/66Zn 1.99881, 66/64Zn 1.9969, and 56/54Fe 1.99533) are used to identify metal-containing species in both elemental and molecular mass spectrometry datasets.

Further, MS-based analysis of lung, urinary tract and central nervous system (CNS) infections is elaborated. In lung infections, the airways represent a common entry point for fungal spores (Fig. 5.5). Inoculation of rat model with *Aspergillus* conidia was found to induce secretion of TafC and Fc siderophores into the urine, serum, and lung tissue where the site of infection was investigated by positron emission tomography (PET) [39]. Another study demonstrated the use of MS imaging to visualize the distribution of microbial siderophores in infected rat lungs to detect the site of infection [40]. The fungal burden in rat lung tissue was determined by combining ICP-MS and scanning electron microscopy. This revealed a noticeable increase in the iron concentration in infected areas, attributing to both severe haemorrhage and secretion of fungal siderophores. The experiments with inoculation of variable conidial loads were conducted in immunocompromised rats to understand the difference in siderophore biomarker levels in neutropenic and non-neutropenic hosts. With higher inoculation with 10<sup>8</sup> *Aspergillus* conidia, the first *A. fumigatus* siderophore biomarkers (TafC and Fc) were detected in host urine as early as 4h post infection [41]. However, with a lower inoculation dose of 10<sup>4</sup> conidia to mimic the situation in immunocompetent hosts, a detectable MS signal was first observed 30 h after inoculation. Animal model studies have revealed that infectious fungal species exhibit high biological diversity, and MS methods can be used to monitor the

distribution and metabolism of fungal siderophores *in vivo*. Moreover, *A. fumigatus* siderophore TafC has soon reported in human serum [42] and urine samples [32]. In mixed infection rat models and critically ill patients, mixed bacterial and fungal secondary metabolites were detected in the urine, indicating a distant lung infection. Similarly, analysis of breath condensate revealed an early infection by *P. aeruginosa* [43].

The application of infection metallomics in uropathogen characterization is another well-developed field of clinical MS. *E. coli* is the most frequent pathogen, followed by *Klebsiella*, *Enterobacter*, *Proteus* spp., and *Citrobacter* isolated from urine in hospital settings [44]. *E. coli* is known to secrete siderophores, enterobactin and aerobactin, as well as the secondary metabolites dihydroxy-benzoylserine, its dimer and trimer, and dihydroxybenzoic acid (Hider & Kong, 2010). Enterobactin production has also been reported in urinary isolates of *Klebsiella*, *Enterobacter*, and *Citrobacter*. Siderocalin, a soluble protein with high ferric ion affinity, can starve *E. coli* for iron during urinary tract infections. Another uropathogen *Staphylococcus aureus* producing metallophores, staphylopin with binding affinity to Co, Ni, Zn, and Cu [45] and staphyloferrins A, B [46], which were found to be heterogeneously distributed within infectious foci [47]. Several uropathogenic strains, such as *Yernia* spp. *Enterobacter* spp. and *Klebsiella* spp. secrete the common biomarker yersiniabactin which binds iron, copper, and some other metals. The fungal pathogens *Candida* spp. and *Aspergillus* spp. are often associated with nosocomial infections in critically ill patients, including the CNS. Due to the blood-brain barrier, diagnosing and treating CNS infections in neonates, children, and adults is particularly challenging. The meningitis-causing microbe *Neisseria* spp. use heterologous siderophores secreted by other bacteria like *E. coli* [48]. Additionally, it was revealed that *L. monocytogenes* utilizes iron-bound transferrin as its sole source of iron and also uses epinephrine and 3,4-dihydroxyphenylalanine as well as xenosiderophores produced by other bacterial and fungal pathogens such as pyoverdine and ferrioxamine B [49]. Infection metallomics using MS imaging could play a key role in describing pathogen routing pathways and mechanisms in CNS infections by visualizing the metallophores secreted by invading pathogens overlaid with the molecular signals of host defence molecules.

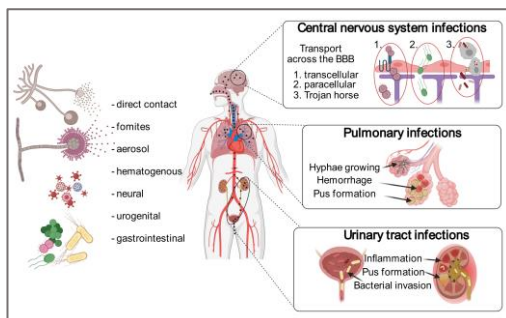


**Figure 5.5** Entry of pathogens into a critically ill patient. Around 70% of all intensive care unit cases are related to bacterial infections predominated with Gram-negative bacteria, whereas viral, fungal, and mixed infections account for around 20% of cases [50, 51].

Lastly, we compared the performance of infection metallomics-based diagnosis to that of four routinely used clinical approaches, mainly culturing, microscopy and PCR in IPA (**Fig. 5.6**). Infection metallomics either outperformed or matched all existing diagnostic methods to four critical parameters such as sensitivity, specificity, invasivity and timeliness. Maximizing analytical dynamic range is the key technical challenge to overcome while developing any diagnostic tool. Infection metallomics combined with isotopic data filtration can achieve a wide dynamic range by utilising microbes' tremendous capacity to secrete biomarker molecules into a host. For instance, *P. aeruginosa* is known to secrete  $10^{11}$  pyoverdine molecules per cell per time point [52]. This vast production of virulence factors could be why the metabolomic approach outperformed other omics strategies in terms of sensitivity except for PCR.

Method	Sensitivity	Specificity	Invasivity	Timeliness
sCulturing	Yellow	Green	Red	Red
sGM/sPCR	Yellow	Green	Red	Green
bGM/bPCR	Green	Green	Red	Green
bMicroscopy	Yellow	Yellow	Red	Green
<i>Infection metallomics</i>	Green	Green	Green	Green

**Figure 5.6** Performance of infection metallomics and four other techniques for diagnosing *Aspergillus* infections with respect to four key criteria. sGM denotes galactomannan serology. bGM denotes galactomannan in bronchoalveolar lavage fluid. Performance is indicated using the following colour code: **excellent**, **fair**, and **poor**. Data presented from [43, 53] and [32]. b, bronchoalveolar lavage; PCR, polymerase chain reaction; s, serum.

Alike every other new technique, infection metallomics also has some limitations. Although the clinical analysis of metallophores is attractive due to its non-invasivity, original site of certain infections such as pulmonary and CNS infections cannot be determined using non-invasive sampling. However, by combining infection metallomics with PET imaging also being non-invasive, it becomes possible to observe the specific accumulation of radioactive  $^{68}\text{Ga}$ -siderophores in animals infected by bacteria or fungi. On the other hand, invasive sampling involving BALF and cerebrospinal fluid can reflect infection site in pulmonary and CNS infections. Currently, no tools can describe the interplay between viral, bacterial, and fungal infections. However, infection metallomics, at minimum, can assess and quantify the interplay between bacterial and fungal pathogen interaction in a host and monitor the microbiome's dynamic response to antibiotic, antiviral, and antimycotic therapies. Combined analysis of metallophores and their dynamics can determine how the infected pathogens are infiltrating into and proliferating within specific tissues and shed light on coinfections where eliminating one pathogen may lead to increased activity by another. This study shows that infection metallomics can potentially improve outcomes in intensive care medicine by allowing safe sampling of highly infective patients with fungal, bacterial, and mycobacterial infections with minimal risk of disease transmission as well as reducing the financial and technical burden in hospital settings. Infection metallomics may thus advance medical MS, like the introduction of the MALDI Biotyper in 2009.

## **5.2 Liquid chromatography-mass spectrometry (LC-MS) based characterization of *R. microsporus* siderophores**

The results of this section have been published in the following article: A. Škríba, R.H. Patil, P. Hubáček, R. Dobiáš, A. Palyzová, H. Marešová, T. Pluháček V. Havlíček, Rhizoferrin glycosylation in *Rhizopus microsporus*. *J Fungi* 6(2020)89 [54].

Metabolomic studies of *R. microsporus* are scarce, as a result, the metabolome of a *R. microsporus* patient isolate was reported in this study. The urinal and *in vitro* metabolic profiles of the same patient with proven *R. microsporus* invasive infection were compared. Additionally, a new chromatographic method for the separation of carboxylate siderophore was developed. Initially, for chromatographic method development for RHF, a standard Waters Acquity HSS T3 ( $1.0 \times 150$  mm,  $1.8 \mu\text{m}$ ) column was used. The stationary phase revealed significant adsorption of desferri- RHF. Therefore, the ferri form of RHF was utilised for better separation of molecules. Positive and negative ion modes were tested for the detection of RHF and its analogues. Further, the desolvation temperature and ion transfer optic parameters were

optimized to decrease the in-source fragmentation. Using developed chromatography and MS method, *R. microsporus* cultivation under iron-limited conditions and D-glucose as a carbon source provided RHF ( $345.3 \pm 13.5$  mg/g) and imido-RHF ( $1.2 \pm 0.03$  mg/g) as two dominant products in continuous accumulation of selected ions (CAS) 200–700 mass window (**Fig. 5.7**). The RHF trace was visible with a deteriorated peak shape of the protonated molecules at  $m/z$  437.140 while imido-RHF trace was detected for protonated molecules at  $m/z$  419.130 (**Fig. 5.7 E, D**). Further, we found that storage of samples, even in a lyophilized state for up to five months at room temperature, caused extensive RHF decomposition to the imido- and bis-imido-RHF forms (**Fig. 5.7 B**). The citryl-RHF intermediate with an elution time of 2.36 min was characterized by the accurate mass of the protonated molecule at  $m/z$  263.124 (263.124 calculated for  $C_{10}H_{18}N_2O_6$ ). For the first time in this study, we report the production of glycosylated RHF analogues in directed cultivation (**Fig. 5.7 G–I**).

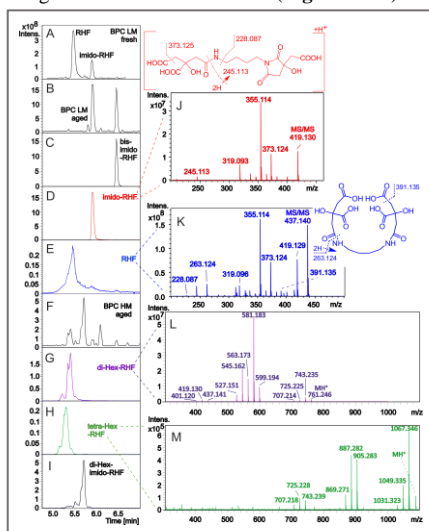


**Figure 5.7** Chromatographic separation and tandem mass spectrometry of *R. microsporus* secondary metabolites. BPC: base peak chromatogram, Hex: hexose. (**A, B**) BPC in the 200–700 Daltons mass range of fresh or aged (5 months) lyophilizates; (**C–E**), extracted ion chromatograms corresponding to bis-imido-RHF, imido-RHF, and RHF, respectively (0.005 Dalton window), (**F–I**) BPC and selected ion chromatograms of di-Hex-RHF, tetra-Hex-RHF, and di-Heximido-RHF, respectively. (**J–M**) refer to the product ion mass spectra (10 eV collisional energy) of imido-RHF, RHF, di-Hex-RHF, and tetra-Hex-RHF, respectively. The structure on the top indicates the intrinsic fragmentation in the RHF.

The positive-ion ESI mass spectra provided clusters of protonated and cationized species. Ion signals of the putative mono- and tri-Hex-RHFs co-eluted with the corresponding di- and tetra-analogues. Although the formation of mono- and tri-Hex-RHFs cannot be excluded, we concluded that the corresponding ionic species represent fragments rather than biosynthetic intermediates. Alternatively, di-Hex-imido-RHF was well separated (**Fig. 5.7I**). The tandem MS of the di- and tetra-Hex analogues revealed the consecutive losses of Hex units from the protonated molecules (**Fig. 5.7 L, M**) and the intrinsic fragmentations in the RHF (**Fig. 5.7 J, K**). The fragmentation pattern indicated in **Fig. 5.7** correlated with the ion compositions derived from exact mass measurements. Moreover, CycloBranch software directly annotated other metabolites summarized in this study.

Glycosylation of RHF provided more polar and possibly more enzymatically stable products. We speculated that RHF glycosylation could benefit the producer; e.g., *R. microsporus* converted zearalenone to its more soluble 4- $\beta$ -D-glucopyranoside [55]. Our results suggested that RHF is an analytically complex molecule for direct detection in patients with invasive mucormycosis, and its metabolic fate in the host body remains uncertain. Aged lyophilized samples exhibited considerable RHF and imido-RHF instabilities (**Fig. 5.7 B**). This instability in human serum or urine is expected to be even more compromised owing to enzymatic processes in those matrices. Hence, bis-imido-RHF or its metabolic products should be among the few *R. microsporus* biomarkers remaining in bodily fluids for targeted metabolomics. Our experiments for detecting RHF analogues directly in patient urine or serum samples were also inconclusive. The reason was the antifungal treatment which most likely stopped siderophore production before sampling. However, analysis of patient urine suffering from pulmonary mucormycosis revealed the detection of the antifungal drug posaconazole along with all its major metabolites, including hydroxyderivatives or glucuronides, in a single LC-MS run. Nevertheless, RHF is the dominant product of *R. microsporus* cultivation under iron-restricted conditions. Although RHF and its analogues could serve as potential candidates for zygomycete diagnostics, future studies are required to determine the biotransformations of RHF in the host and to reveal its chemical stability and protein binding precisely.



### 5.3 LC-MS-based *A. fumigatus* growth-specific siderophore and mycotoxin quantitation to distinguish between colonization and invasive infection

The results of this section have been published in the following article: D. Luptakova, R.H. Patil, R. Dobias, D.A. Stevens, T. Pluhacek, A. Palyzova, M. Kanova, M. Navratil, Z. Vrba, P. Hubacek V. Havlicek, Siderophore-Based Noninvasive Differentiation of *Aspergillus fumigatus* Colonization and Invasion in Pulmonary Aspergillosis. *Microbiol Spectr.* 11(2023) [56].

Distinguishing invasive disease from benign colonization is a crucial biological challenge in clinical settings. Overdiagnosis and unnecessary treatment can occur if colonization is mistaken for infection. The importance of this study lies in demonstrating that siderophore analysis can distinguish between asymptomatic colonization and invasive pulmonary aspergillosis. We reported clear associations between fungal development phases, from conidial germination to the proliferative stage of invasive aspergillosis, and changes in secondary metabolite secretion.

In order to analyze siderophore production during growth of *A. fumigatus* we first observed key stages of conidial germination using bright field microscopy. The conidia from the clinical isolate of *A. fumigatus* were incubated at 37°C in an iron-limited medium with glucose as a carbon source for 72 h. During the first 3h of incubation, no morphological changes were observed in conidia, indicating conidial dormancy. Isotropic growth was observed between 3 and 6 h post-inoculation, wherein at 6h, most conidia began swelling and doubled in size. Polarized growth began 6h after inoculation. By 8h, the majority of conidia had germ tubes growing from one side of the cell (**Fig. 5.8**). All these processes are asynchronous. As a result, the growth curves have broader distribution.

The results summarized in **Fig. 5.8 B** and **Fig. 5.9** revealed evident germination phase-dependent variations in the abundances of *A. fumigatus* siderophores involved in iron homeostasis, quantified by HPLC-MS-based infection metallomics. Intracellular Hfc was mainly detected in dormant conidia. Further, its reappearance in residual fungal mass after 48 h indicated the formation of asexual conidiophores at the air-glass interface, which cannot be eliminated in shaken cultures. Predominantly intracellular Fc marked the onset of isotropic growth, exhibited by the swelling of conidia. There was an exponential increase in its content, up to the constant level in the residual fungal mass, reflecting the need for iron accumulation necessary for hyphal growth and further conidiation.

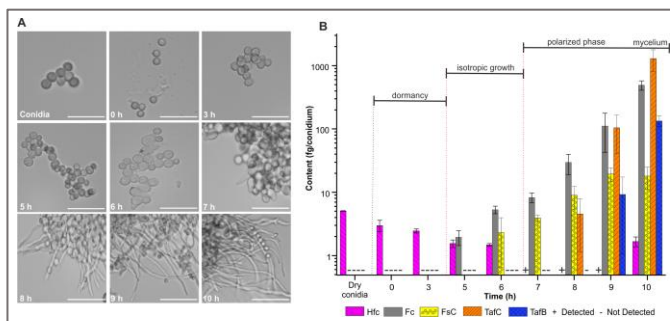


**Figure 5.8** A) Transition of *A. fumigatus* conidia during germination, observed by bright-field microscopy. Bar represents 10  $\mu\text{m}$ . Top row- dormancy, middle row- isotropic growth and bottom row- polarised growth. B) Levels of intra and extracellular siderophores during *A. fumigatus* conidial germination. Data are presented as means  $\pm$  standard deviations.

Fc reported to be transcellular [57], was also detected in the supernatant in this study. The gradual increase in FsC secretion was already detected at the beginning of the isotropic phase. It was followed by the secretion of TafC and its hydrolytic derivative triacetylfusarinine B (TafB) during the fungal transition to polarized growth. An inverse relationship of the abundances of TafC and TafB at the stationary phase of growth reflected the iron capture, release, or storage managed by *Aspergillus*. Moreover, the detection of mycotoxins, including fumigaclavine A, fumiquinazoline C, fumiquinazoline D, 3-hydroxy-fumiquinazoline A, and tryptoquivaline F/J, exclusively in conidia, demonstrated the ability of *A. fumigatus* to adapt to environmental conditions.

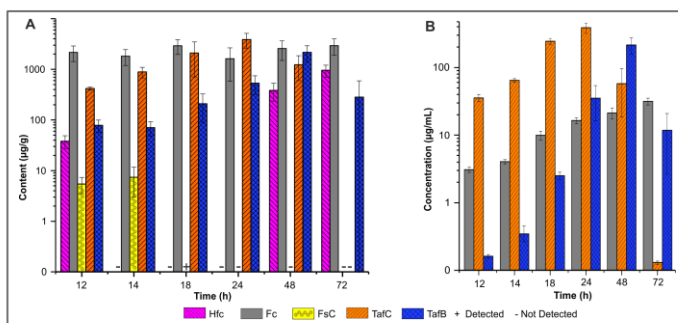


**Figure 5.9** Time-related quantitative siderophore analysis in *A. fumigatus* in **A)** residual fungal mass and **B)** supernatant from 12 to 72 h postinoculation. Data are presented as means  $\pm$  standard deviations.

In this study, each *A. fumigatus* morphotype demonstrated both qualitatively and quantitatively different profiles of siderophores. The results showed that Hfc and Fc indicated the beginning of germination and isotropic growth of *A. fumigatus*, respectively, whereas TafC and TafB produced during later stages of germination marked the phase of proliferation.

### 5.3.1 *A. fumigatus* siderophores and mycotoxins production during interaction with neutrophils and *P. aeruginosa*

As mentioned earlier, siderophore and mycotoxins play a crucial role in *A. fumigatus* virulence, we sought to describe the dynamics of these metabolite's production during *A. fumigatus* interaction *in vitro*. The interaction between *Aspergillus* and host cells is crucial for successful invasion. Moreover, *Aspergillus* co-exists with other pathogens in nature and the host. Based on this, we designed an interaction experiment with innate immune cells, mainly blood-derived neutrophils, since they are part of the primary line of defence and with bacterial pathogen *P. aeruginosa*, which is most commonly found to cohabit with *A. fumigatus*.

Firstly, we developed a new extraction protocol for sensitive and simultaneous detection of both Gtx and BmGtx using LC-MS, thereby avoiding suppression by huge siderophore secretion. SPE involving washing in a double volume of 60% MeOH +0.1FA followed by elution in 100% MeOH+0.1FA provided the best results for improved detection of Gtx and BmGtx with reduced carry over of siderophores.

The analysis of co-culture supernatant with *A. fumigatus* and *P. aeruginosa* showed that Fc secretion was significantly suppressed in the presence of *P. aeruginosa* over 72h of incubation (**Fig. 5.10 A**). TafC was first detected at 12h in only single *A. fumigatus* culture with significantly lower production from the stationary phase of bacterial growth, i.e., from 18h in dual culture samples (**Fig. 5.10 B**). Conversely, TafB secretion was detected at 24h, only in dual culture however, further growth from 36h resulted in reduced TafB secretion contrast to single culture (**Fig. 5.10 C**).

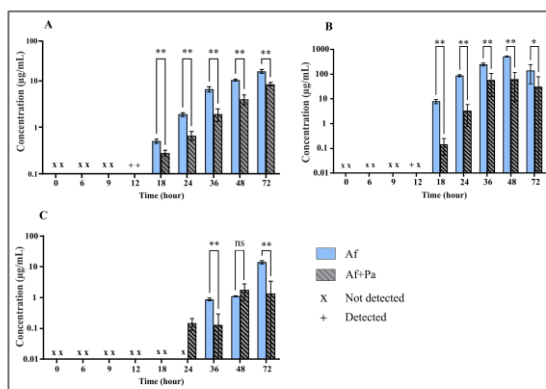


**Figure 5.10** Kinetics of siderophore production in *A. fumigatus* and *P. aeruginosa* during co-culture. Secretion of **A)** Fc and **B)** TafC was significantly higher in single culture of *A. fumigatus* than during co-culture with *P. aeruginosa* over 72 h. **C)** TafB was first quantified at 24h only in co-culture samples with further decreased in its production compared to single *A. fumigatus* culture. Data are presented as means  $\pm$  SDs. The statistical significance (Mann-Whitney test) is indicated by ns (not significant), \* ( $P < 0.05$ ), \*\* ( $P < 0.01$ ). Af, *A. fumigatus*; Pa, *P. aeruginosa*

Our results indicated that during the competition for iron in a shared environment, *P. aeruginosa* dominates *A. fumigatus* by modulating iron acquisition strategies. Nevertheless, in this study, even using a developed extraction protocol, we could not detect Gtx or its metabolites. This contradicts the other findings [58, 59]; however, given that the growth conditions used in those two studies differ than this study could have implications on Gtx secretion.

Further, we determined siderophore and mycotoxins production in the interaction processes between neutrophil and *A. fumigatus*. Neutrophils are reported to respond specifically to hyphal forms of *A. fumigatus* [60] as a result, the experiment was carried out using neutrophil ( $1 \times 10^6$  cells/mL) and *A. fumigatus* hyphae (100  $\mu\text{g/mL}$ ). The results summarized in **Fig. 5.11** showed that content of Fc, TafC and TafB was significantly higher during the incubation of *A. fumigatus* with neutrophils till 36 h. The higher content of Fc and TafC was also detected at 48 h in *A. fumigatus* infected neutrophil samples, however, due to biological variation observed between replicates it was statistically insignificant. Interestingly TafB was continuously detected till 48 h with neutrophil incubation, while single *A. fumigatus* culture showed detection till 18 h (**Fig. 5.11 C**). None of these siderophores were detected in control neutrophil supernatant or pellet samples.

The more siderophore content detected from the beginning of experiment was mainly due to incubation of neutrophils with lyophilized *A. fumigatus* hyphae. From these result, we concluded that experiment involving incubation of *A. fumigatus* germinating conidia with neutrophils is necessary to study kinetics of siderophore production during host cell interaction.

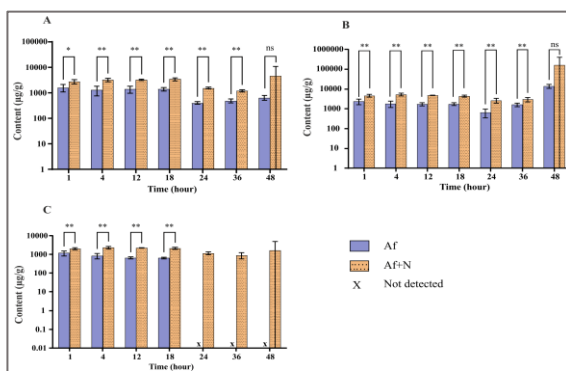


**Figure 5.11** *A. fumigatus* siderophore production upon incubation of hyphae with neutrophils over the time course. All siderophores content **A)** Fc, **B)** TafC and **C)** TafB, was elevated during interaction with neutrophils than single *A. fumigatus* culture. Data are presented as means  $\pm$  standard deviations. The statistical significance (Mann-Whitney test) is indicated by ns (not significant), \* ( $P < 0.05$ ), \*\* ( $P < 0.01$ ). Af, *A. fumigatus*; N, neutrophils

Regarding mycotoxins, we mainly targeted the detection of Gtx and its metabolites due to their immunosuppressive properties, as mentioned earlier. We quantified both Gtx and BmGtx in supernatant samples at 48h (Fig. 5.12). The detection of Gtx only at 48h could be result of a possible defense strategy used by *A. fumigatus* against neutrophils. On the other hand, low zinc concentration reported to play important role in Gtx regulation (in this case 4.2  $\mu$ M) could also be the trigger for Gtx production.

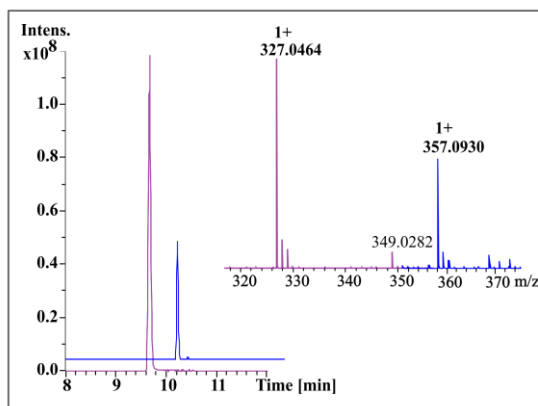


**Figure 5.12** Extraction of Gtx (M+H)<sup>1+</sup>(pink) and BmGtx (M+H)<sup>1+</sup>(blue) with their annotation in *A. fumigatus* incubated neutrophil supernatant at 48h. Gtx, gliotoxin; BmGtx, bismethylgliotoxin

Our results indicated that siderophores, Fc, TafC, TafB and mycotoxins Gtx and BmGtx were the main molecules detected during an exposure of *A. fumigatus* hyphae to neutrophil cells. However, further experiments to overcome the mentioned limitations are necessary to confirm the findings.

### 5.3.2 *A. fumigatus* siderophores and mycotoxins production during interaction with polymycovirus

The results of one part of this section have been published in the following article:

R.H. Patil, I. Kotta-Loizou, A. Palyzová, T. Pluháček, D.A. Stevens, V. Havlíček, Freeing *Aspergillus fumigatus* of the polymycovirus makes it more resistant in the competition with *Pseudomonas aeruginosa* due to altered iron-acquiring tactics (2021) [61].

Mycoviruses can affect a range of host phenotypes including virulence and toxin production. One of our colleagues reported that mycovirus (AfuPmV-1) infection weakened *A. fumigatus* in competition with *P. aeruginosa* via altering fungal stress responses by a mechanism somehow linked to iron metabolism [12]. As a result, in this study, *A. fumigatus* iron-acquiring tactics are described during *A. fumigatus* polymycovirus-1 (AfuPmV-1) infection. Moreover, the effect of mycovirus on *A. fumigatus* mycotoxins (Gtx and BmGtx) production is also described. The results summarized in **Fig. 5.13** revealed differential secretion kinetics of siderophores in virus-free (VF) and virus-infected (VI) strains. The differences in the secretion rate of extracellular TafC between the VF and the VI strains were statistically significant (Kruskal–Wallis,  $p < 0.01$ ) in the early (24 and 31 h) and stationary growth phase (48, 54, 72 h) (**Fig. 5.13**). Similar secretion kinetics was observed for Fc detection in the supernatant. As Hfc and Fc are siderophores involved in the storage of iron, we also determined their content in conidia and fungal pellets in the stationary phase of growth. However, the sum of both Fc and Hfc content ( $\mu\text{g}$  per g of a pellet) was similar in VF and VI strains in the pellet and also in conidia.

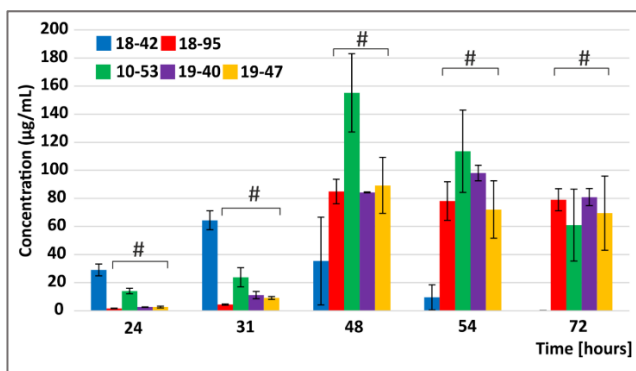


**Figure 5.13** TafC secretion in *A. fumigatus* supernatant. TafC production was earlier in VF than in the VI strains, indicated by an # symbol. The error bars show a standard error of mean n=9.

Our study showed that polymycovirus infection altered the iron-acquiring tactics of *A. fumigatus* supported by rapid secretion of siderophores by VF than VI strains in the exponential growth of *A. fumigatus*. Thus, the VF strain was more resistant in iron competition against *P. aeruginosa*. Notably, we would like to state that rather than only selected time points, a study of a whole time course is essential, as the data could have been interpreted differently if only selected time points had been used for reaching conclusions (**Fig. 5.13**) TafC secretion at 31 versus 72 h). Pigment production was another phenotype that we checked upon mycovirus infection. On solid media of malt extract agar, no differences in colouration between the five strains were visible. Conversely, in an iron-limited liquid medium, green colour pigment secretion was visible only in VI strains. As mentioned earlier, *A. fumigatus* secretes different forms of melanin; as a result, this observation was verified using matrix-assisted laser desorption MS for melanin detection in VI samples. None of the melanin or its precursors was detectable in our culture; therefore, we concluded that pigments secreted in VI strains were not associated with melanin production. Our data suggested that the presence of the virus in the infected fungal cell represents a substantial metabolic burden where AfuPmV-1 proteins or RNA interfered with fungal siderophore synthesis and iron metabolism. As a result, fungal virulence attenuation through transfection of *Aspergillus* with mycoviruses could represent a promising experimental approach analogous to antibacterial phage therapy.



As a next step, we have investigated whether AfuPmV-1 influences the production of mycotoxins in *A. fumigatus*. Gtx production is dependent on the presence of nutrients therefore, this experiment was performed in a media containing all nutrients and trace elements keeping AfuPmV-1 as a sole source of a stress factor. The analysis of the supernatants in this kinetic study revealed that Gtx and BmGtx were first detected at 36 h of incubation in VI strains (except for BmGtx in 19-40 detected at 24h) (**Fig. 5.14**). Gtx secretion was mainly observed in the stationary phase of fungal growth (36, 48 and 60h) in all VI strains (**Fig. 5.14A**).

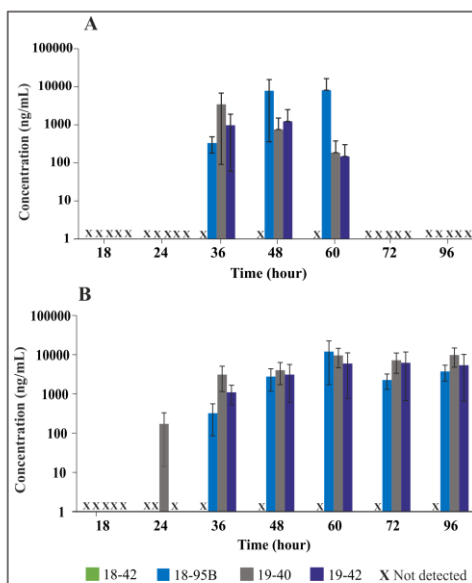


**Figure 5.14 A) Gtx and B) BmGtx production in supernatant over the time course of 96 h in VI strains.**

On the other hand, BmGtx production was continuously detected over the complete time course of the study till 96h in VI strains (**Fig. 5.14B**). No Gtx nor BmGtx were detected in the VF strain at any time point of our study. Moreover, increased levels of BmGtx after 60h appear to correlate with a decrease in Gtx levels since BmGtx is a negative regulator of Gtx biosynthesis upon an increase in Gtx levels [62]. Our results support the hypothesis that Gtx thiomethylation is a potential *A. fumigatus* mechanism of protection against Gtx

toxicity. Results in this work indicated that AfuPmV-1 infection is a stress factor for *A. fumigatus* supported by differential secretion of *A. fumigatus* antibacterial mycotoxins, particularly Gtx and its derivative bmGtx.

Among several nutrients, Gtx production is inversely related to zinc availability. Based on this observation and to further confirm previous LC-MS results, we performed gene expression analysis targeting Gtx biosynthesis genes, mainly *gliG*, *gliN*, *gliT*, *gliA* and BmGtx gene *gtxA*. Here similar VF and VI strains were grown under zinc-depleted media for 48h. Initially, we confirmed the presence and content of AfuPmV-1 in all strains (**Fig. 5.15A**). Our results indicated that expression of all the Gtx biosynthesis genes tested, i.e., *gliG*, *gliN*, *gliT* and *gliA*, were upregulated in VI strains than VF (**Fig. 5.15B**). *gtxA* involved in BmGtx synthesis was also found to be expressed more in VI strains. As stated previously the study of the whole time course is essential, which is a limitation of this experiment. However, these results proved that zinc availability plays a vital role in Gtx production, supported by two studies indicating the upregulation of Gtx genes in zinc depletion and no detection of Gtx in the zinc-containing media in the VF strain.

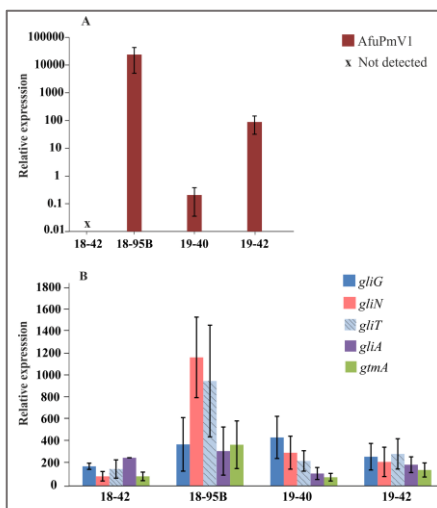


**Figure 5.15** Relative expression of **A)** AfuPmV-1 in VI strains **B)** *gli* biosynthetic cluster including *gliG*, *gliN*, *gliT* and *gliA* together with *gtxA* in VF and VI strains in zinc-depleted media at 48h.

## 5.4 Infection metallomics-based diagnosis

All the knowledge obtained throughout the preparation of section 5.1 and 5.3 was utilized to demonstrate the potential utility of infection metallomics for diagnosing aspergillosis. *Aspergillus* spp. infections are frequent in both humans and animals; therefore, we conducted this study in the diagnosis of aspergillosis in humans as well as horses.

Results shown in this section have been published in the following articles:

D. Luptakova, R.H. Patil, R. Dobias, D.A. Stevens, T. Pluhacek, A. Palyzova, M. Kanova, M. Navratil, Z. Vrba, P. Hubacek V. Havlicek, Siderophore-Based Noninvasive Differentiation of *Aspergillus fumigatus* Colonization and Invasion in Pulmonary Aspergillosis. *Microbiol Spectr.* 11(2023) [56].

R. Dobias, P. Jahn, K. Tothova, O. Dobesova, D. Visnovska, R. Patil, A. Skriba, P. Jaworska, M. Skoric, L. Podojil, M. Kantorova, J. Mrazek, E. Krejci, D.A. Stevens V. Havlicek, Diagnosis of Aspergillosis in Horses. *J Fungi* 9(2023) [63].

### 5.4.1 Human invasive pulmonary aspergillosis

The whole idea behind this work is based on the hypothesis that fungal growth-dependent production of siderophores can allow differentiation of colonization and invasive infection in critically ill patients. Depending on the host's status, once a conidial niche is established, with subsequent germination, tissue invasion, and angioinvasion, fungal virulence factors are disseminated via the bloodstream to other organs (**Fig. 5.15**). *A. fumigatus* excreted siderophores are, distributed from the site of infection to the circulation system from where they are filtered into the urine (**Fig. 5.15C**). On the top, their concentrations could be affected by viability of the pathogen in response to host factors or antifungal treatment (**Fig. 5.15B**).

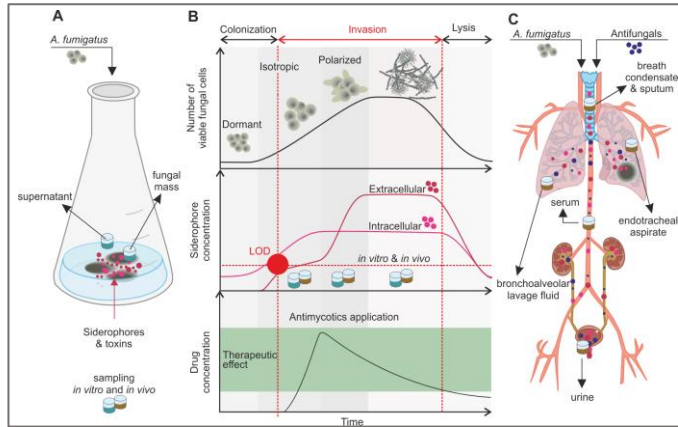


**Figure 5.15** Conceptual overview for characterization of *A. fumigatus* colonization and invasion in critically ill patients. The *in vitro* observations were transferred to human diagnostics.

Therefore, the results from *in vitro* *A. fumigatus* germination study were applied to diagnosing invasive pulmonary aspergillosis *in vivo*. In this 3-year observational, retrospective, noninterventional clinical study, 35 patients were enrolled, of which 22 patients with non-IPA infections served controls and 13 patients were diagnosed with probable IPA [64]. Applying our infection metallomics strategy, the characteristic *A. fumigatus* siderophores identified from *in vitro* study (section 4.3) were screened in urine and serum samples of all patients. Fc, TafC, TafB, and Gtx were the primary, secondary metabolites detected in IPA patients (**Fig. 5.16**). Importantly, none of these metabolites were detected in the controls. For urine analysis, biological variability in patients with diverse renal functions was partly compensated by applying a creatinine index.

Underlying disease	Risk factor(s)	Infection metallomics (mean value $\pm$ SD) <sup>a</sup>				Conventional biomarker		Death
		uGtx/Crea index	uFc/Crea index	uTafC/Crea index	uTafB/Crea index	sGM (ODI)	sBDG (pg/mL)	
Multiple myeloma	Neutropenia, IST	15.8 $\pm$ 1.0	Det	17.2 $\pm$ 0.2	ND	1.56	501	No
Non-Hodgkin lymphoma	Neutropenia, IST	Det	ND	32.1 $\pm$ 0.4	ND	3.14	115	No
Multiple myeloma	Neutropenia, IST	ND	ND	Det	ND	0.17	ND	Yes
Bronchopneumonia	Flu (H1N1)	85.2 $\pm$ 3.7	8.3 $\pm$ 0.7	82.9 $\pm$ 1.5	5.4 $\pm$ 0.1	5.9	276	Yes
COPD	Steroids	ND	11.9 $\pm$ 2.7	35.7 $\pm$ 0.4	11.5 $\pm$ 0.4	0.89	>523	Yes
COPD	Flu (H1N1)	ND	ND	Det	ND	0.1	161	No
DM II	Ketoacidosis	33.8 $\pm$ 1.4	4.2 $\pm$ 0.5	2.3 $\pm$ 0.1	ND	0.26	155	No
Bronchopneumonia	Flu (H1N1), steroids	67.9 $\pm$ 6.6	40.6 $\pm$ 2.2	3,117.4 $\pm$ 78.2	59.6 $\pm$ 3.0	7.9	>523	Yes
Liver transplant	Steroids, IST	ND	ND	27.6 $\pm$ 0.3	4.7 $\pm$ 0.3	0.06	221	No
Bronchopneumonia	Steroids	ND	ND	12.9 $\pm$ 0.3	ND	0.56	>523	No
Polytrauma	Steroids	ND	ND	ND	ND	0.24	75	No
COPD	DC	596.3 $\pm$ 13.1	505.1 $\pm$ 8.0	1,071.1 $\pm$ 5.6	250.4 $\pm$ 2.2	0.126	>523	No
Burns	ND	ND	ND	Det	ND	0.121	ND	No

<sup>a</sup>All cases (13 in total) were classified as "probable aspergillosis" [26, 27]. uFc, ferriochin in urine; uTafC, triacetylflusarinine C in urine; uTafB, triacetylflusarinine B in urine; uGtx, gliotoxin in urine; sGM, galactomannan in serum; sBDG,  $\beta$ -D-glucan in serum; ND, not detected; Det, detected; Crea, creatinine; ODI, optical density index; COPD, chronic obstructive pulmonary disease; DM II, diabetes mellitus type II; IST, immunosuppressants; DC, decompensated cirrhosis; Flu, influenza.

<sup>b</sup>For creatinine indexing, see reference 21.

**Figure 5.16** Non-invasive detection of IPA in human urine of immunocompromised and immunocompetent patients.

The results summarized in **Fig. 5.17** indicated that the TafC/creatinine index provided the highest detection sensitivity of 92.3% (95% confidence interval [CI], 64.0 to 99.8%) and specificity of 100% (95% CI, 84.6 to 100%), substantially better than the indications provided by GM and BDG serology. The serum GM and BDG sensitivities were 46.2 and 76.9%, respectively, and their specificities were 86.4 and 63.6% for the same patient cohort. Interestingly, we obtained poor sensitivity for TafC in serum (2 of 13 patients with IPA).

Biomarker	LOD threshold	Sensitivity (%) (95% CI)	Specificity (%) (95% CI)
<b>Infection metallomics<sup>b</sup></b>			
uGtx/Crea index	≥2.7 ng/mL	46.2 (19.2–74.9)	100 (84.6–100)
uFc/Crea index	≥0.9 ng/ml	46.2 (19.2–74.9)	100 (84.6–100)
uTafC/Crea index	≥0.6 ng/mL	92.3 (64.0–99.8)	100 (84.6–100)
uTafB/Crea index	≥0.6 ng/mL	38.5 (13.9–68.4)	100 (84.6–100)
<b>Conventional approaches</b>			
sGM	≥0.5 ODI	46.2 (19.2–74.9)	86.4 (65.1–97.1)
sBDG	≥80 pg/mL	76.9 (46.2–95.0)	63.6 (40.7–82.8)

<sup>a</sup>All cases (13 in total) were classified as “probable aspergillosis” (26, 27). uFc, ferricrocin in urine; uTafC, triacetylfusarinine C in urine; uTafB, triacetylfusarinine B in urine; uGtx, gliotoxin in urine; sGM, galactomannan in serum; sBDG,  $\beta$ -D-glucan in serum; Crea, creatinine; CI, confidence interval.

<sup>b</sup>For creatinine indexing, see reference 21.

**Figure 5.17** Comparison of infection metallomics-based urine diagnosis with conventional serology indicating LOD, sensitivity, and specificity values for patients with IPA

Besides, this work is the first report of TafB and Gtx detection in human urine samples. However, our study is subject to certain limitations, including the low clinical sample size and prospective cohort studies are needed to validate our approach for routine clinical diagnosis. Nevertheless, we demonstrated the potential utility of infection metallomics by non-invasive determination of an array of biomarkers such as TafC, Fc, TafB and Gtx in a single analysis for reliable diagnosis of IPA. We presented clear links between germination or infection phase-dependent siderophore production and observations in critically ill patients.

## 5.4.2 Equine aspergillosis

*A. fumigatus*, *A. niger*, *A. flavus*, *A. nidulans*, and *A. versicolor* are the dominating species in equine aspergillosis [65]. In horses, *aspergilli* are known to cause guttural pouch mycosis [66] and rare equine invasive pulmonary aspergillosis with almost 100% mortality [67]. Similar to humans, diagnosis of IPA is challenging in veterinary medicine also. In this study, we combined PCR, GM and BDG serology and infection metallomics-based metabolites detection.

The study involved BALF and serum samples collected from 18 horses suffering from IPA (n = 1), equine asthma (n = 12), and 5 healthy controls. In this study, measurement of GM levels in BALF provided sensitivity and specificity close to 100% and 94%, respectively, in the diagnosis of IPA (Fig. 5.18), which is consistent with the results obtained for the same approach in human intensive care [68]. Moreover, only Gtx was detected in the BALF and lung tissue samples, and confirmed the ongoing IPA. However, *Aspergillus*-DNA offered lower specificities due to the presence of *Aspergillus spp.* in the BALF of the healthy control horses.

	bGM (PI = 2.56)	bc <i>Aspergillus</i> -DNA	bGtx (86 ng/mL)	sGM (PI = 0.409)	sBDG (1142 pg/mL)
Sensitivity (95% CI)	100% (0.02-1)	100% (0.02-1)	100% (0.02-1)	100% (0.16-1)	100% (0.16-1)
Specificity (95% CI)	94% (0.71-1)	88% (0.64-0.99)	100% (0.8-1)	55% (0.32-0.77)	92% (0.62-1)
PPV	18% (0.01-0.99)	33% (0.01-0.91)	100% (0.02-1)	18% (0.02-0.52)	67% (0.08-0.99)
NPV	100% (0.79-1)	100% (0.78-1)	100% (0.8-1)	100% (0.72-1)	92% (0.72-1)
AUC	0.941	0.941	1	0.625	0.95

GM, galactomannan; b, bronchoalveolar lavage fluid; PPV, Positive Predictive Value; NPV, Negative Predictive Value; AUC, Area under the Curve; Gtx, gliotoxin; s, serum; BDG, 1,3-β-D-glucan; PI, Positivity Index.

**Figure 5.18** Equine serum and BALF analysis for aspergillus biomarkers of invasive aspergillosis

In the same study, for the horses with guttural pouch mycoses (GPM) (n=2), the presence of *A. fumigatus* was confirmed by culture, DNA, and microscopy on tissue samples in case report 1 on day one sampling. In biomarker analysis, intracellular fungal components, i.e., GM and Fc, were positively detected; however, the extracellular fungal markers TafC and Gtx were not detected, specifying the presence of a non-proliferating localized fungal ball. However, the repeated sampling on day 7 revealed *A. nidulans* by culture with GM and Fc biomarkers.

In the case report 2 on GPM, the elevated Fc and GM levels were attributed to *A. nidulans* based on culture, *Aspergillus*-DNA, and microscopic analysis (Fig. 5.19). *A. nidulans* was the dominant species involved in both equine GPM cases examined in this work; as a result, panfungal biomarker Fc was detected. For better inference, larger clinical studies are required, though our results indicate that combining two techniques could be helpful in the early equine IPA diagnosis.

GP	Day	Tool			Biomarker		
		Culture	<i>Aspergillus</i> -DNA	Microscopy (BSH)	GM (PI > 0.5)	Fc (ng/mL)	Sampling
GPM1 associated with nasopharyngeal dysphagia							
Left	1	<i>A. fumigatus</i>	<i>A. fumigatus</i>	Positive	9.72	492	BAT
Left	7	<i>A. nidulans</i>	<i>Aspergillus spp.</i>	Positive	10.4	1364	AS
GPM2 associated with oral dysphagia							
Left	1	<i>A. nidulans</i>	<i>Aspergillus spp.</i>	Positive	8.64	597	BAT
Right	1	<i>A. nidulans</i>	<i>Aspergillus spp.</i>	Positive	8.63	3574	BAT
Left	15	<i>A. nidulans</i>	Negative	Negative	7.54	496	AS
Right	15	Negative	Negative	Negative	7.65	ND	AS

GP, guttural pouch; GPM, guttural pouch mycosis; BSH, branching septated hyphae; GM, galactomannan; Fc, ferritinosis; BAT, before antifungal therapy; AS, after surgery; PI, positivity index; ND, not detected.

**Figure 5.19** *A. fumigatus* diagnostic tools and biomarkers detection in equine guttural pouch debridement.

## 6 CONCLUSION

This work introduced infection metallomics, a MS platform for detecting microbial metallophores, which are specific, sensitive, noninvasive, and promising biomarkers of invasive infectious diseases. This diagnostic minimises false positivity as mammalian cells do not synthesize microbial siderophores or mycotoxin molecules. Instrumentally, the concept was built on isotopically-filtered MS data (LC-MS and imzML formats with fine isotope structure resolution), which enabled untargeted metallophore analysis in microbes with understudied metabolomes or limited molecular studies. Specific isotopic profiles in  $\text{Fe}^{3+}$ ,  $\text{Zn}^{2+}$ ,  $\text{Cu}^{2+}$ ,  $\text{Ni}^{2+}$ , and other elements made it possible to design new functional studies tools involving extra and intracellular metallophores relevant to lung, CNS, or urogenital tract infections.

The metabolome mainly targeting siderophores was characterized for *R. microsporus* causing mucormycosis and *A. fumigatus* responsible for IPA using LC-MS. For the first time, the glycosylation of RHF, a siderophore of *R. microsporus* was described in a clinical isolate by LC-MS and accurate tandem MS. The stage-specific germination of *A. fumigatus* conidia and production of siderophores, mainly HfC, Fc, TafC, and FsC, was characterised for each *A. fumigatus* morphotype. This study showed that both qualitatively and quantitatively different profiles of siderophores could distinguish asymptomatic colonization and invasive infection. The role of siderophores and mycotoxins was further monitored to study the interplay among microbes involving *A. fumigatus* interaction with *P. aeruginosa* and polymycovirus as well as with host neutrophils *in vitro*. The data indicated that *P. aeruginosa* took the upper hand in co-culture with *A. fumigatus*, suppressing *A. fumigatus* siderophore production. Incubation of *A. fumigatus* with neutrophils indicated elevated siderophores levels and immunosuppressive Gtx and BmGtx detection. The AfuPmV-1 modified the expression of genes involved in Gtx biosynthesis, leading to upregulation of Gtx and BmGtx production in VI strains over VF strain demonstrated using qRT-PCR and LC-MS analysis. The AfuPmV-1 infection also interfered with the iron uptake strategies of *A. fumigatus* showed by the slowest onset of siderophore synthesis in VI strains than VF over the time course.

The application of next-generation infection diagnostics was then documented in human and equine aspergillosis. The *in vitro* results from *A. fumigatus* germination were translated to the bedside, where detection of fungal siderophores in urine (a clinical specimen distant from a deep infection site) enabled early, specific, and non-invasive diagnosing of patients suffering from IPA. This work is also the first report on the secretion of TafB and Gtx into human urine samples. In the one-health concept, the diagnosis of aspergillosis was elaborated in horses. Along with routine diagnostic methods such as BDG and GM detection, Gtx was found in the lung tissue and BALF in the fatal

invasive aspergillosis case. However, in guttural pouch aspergillosis cases, two horses positively responded to antimycotic therapies; as a result drop in the concentration of intracellular and panfungal *Aspergillus* siderophore Fc was detected in the debridement.

In the near future, infection metallomics may expand to new application fields. Until now, mostly inter-cellular phenomena were interpreted and upgraded into the next generation infection diagnostics. Although initially developed with FTICR-MS, transfer to widely spread MALDI TOF instruments is feasible. The concept can be used in intracellular pathogens and may shift from infection metallomics to functional metallomics. Definition of emerging metallophore targets in the host cells, research on new chemical structures of metal-bound chelators, discoveries of NRPS systems coding metallophores in understudied species, and definition of new treatment intervention sites represent just a reduced list of areas in which infection metallomics might be of help.



## REFERENCES

- [1] F. Bongomin, S. Gago, R.O. Oladele D.W. Denning, *Journal of Fungi*. 3 (2017) 10.3390/jof3040057.
- [2] E.M. Negm, M.S. Mohamed, R.A. Rabie, W.S. Fouad, A. Beniamen, A. Mosallem, A.E. Tawfik H.M. Salama, *BMC Infect Dis*. 23 (2023) 246.
- [3] (2022).
- [4] B. Mousavi, M.T. Hedayati, N. Hedayati, M. Ilkit S. Syedmousavi, *Curr Med Mycol*. 2 (2016) 36-42.
- [5] J. Pfister, Summer, D., Petrik, M., Khoylou, M., Lichius, A., Kaeopookum, P., Kochinke, L., Orasch, T., Haas, H. and Decristoforo, C, (2020).
- [6] M. Schrettel, E. Bignell, C. Kragl, Y. Sabiha, O. Loss, M. Eisendle, A. Wallner, H.N. Arst, Jr., K. Haynes H. Haas, *PLoS Pathog*. 3 (2007) 1195-1207.
- [7] H. Tamiya, E. Ochiai, K. Kikuchi, M. Yahiro, T. Toyotome, A. Watanabe, T. Yaguchi K. Kamei, *J Infect Chemother*. 21 (2015) 385-391.
- [8] M.A. Mehedi MA, Khondkar PR, Sultana S, Islam MA, Rashid MA, Chowdhury R., (2010).
- [9] X.J. Li, Q. Zhang, A.L. Zhang J.M. Gao, *J Agric Food Chem*. 60 (2012) 3424-3431.
- [10] R.H. Du, E.G. Li, Y. Cao, Y.C. Song R.X. Tan, *Life Sci*. 89 (2011) 235-240.
- [11] R. Amin, A. Dupuis, S.D. Aaron F. Ratjen, *Chest*. 137 (2010) 171-176.
- [12] H. Nazik, I. Kotta-Loizou, G. Sass, R.H.A. Coutts D.A. Stevens, *Viruses*. 13 (2021).
- [13] J. Jennessen, J. Schnurer, J. Olsson, R.A. Samson J. Dijksterhuis, *Mycol Res*. 112 (2008) 547-563.
- [14] Y. Ogawa, S. Tokumasu K. Tubaki, *Mycoscience*. 45 (2004) 271-276.
- [15] M.M. Roden, T.E. Zaoutis, W.L. Buchanan, T.A. Knudsen, T.A. Sarkisova, R.L. Schaufele, M. Sein, T. Sein, C.C. Chiou, J.H. Chu, D.P. Kontoyiannis T.J. Walsh, *Clinical Infectious Diseases*. 41 (2005) 634-653.
- [16] E. Alvarez, D.A. Sutton, J. Cano, A.W. Fothergill, A. Stchigel, M.G. Rinaldi J. Guarro, *J Clin Microbiol*. 47 (2009) 1650-1656.
- [17] H. Prakash, A.K. Ghosh, S.M. Rudramurthy, P. Singh, I. Xess, J. Savio, U. Pamidimukkala, J. Jillwin, S. Varma, A. Das, N.K. Panda, S. Singh, A. Bal A. Chakrabarti, *Med Mycol*. 57 (2019) 395-402.
- [18] T.J. Walsh, M.N. Gamaletsou, M.R. McGinnis, R.T. Hayden D.P. Kontoyiannis, *Clin Infect Dis*. 54 Suppl 1 (2012) S55-60.
- [19] K. Voigt, T. Wolf, K. Ochsenreiter, G. Nagy, K. Kaerger, E. Shelest T. Papp, 15 Genetic and Metabolic Aspects of Primary and Secondary Metabolism of the Zygomycetes, in *Biochemistry and Molecular Biology*, D. Hoffmeister, Editor. 2016, Springer International Publishing: Cham. p. 361-385.

- [20] W.M. Artis, J.A. Fountain, H.K. Delcher H.E. Jones, *Diabetes*. 31 (1982) 1109-1114.
- [21] J.R. Boelaert, A.Z. Fenves J.W. Coburn, *Am J Kidney Dis*. 18 (1991) 660-667.
- [22] H.M. Drechsel, J.; Freund, S.; Jung, G.; Boelaert, J.R.; Winkelmann, G., (1991).
- [23] H. Drechsel, Tschierske, M., Thieken, A., Jung, G., Zähler, H. and Winkelmann, G, (1995).
- [24] C.S. Carroll, C.L. Grieve, I. Murugathasan, A.J. Bennet, C.M. Czekster, H. Lui, J. Naismith M.M. Moore, *Int. J. Biochem. Cell Biol*. 89 (2017) 136-146.
- [25] M. de Locht, J.R. Boelaert Y.J. Schneider, *Biochem Pharmacol*. 47 (1994) 1843-1850.
- [26] E. Layre, L. Sweet, S. Hong, C.A. Madigan, D. Desjardins, D.C. Young, T.-Y. Cheng, J.W. Annand, K. Kim I.C. Shamputa, *Chemistry & biology*. 18 (2011) 1537-1549.
- [27] (2018).
- [28] J. Novak, A. Škríba V. Havlíček, *Anal Chem*. 92 (2020) 6844-6849.
- [29] L. Kanhayuwa, I. Kotta-Loizou, S. Ozkan, A.P. Gunning R.H. Coutts, *Proc Natl Acad Sci U S A*. 112 (2015) 9100-9105.
- [30] R.H. Patil, I. Kotta-Loizou, A. Palyzova, T. Pluháček, R.H.A. Coutts, D.A. Stevens V. Havlíček, *J Fungi (Basel)*. 8 (2022).
- [31] E.J. Want, I.D. Wilson, H. Gika, G. Theodoridis, R.S. Plumb, J. Shockey, E. Holmes J.K. Nicholson, *Nat Protoc*. 5 (2010) 1005-1018.
- [32] M. Hoenigl, T. Orasch, K. Faserl, J. Prattes, J. Loeffler, J. Springer, F. Gsaller, F. Reischies, W. Duettmann, R.B. Raggam, H. Lindner H. Haas, *J Infection*. 78 (2019) 150-157.
- [33] R.H. Patil, D. Luptakova V. Havlíček, *Mass Spectrom Rev*. 42 (2023) 1221-1243.
- [34] T. Pluháček, A. Škríba, J. Novák, D. Luptáková V. Havlíček, Analysis of microbial siderophores by mass spectrometry, in *Methods in Molecular Biology*, S.K. Bhattacharya, Editor. 2019, Springer Nature.
- [35] T. Pluháček, K. Lemr, D. Ghosh, D. Milde, J. Novák V. Havlíček, *Mass Spectrometry Reviews*. 35 (2016) 35-47.
- [36] J. Novák, A. Škríba, J. Zápal, M. Kuzma V. Havlíček, *J Mass Spectrom*. 53 (2018) 1097-1103.
- [37] J. Novák, A. Škríba V. Havlíček, *Anal Chem*. 92 (2020) 6844-6849.
- [38] J. Privratsky J. Novak, *J Cheminform*. 13 (2021) 51.
- [39] D. Luptáková, T. Pluháček, M. Petřík, J. Novák, A. Palyzová, L. Sokolová, A. Škríba, B. Šedivá, K. Lemr V. Havlíček, *Sci Rep*. 7 (2017) 16523.
- [40] T. Pluháček, M. Petřík, D. Luptáková, O. Benada, A. Palyzová, K. Lemr V. Havlíček, *Proteomics*. 16 (2016) 1785-1792.
- [41] A. Škríba, T. Pluháček, A. Palyzová, Z. Novy, K. Lemr, M. Hajduch, M. Petřík V. Havlíček, *Front Microbiol*. 9 (2018) 2356.
- [42] C.S. Carroll, L.N. Amankwa, L.J. Pinto, J.D. Fuller M.M. Moore, *PLoS One*. 11 (2016) e0151260.

- [43] R. Dobias, A. Skriba, T. Pluhacek, M. Petrik, A. Palyzova, M. Kanova, E. Cubova, J. Houst, J. Novak, D.A. Stevens, G. Mitulovic, E. Krejci, P. Hubacek V. Havlicek, *J Fungi (Basel)*. 7 (2021).
- [44] K. Gupta, L. Grigoryan B. Trautner, *Ann Intern Med*. 167 (2017) ITC49-ITC64.
- [45] G. Ghsssein, C. Brutesco, L. Ouerdane, C. Fojcik, A. Izaute, S. Wang, C. Hajjar, R. Lobinski, D. Lemaire, P. Richaud, R. Voulhoux, A. Espaillat, F. Cava, D. Pignol, E. Borezée-Durant P. Arnoux, *Science*. 352 (2016) 1105-1109.
- [46] J.L. Cotton, J. Tao C.J. Balibar, *Biochemistry*. 48 (2009) 1025-1035.
- [47] W.J. Perry, J.M. Spraggins, J.R. Sheldon, C.M. Grunenwald, D.E. Heinrichs, J.E. Cassat, E.P. Skaar R.M. Caprioli, *Proc Natl Acad Sci USA*. 116 (2019) 21980-21982.
- [48] D. Perkins-Balding, M. Ratliff-Griffin I. Stojiljkovic, *Microbiol Mol Biol Rev*. 68 (2004) 154-171.
- [49] N. Simon, V. Coulanges, P. Andre D.J. Vidon, *Appl Environ Microb*. 61 (1995) 1643-1645.
- [50] J.L. Vincent, J. Rello, J. Marshall, E. Silva, A. Anzueto, C.D. Martin, R. Moreno, J. Lipman, C. Gomersall, Y. Sakr, K. Reinhart E.I.G.o. Investigators, *JAMA*. 302 (2009) 2323-2329.
- [51] J.L. Vincent, Y. Sakr, M. Singer, I. Martin-Loeches, F.R. Machado, J.C. Marshall, S. Finfer, P. Pelosi, L. Brazzi, D. Aditianiingsih, J.F. Timsit, B. Du, X. Wittebole, J. Maca, S. Kannan, L.A. Gorordo-Delsol, J.J. De Waele, Y. Mehta, M.J.M. Bonten, A.K. Khanna, M. Kollef, M. Human, D.C. Angus E.I. Investigators, *JAMA*. 323 (2020) 1478-1487.
- [52] A. Johnová, M. Dobišová, M.A. Abdallah P. Kyslík, *Biotechnol Lett*. 23 (2001) 1759-1763.
- [53] R. Dobiáš V. Havlíček, Microbial siderophores: markers of infectious diseases, in *Microbial and natural macromolecules: synthesis and applications*, S. Das and H.R. Das, Editors. 2021, Academic Press, Elsevier, USA.
- [54] A. Škríba, Patil, R.H., Hubáček, P., Dobiáš, R., Palyzová, A., Marešová, H., Pluháček, T. and Havlíček, V., (2020).
- [55] H. Kamimura, *Appl Environ Microbiol*. 52 (1986) 515-519.
- [56] D. Luptakova, R.H. Patil, R. Dobias, D.A. Stevens, T. Pluhacek, A. Palyzova, M. Kanova, M. Navratil, Z. Vrba, P. Hubacek V. Havlicek, *Microbiol Spectr*. 11 (2023) e0406822.
- [57] I. Happacher, M. Aguiar, M. Alilou, B. Abt, T.J.H. Baltussen, C. Decristoforo, W.J.G. Melchers H. Haas, *Microbiol Spectr*. 11 (2023) e0049623.
- [58] A. Margalit, D. Sheehan, J.C. Carolan K. Kavanagh, *Microbiology (Reading)*. 168 (2022).
- [59] E.K. Manavathu, D.L. Vager J.A. Vazquez, *BMC Microbiol*. 14 (2014) 53.
- [60] B.P. Knox, Q. Deng, M. Rood, J.C. Eickhoff, N.P. Keller A. Huttenlocher, *Eukaryot Cell*. 13 (2014) 1266-1277.
- [61] R.H. Patil, I. Kotta-Loizou, A. Palyzova, T. Pluhacek, R.H.A. Coutts, D.A. Stevens V. Havlicek, *J Fungi (Basel)*. 7 (2021).

- [62] S.K. Dolan, R.A. Owens, G. O'Keeffe, S. Hammel, D.A. Fitzpatrick, G.W. Jones S. Doyle, *Chem Biol.* 21 (2014) 999-1012.
- [63] R. Dobias, P. Jahn, K. Tothova, O. Dobesova, D. Visnovska, R. Patil, A. Skriba, P. Jaworska, M. Skoric, L. Podojil, M. Kantorova, J. Mrazek, E. Krejci, D.A. Stevens V. Havlicek, *J Fungi (Basel)*. 9 (2023).
- [64] M. Bassetti, E. Azoulay, B.-J. Kullberg, M. Ruhnke, S. Shoham, J. Vazquez, D.R. Giacobbe T. Calandra, *Clin Infect Dis.* 72 (2021) S121-S127.
- [65] C. Cafarchia, L.A. Figueredo D. Otranto, *Vet Microbiol.* 167 (2013) 215-234.
- [66] O. Dobesova, B. Schwarz, K. Velde, P. Jahn, Z. Zert B. Bezdekova, *Vet Rec.* 171 (2012) 561.
- [67] L.W. Pace, N.R. Wirth, R.R. Foss W.H. Fales, *J Vet Diagn Invest.* 6 (1994) 504-506.
- [68] J.P. Donnelly, S.C. Chen, C.A. Kauffman, W.J. Steinbach, J.W. Baddley, P.E. Verweij, C.J. Clancy, J.R. Wingard, S.R. Lockhart, A.H. Groll, T.C. Sorrell, M. Bassetti, H. Akan, B.D. Alexander, D. Andes, E. Azoulay, R. Bialek, R.W. Bradsher, Jr, S. Bretagne, T. Calandra, A.M. Caliendo, E. Castagnola, M. Cruciani, M. Cuenca-Estrella, C.F. Decker, S.R. Desai, B. Fisher, T. Harrison, C.P. Heussel, H.E. Jensen, C.C. Kibbler, D.P. Kontoyiannis, B.-J. Kullberg, K. Lagrou, F. Lamoth, T. Lehrnbecher, J. Loeffler, O. Lortholary, J. Maertens, O. Marchetti, K.A. Marr, H. Masur, J.F. Meis, C.O. Morrissey, M. Nucci, L. Ostrosky-Zeichner, L. Pagano, T.F. Patterson, J.R. Perfect, Z. Racil, E. Roilides, M. Ruhnke, C.S. Prokop, S. Shoham, M.A. Slavin, D.A. Stevens, G.R. Thompson, III, J.A. Vazquez, C. Viscoli, T.J. Walsh, A. Warris, L.J. Wheat, P.L. White, T.E. Zaoutis P.G. Pappas, *Clin Infect Dis*, (2019).

## CURRICULUM VITAE

**Name:** RUTUJA HIRAJI PATIL  
**Year and place of birth:** 1995, Maharashtra, India  
**E-mail:** rutuja.patil@biomed.cas.cz

**Education:**

2013 - 2016 Bachelor of Science in Biotechnology, Maharashtra Education Society Abasaheb Garware College, Pune, India.

2016 - 2018 Master of Science in Biotechnology, Pondicherry University, India. Title: Standardization of inflammation induced sepsis in Sprague Dawley rats. (Supervisor: Prof. A. Hannah Rachel Vasanthi).

2018-2019 Advanced Post Graduate-Diploma in life science technologies, Sri Ramaswamy Memorial (SRM)- Department of Biotechnology Platform (DBT), SRM Institute of Science and Technology, Chennai, India. Topic: Urinary metabolomics analysis for biomarker identification in diabetic nephropathy. (Supervisor: Dr. M.Vairamani and Dr. K.M. Ramkumar).

2019 - Current PhD Student, Department of Analytical Chemistry, Faculty of Science, Palacký University, Olomouc, Czech Republic. Topic: Metabolomics of clinically important *Aspergillus fumigatus* and *Rhizopus microsporus* in diagnoses of invasive infections (Supervisor: Prof. Ing. Vladimír Havlíček).

**Internships:**

2017 Research stay, School of life science, University of Hyderabad, India (3 months) Title: Cloning of dopamine receptors in *Clarias gariepinus* (Supervisor: Prof. B. Senthilkumaran).

2022-2023

PhD Research stay, Imperial College London, Department of Life Sciences, London, United Kingdom, (3 months) Title: Mycotoxin gene expression analysis in *A. fumigatus* polmycovirus strains (Supervision: Dr. Ioly Kotta-Loizou)

#### Grants:

- Principal investigator: Doctoral student grant competition at Palacký University Olomouc, grant no. DSGC-2021-0144 (2022), Title: Small molecular weight neutrophil secretome stimulated by *Aspergillus fumigatus*.
- Team member: Internal Grant Agency of Palacký University grant IGA\_PrF\_2022\_023.
- Team member: Czech Science Foundation, grant No. 21-17044S (2021-2023), Next Generation Infection Diagnostics.
- Team member: Czech Health Research Council, grant No. NU23-05-00095 (2023-2026), A prospective study on invasive pulmonary aspergillosis.

#### Publications:

- Škríba, A., Patil, R.H., Hubáček, P., Dobiáš, R., Palyzová, A., Marešová, H., Pluháček, T. and Havlíček, V., 2020. Rhizoferrin glycosylation in *Rhizopus microsporus*. *Journal of Fungi*, 6, p.89. DOI: 10.3390/jof6020089.
- Patil, R.H., Kotta-Loizou, I., Palyzová, A., Pluháček, T., Coutts, R.H., Stevens, D.A. and Havlíček, V., 2021. Freeing *Aspergillus fumigatus* of polmycovirus infection renders it more resistant to competition with *Pseudomonas aeruginosa* due to altered iron-acquiring tactics. *Journal of Fungi*, 7, p.497. DOI: 10.3390/jof7070497.
- Dobiáš, R., Jahn, P., Tóthová, K., Dobešová, O., Višňovská, D., Patil, R., Škríba, A., Jaworská, P., Škorič, M., Podojil, L. and Kantorová, M., 2023. Diagnosis of Aspergillosis in Horses. *Journal of Fungi*, 9, p.161. DOI: 10.3390/jof9020161
- Luptáková, D., Patil, R.H., Dobiáš, R., Stevens, D.A., Pluháček, T., Palyzová, A., Káňová, M., Navrátil, M., Vrba, Z., Hubáček, P. and Havlíček, V., 2023. Siderophore-based noninvasive differentiation of *Aspergillus fumigatus* colonization and invasion in pulmonary

aspergillosis. *Microbiology Spectrum*, 11, pp.e04068-22. DOI: 10.1128/spectrum.04068-22.

- Patil, R.H., Luptáková, D. and Havlíček, V., 2023. Infection metallomics for critical care in the post-COVID era. *Mass Spectrometry Reviews*. DOI: 10.1002/mas.21755.

#### **Conference poster presentations:**

- Patil, R.H., Kotta-Loizou, I., Palyzová, A., Pluháček, T., Stevens D.A., Havlíček, V., Freeing the *Aspergillus fumigatus* of the polymycovirus makes it more resistant in the competition with *Pseudomonas* due to the altered iron-acquiring tactics. European Congress of Clinical Microbiology and Infectious Diseases, online, July 9-12, 2021, Poster No. 04053.
- Patil, R.H., Kotta-Loizou, I., Palyzová, A., Pluháček, T., Coutts, R., Stevens, D.A., Havlíček, V., Mycotoxin secretion by *Aspergillus fumigatus* as a response to mycovirus infection. The Advances against Aspergillosis and Mucormycosis virtual conference, Feb 2-3, 2022, Poster No. 42. One of the outstanding posters presented at the conference.
- Patil, R. H., Luptáková, D., Havlíček, V., Infection metallomics based functional studies in *Aspergillus fumigatus*. Proceedings of Advances in Chromatography and Electrophoresis & Chiral, Olomouc June 13-16, 2022, Czech Republic.

#### **Conference oral presentations:**

- Patil, R.H., Dobiáš, R., Škríba, A., Pluháček, T., Luptáková, D., Palyzová, A., Havlíček, V., On the threshold between *Aspergillus fumigatus* colonization and proliferation in a host. The 31st MassSpec Forum, Feb 25-26, 2020, Vienna, Austria.
- Patil, R.H., Luptáková, D., Dobiáš, R., Pluháček, T., Palyzová, A., Havlíček, V., Extracellular secretome in polarized *Aspergillus fumigatus* growth triggers the invasive aspergillosis in a host. The Ninth Annual Conference of the Czech Society for Mass Spectrometry, Oct 11-12, 2021, Prague, Czech Republic.
- Patil, R.H., Kotta-Loizou, I., Palyzová, A., Pluháček, T., Coutts, R., Stevens D.A., Havlíček, V., Freeing *Aspergillus fumigatus* of Polymycovirus Infection Renders it More Resistant to Competition

with *Pseudomonas aeruginosa* due to Altered Iron-Acquiring Tactics. Prague Meeting on Historical Perspectives of Mass Spectrometry & Opening of the Czech Mass Spectrometry Museum, Oct 13-14, 2021, Prague, Czech Republic.

- EU FT-ICR MS 2<sup>nd</sup> advanced user school Prague, Czech Republic (2021).
- Patil, R.H., Luptáková, D., Dobiáš, R., Stevens, D.A., Pluháček, T., Palyzová, A., A., Havlíček, V., Infection metallomics-based differentiation of *Aspergillus fumigatus* colonization and invasion. The 24th International Mass Spectrometry Conference, Maastricht, The Netherlands, 27 Aug-2 Sept 2022.
- Patil, R.H., Juříková T., Mácha H., Hrdý J., Marešová H., Palyzová A., Benada O. and Havlíček V., *Aspergillus fumigatus* and *Pseudomonas aeruginosa* interplay at a host interface. The Eleventh Annual Conference of the Czech Society for Mass Spectrometry, June 19-21, 2023, Brno, Czech Republic.

#### Scholarships and awards

- J. L. Fisher scholarship, Olomouc, Czech Republic (2019 - Present).
- Nico Nibbering Student Travel Award to attend the 24th International Mass Spectrometry Conference, Maastricht, The Netherlands (2022).
- Austrian Proteomics & Metabolomics Association (APMA) travel grant for the 31st MassSpec Forum Vienna, Austria (2020).
- SRM-DBT fellowship, Chennai, India (2018 - 2019).
- Jawaharlal Nehru University (JNU-DBT) fellowship, Delhi, India (2016 - 2018).

#### Trainings

- EU FT-ICR MS 2<sup>nd</sup> advanced user school Prague, Czech Republic (2021).
- A course in Mass Spectroscopy: “Fundamentals and Applications” organized by SRM-IST, Chennai, India (2018).
- Industrial training at Serum institute of India PVT. LTD. Pune India on large scale manufacturing of Diphtheria, Tetanus, Pertussis, Hib, BCG, r- Hepatitis B, Measles vaccines production and its quality control (2016).